QUALITY OF SERVICE FOR MULTI-RATE DS/CDMA SYSTEMS WITH MULTI-USER DETECTION

BY MOHAMMAD SAQUIB

A dissertation submitted to the

Graduate School—New Brunswick

Rutgers, The State University of New Jersey

in partial fulfillment of the requirements

for the degree of

Doctor of Philosophy

Graduate Program in Electrical and Computer Engineering

Written under the direction of

Professor Roy D. Yates

and approved by

New Brunswick, New Jersey

January, 1998

ABSTRACT OF THE DISSERTATION

Quality of Service for Multi-rate DS/CDMA Systems with Multi-user Detection

by Mohammad Saquib

Dissertation Director: Professor Roy D. Yates

This thesis addresses the use of decorrelators for a dual-rate synchronous DS/CDMA system that serves both low bit rate and high bit rate users. Here it is assumed that in an interval of duration T, a low rate user transmits one bit while a high rate user transmits M bits. Applying a standard decorrelator to the interval of duration T yields an M bit processing delay for high rate users and a computational complexity that grows with M. This situation prompts us to propose a decorrelator that generates bit decisions for each high rate user in every subinterval of duration T/M. To decode a low rate user, a soft decoding rule applies maximal ratio combining on M separate decorrelated outputs of each low rate user. It is proven that the bit error rate of the standard decorrelator is less than or equal to that of the soft decoding decorrelator. In addition, we develop a dual-rate decision feedback decorrelator which retains the desirable properties of the soft decoding decorrelator and outperforms the standard decorrelator.

For an asynchronous multi-rate DS/CDMA system, a truncated window decorrelator is proposed. We prove that the performance of any truncated window decorrelator improves monotonically with the observation window length. On the other hand, a longer observation window results in greater computational complexity. Therefore, we

decode a user by extending the observation window over sufficient number of its bits. We develop simple upper and lower bounds for the asymptotic efficiency of both the truncated window and infinite window decorrelators to characterize practical window sizes.

Using a decorrelator in a multi-rate DS/CDMA system, it may be necessary for different users to combat the noise enhancement and the propagation losses to varying degrees depending on individual requirements. In this context, we propose an iterative power control algorithm which is suitable for a class of BER objectives. If the uplink channel gain of the desired user is known, then it is simple to choose the transmitter power needed to meet its target BER objective. In practice, however, the uplink channel gain is often difficult to measure. To avoid this measurement, we employ stochastic approximation methods to develop the power control algorithm.

Acknowledgements

First, I would like to acknowledge my advisor Prof. Roy D. Yates. I am deeply grateful to him for his constant support, guidance and encouragement during all phases of my graduate student life including seeking employment. His deep insight and rigorous style of problem solving influenced and inspired me throughout my tenure at WINLAB. Prof. Yates' unlimited encouragement, availability to listen to my ideas and to answer my questions, both in and out-of-hours, kept me motivated during all stages of this work.

My heartfelt gratitude goes to Prof. Narayan B. Mandayam for his useful ideas and insightful discussions during the evolution of the work. I also would like to thank Prof. Jack M. Holtzman for several helpful ideas and discussions at different stages of this dissertation. Many thanks to Prof. Sophocles J. Orfanidis for serving my thesis committee and for showing keen interest in the progress of this work. I would specially like to acknowledge my outside committee member, Dr. Howard C. Huang of Lucent Bell Labs for taking time from his busy schedule to participate in my dissertation. I am grateful to Prof. David J. Goodman for providing me the opportunity to be a part of WINLAB. My special thanks to Anand Ganti for collaborating me on the background work and publications that are parts of this dissertation. To Tuhin Mahmud, Sudhir Ramakrishna, Kamesh Medepalli, Aylin Yener, Sennur Ulukus, Ashwin Sampath, Shehzad Hussain, Mathew Thomas, Mark Wehle and all my other friends at Rutgers, thanks for their invaluable companionship.

I am and will always be very grateful to my parents and my brother Dr. Mohammad Farooque who have supported me with their love, advice and encouragement in my last twenty years of schooling. Finally, my most grateful gratitude goes to my wife Rehana Saquib who has taught me the true meaning of companionship and provided me endless love and caring from the beginning to the end of this work.

Dedication

This thesis is dedicated to my *Abba* and *Ma*. Without their love, guidance and encouragement, I would not have been able to complete this dissertation.

Table of Contents

List of Figures

Chapter 1

Introduction

In a code division multiple access (CDMA) system, multiple users are allowed to share the limited resources of frequency and time. There are two primary CDMA schemes, namely frequency hopping and direct sequence. We will focus on direct sequence CDMA or DS/CDMA. The DS/CDMA system has several properties, such as i) soft capacity, ii) soft handoff, iii) anti-multipath capabilities, etc., which make it more attractive in terms of capacity [13] over other multiple access methods, such as FDMA and TDMA. A detailed literature on DS/CDMA can be found in [69]. In the following section we will review the DS/CDMA system with matched filter receivers which is also known as the conventional DS/CDMA system.

1.1 Conventional DS/CDMA System

In a conventional DS/CDMA system, each user is treated separately by considering the other users as interference called *multiple access* or *multi-user interference*. If the interference due to other users increases, the equivalent noise results in the degradation of the desired users' performance. In a conventional DS/CDMA system, a user's performance degrades as the received powers of the interfering users increase. When all the users are transmitting at the same power level and an interferer is much closer to the base station, then the desired user's signal-to-interference ratio will be low and the bit error rate will be high. This phenomenon is known as the *near/far* effect. Basically, the conventional DS/CDMA system is very sensitive to the near/far effect and in order to overcome this sensitivity, power control must be employed. For the conventional DS/CDMA system, the following two key limitations have drawn significant attention.

- All users interfere with each other. This results in performance degradation for every user.

- To combat the near/far problem and to guarantee quality of service objectives, power control is required.

1.2 DS/CDMA System with Multiuser Detectors

In order to resolve the shortcomings of the conventional DS/CDMA system, multiuser detection has been proposed. Unlike conventional matched filter detection, multiuser detection exploits interfering users' received signals to decode a user. Under multiuser detection, each transmitter needs to know only its own signature waveforms, whereas, the base station detects all the transmitted signals by utilizing full/partial knowledge of all users' transmitted signature waveforms.

Verdú [66,67] proposed the *optimum multiuser receiver* or *maximum-likelihood (ML) receiver* in which all users' signals are jointly decoded. The ML receiver can be realized by following the matched filter bank with a Viterbi algorithm. This receiver minimizes the bit error probability, however, it suffers from exponential complexity and requires the perfect knowledge of the received energies. The computational complexity of the ML receiver prompted the development of a number of sub-optimal receivers.

Among all the sub-optimal receivers, a significant amount of attention has been devoted to linear multi-user detectors. The first linear multi-user detector extensively analyzed was the *decorrelating detector* or *decorrelator* [28]. This receiver has probably drawn more attention than any other multi-user detector. The decorrelator applies the inverse of the cross-correlation matrix at the outputs of bank of matched filter. It operates without estimating the received energies. The main disadvantage of this receiver is that it enhances the noise variance. The decorrelating detector is exactly analogous to the zero-forcing equalizer used to combat ISI [41]. Reference [33] showed that when the cross-correlations between the signature waveforms are relatively small, a first-order approximation of the decorrelating detector exhibits good performance.

Another very efficient linear multi-user is the Minimum Mean-Square (MMSE) multiuser detector [74]. This receiver chooses the linear transformation which minimizes the mean-squared error between the transmitted data and the soft output of the matched filter. A training sequence-based adaptive MMSE receiver was implemented in reference [31]. Here it was shown that the MMSE receiver maximizes the signal-to-interference ratio (SIR). References [17, 70] proposed a blind version of the adaptive MMSE receiver. In [34], a stochastic gradient algorithm was used to find the linear detector that minimizes the probability of error. Several other adaptive multi-user receivers were proposed in references [4, 35, 42].

Another class of linear detectors includes subtractive interference cancellation detectors [8, 39, 55, 61, 62]. This group of detectors detects the bit of the strongest user and subtracts its signal from the received signal. This process continues until the weakest user of the system is detected. This successive interference cancellation scheme can be implemented by using any linear receiver such as the matched filter or the decorrelating detector or the MMSE receiver. Reference [8] proposed the decision feedback decorrelator for a DS/CDMA system where users transmit at the same bit rate. To decode a user, this receiver first orthogonalizes the relatively weaker users and then utilizes bit decisions of the stronger users to eliminate their multiuser interference.

1.3 Multi-rate Access Methodologies for DS/CDMA Systems

Significant efforts are being made to integrate the cellular network with fixed networks for communicating both voice and data messages [15, 32, 45]. CDMA systems are being considered to support multimedia traffic in third generation mobile radio systems, such as Future Public Land Mobile Telecommunication Systems (FPLMTS) and Universal Mobile Telecommunication Systems (UMTS) [1, 43]. To provide integrated voice and data communication over cellular networks, several access strategies [20, 37, 72, 73] have been proposed for multi-rate DS/CDMA systems. These include

1. Fixed chip rate, variable processing gain scheme [37, 72, 73]

2. Fixed processing gain, variable chip rate scheme [72, 73]

3. Multi-code method [20, 37]

4. Multi-modulation scheme [37]

A comparative study of the above access strategies 1 and 2 was performed in [72]. In [73], it was found that the access strategy 2 is complicated because the receiver must be synchronized to its particular code rate and the system needs additional frequency planning due to the unequal bandwidth spreading of different users. The access strategy 1 needs simple hardware for building a multi-rate DS/CDMA radio interface. However, in a conventional multi-rate DS/CDMA system, this scheme suffers from performance degradation as the bit rate increases.

In the multi-code access strategy 3, all users multiplex their information bits onto multiple low rate signature waveforms by using BPSK or any other type of modulation scheme such as QPSK. As all the users have the same processing gain, it may be easier to construct signatures with good cross-correlation properties. However, in a conventional multi-rate DS/CDMA system with the multi-code scheme, the mobile as well as the base station require linear amplifiers; see [37].

The multi-modulation access strategy 4 employs an M-ary QAM modulation scheme and varies the modulation-level, M to accommodate multiple bit rates. In the other words, users of different bit rates use different modulation schemes. Under the same signal-to-noise ratio per bit, transmitter powers will be different for different users. High rate users transmit at very high powers and in a conventional multi-rate DS/CDMA system, this will cause a severe near/far problem for the relatively low rate users.

1.4 Multi-rate Multi-user Detectors

Several studies regarding receiver designs for multi-rate CDMA systems have been performed. The performance of jointly optimal detection for multi-rate DS/CDMA systems was studied in [36]. This study was performed for both the variable processing gain access strategy as well as in the context of multi-code scheme with BPSK modulation. Multistage multiuser receivers for multi-rate CDMA communications were introduced in [19]. For minimum mean squared error (MMSE) performance criteria, [18] considered multi-user communication with multiple symbol rates. In [21], a successive

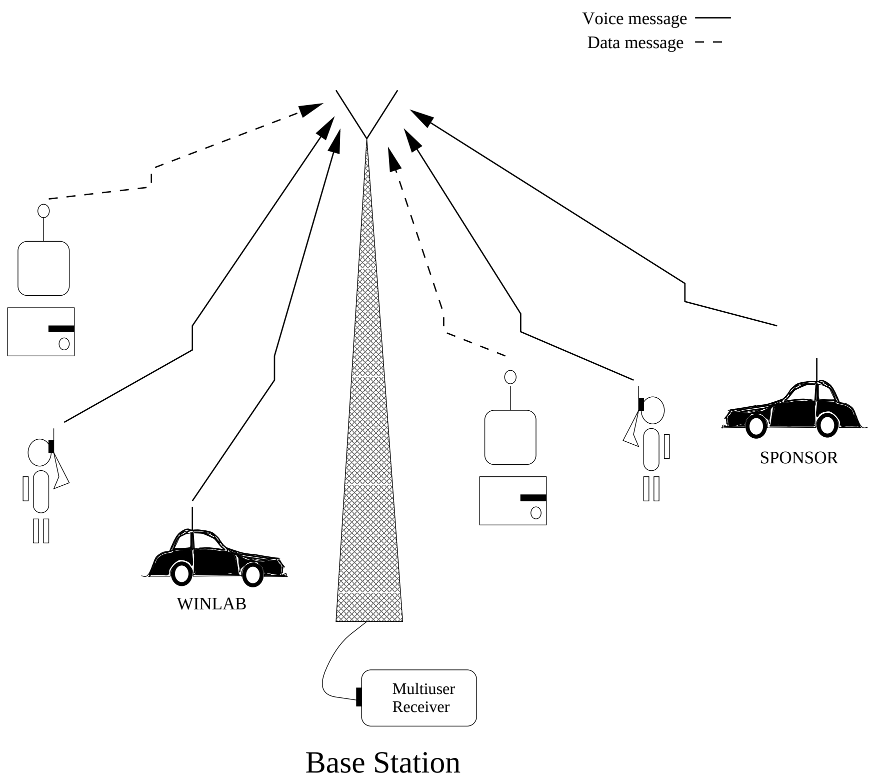

Figure 1.1: Future CDMA cellular network.

interference cancellation scheme for multi-rate CDMA was studied in the context of the multi-modulation scheme as well as the multi-code scheme.

1.5 Thesis Overview

Among all the multi-rate access methods described in Section 1.3, the *fixed chip rate and variable processing gain* access strategy requires the lowest hardware complexity and appears to be the most promising approach towards implementing a multi-rate DS/CDMA radio interface. Consequently, this thesis focuses its attention on the fixed chip rate and variable processing gain access strategy. Using this access strategy, Chapter 2 models a dual-rate synchronous DS/CDMA system where in an interval of duration T, a low rate user transmits one bit while a high rate user transmits M bits. We show how the dual-rate system is equivalent to a single rate system in which each high rate user is modeled as M independent low rate users. For this equivalent low rate system, we derive the log-likelihood function of the optimum receiver. Several multi-user performance measures that are used in this thesis are discussed at the end of Chapter 2.

Chapter 3 addresses the use of decorrelating receivers for a synchronous dual-rate DS/CDMA system. Here we propose a receiver called the *low rate decorrelator* or *LRD* for the dual-rate CDMA system that is simply the standard decorrelator of [28] applied to an equivalent low rate system. The LRD yields an M bit processing delay for high rate users and a computational complexity that increases with M. The complexity of the LRD prompts consideration of a *high rate decorrelator* or *HRD*, in which during the bit interval of a high rate user, each low rate user is modeled as a high rate user. The HRD provides bit decisions for each high rate user in every subinterval of duration T/M. To decode a low rate user, it applies maximal ratio combining technique on M separate decorrelated outputs of each low rate user. It is found that HRD achieves a sizable reduction in complexity though suffering a penalty in terms of bit error probability or asymptotic efficiency. Both LRD and HRD preserve the standard decorrelator's near/far resistance property.

In Chapter 4, a signature assignment technique for a dual-rate DS/CDMA system is proposed. Based on this signature assignment technique, we develop a decorrelator called the *two stage decorrelator* or *2SD*. The 2SD generates bit decisions for each high rate user in every subinterval of duration T/M. In order to decode a low rate user, an orthogonal projection is applied to M separate decorrelated outputs of each low rate user. Similar to the HRD, the 2SD reduces the complexity of the LRD and suffers in terms of bit error rate. It is found that in several cases, the 2SD achieves the performance of the LRD. Furthermore, analyzing the 2SD yields a significant insight into the performance of the HRD.

Motivated by the decision feedback detector of [8], Chapter 5 proposes a bandwidth efficient decision feedback decorrelating detector for a dual-rate synchronous CDMA system. The proposed receiver is referred to as the *high rate decision feedback decorrelator* or *HRDF*. The HRDF provides the high rate bit decisions in every subinterval of duration T/M and the low rate bit decisions at the end of interval, T. Each bit is decoded by utilizing the decisions of all previously decoded users. We study the performance of the HRDF and compare that with the performance of the dual-rate decorrelators (LRD and HRD). By simulation, it is found that the HRDF outperforms the LRD and HRD and as the interferers grow stronger relative to the desired user, the performance of the HRDF for decoding the desired user approaches the single user bound.

Generalizing the synchronous dual-rate system model of Chapter 2, Chapter 6 considers an asynchronous multi-rate DS/CDMA system. For the asynchronous multi-rate DS/CDMA system, we develop a decentralized, truncated window decorrelator called the *asynchronous multi-rate decorrelator* or *AMD*. The AMD will decode bits of a user by employing a set of modified correlators whose signals are simply time shifted versions of one another. Due to the decentralization of our decorrelator, each user will be able to suppress the multiuser interference as long as that user has non-zero asymptotic efficiency [28, 29] over its observation window. Our decentralized model permits a simple proof that the performance of any truncated window decorrelator improves monotonically with the observation window length. It is well known that a longer observation window results in greater computational complexity. Therefore, in order to implement a truncated window decorrelator, a user should only extend the observation window over a reasonable number of bits. For a given observation window, we will derive upper and lower bounds on the performance of the infinite window decorrelator. These bounds, which follow naturally from the implementation of the AMD, are functions of the observation window length. The upper and lower bounds will permit performance comparisons of the proposed truncated window decorrelator with the infinite window decorrelator. In addition, by analyzing these bounds one can obtain significant insights into the performance of a truncated window decorrelator.

The varied Quality of Service (QoS) or bit error rate (BER) requirements of multimedia traffic need the use of power control for CDMA wireless systems employing multiuser detection. Using a decorrelator in a multi-rate DS/CDMA system, it is necessary for different users to combat the noise enhancement and the propagation losses to varying degrees depending on the individual QoS requirement. In this context, for a multi-rate decorrelator, Chapter 7 proposes a power control algorithm called the *target power* or *TP* algorithm. The proposed power control algorithm is suitable for a class of BER based link quality objectives. The criterion that is used for power control is to minimize the total transmitted power while at the same time guaranteeing each user's QoS requirement. If the uplink channel gain of the mobile is known then it is simple to provide each user its QoS objective. In practice, the measurement of the channel gain is non-trivial and neglects the stochastic behavior of the channel. This practical situation leads us to use stochastic approximation methods [44] to develop the TP algorithm. In the TP algorithm, a mobile needs to know only the output of its own decorrelator to update its transmitted power. We prove that when the TP algorithm is feasible, it converges in the mean square sense to an optimal power at which the desired user achieves its QoS requirement.

Most of the results of this thesis have been presented previously. Chapter 3 was presented in part in the IEEE Vehicular Technology Conference [54] and is also accepted for publication in Wireless Personal Communications [52]. The work in Chapter 4 was presented in the IEEE International Conference on Communications [46]. Parts of Chapter 5 were presented in the IEEE Global Telecommunications Conference [53] and the entire work in Chapter 5 will be published in Wireless Networks, special issue on "Multi-user Detection in Wireless Communications" [51]. The work in Chapter 6 was presented in part in the Conference on Information Science and Systems [49] and later submitted to the IEEE Transactions on Communications [47]. Chapter 7 was submitted recently to the IEEE Transactions on Communications [48] and has been presented as an invited paper at the Thirty-fifth Allerton Conference on Communication, Control and Computing [50].

Chapter 2

System Model

2.1 Introduction

For the fixed chip rate and variable processing gain access strategy, this chapter derives a dual-rate synchronous DS/CDMA system where in an interval of duration T_0, a low rate user transmits one bit while a high rate user transmits M bits; see Figure 2.1. This system model permits us to show a dual-rate system as a single rate system in which each high rate user is equivalent to M independent low rate users. For the equivalent single or low rate system, we obtain the log-likelihood function of the optimum receiver. Different multi-user performance measures that will be used in this thesis are addressed at the end of this chapter. Note that in Chapters 3 - 5, several multi-user receivers will be developed for this synchronous dual-rate system model. Furthermore, Chapter 6 will use this synchronous dual-rate system model to derive an asynchronous multi-rate DS/CDMA system.

2.2 Dual-rate Synchronous System Model

In our synchronous dual-rate DS/CDMA system model, each bit results in the baseband transmission of a sequence of pulses, or chips, $p[t]$, each pulse having a duration of one chip period T_c. These pulses are sent over an additive white Gaussian noise channel in which the noise $n(t)$ has power spectral density σ^2.

The users will be grouped by their bit rates. The transmission rate of group g users is denoted by R_g, where $g = 0, 1$ and $R_1 = MR_0$ for an integer $M > 1$. For the K_g group g users, the transmission time of a bit is $T_g = 1/R_g$ and the processing gain is

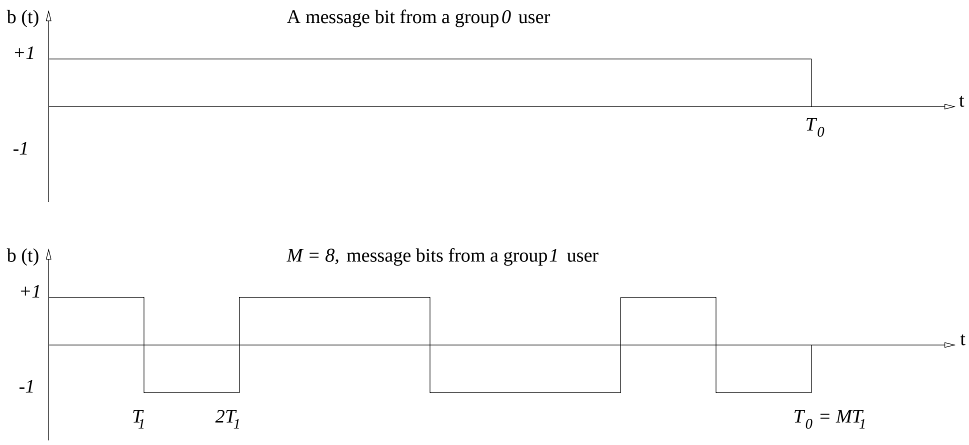

Figure 2.1: Messages from a user of each group in the time interval, $[0, T_0]$ are shown.

$L_g = T_g/T_c$. The signature waveform of the nth group g customer is

$$S_{n,g}(t) = \sum_{m=1}^{L_g} \{a_{n,g}(m) \frac{1}{\sqrt{L_g}} p[t - (m-1)T_c]\} \qquad t \in [0, T_g] \tag{2.1}$$

where $a_{n,g}(m) \in \{-1, 1\}$ denotes the signature sequence of user n of group g. The energy of the pulse $p[t]$ is normalized so that

$$\int_0^{T_g} [S_{n,g}(t)]^2 dt = 1 \qquad g = 0, 1; n = 1, \ldots, K_g \tag{2.2}$$

Note that a group 0 user has a signature waveform of duration T_0 while a group 1 user has a signature waveform of duration $T_1 = T_0/M$. In the interval $[0, T_0]$, each group 0 user transmits one bit while each group 1 user transmits M bits. The jth user from group 0 transmits bit $b_{j,0} \in \{-1, 1\}$ with received energy $E_{j,0}$ in the interval $[0, T_0]$. Similarly, the kth user from group 1 transmits its ith bit $b_{k,1}^{(i)} \in \{-1, 1\}$ with received energy $E_{k,1}^{(i)}$ in the ith subinterval $[(i-1)T_1, iT_1]$ using the signature waveform

$$S_{k,1}^{(i)}(t) = S_{k,1}(t - (i-1)T_1) \tag{2.3}$$

Over the interval $[0, T_0]$, the received baseband signal can be written as

$$r(t) = \sum_{j=1}^{K_0} \sqrt{E_{j,0}} b_{j,0} S_{j,0}(t) + \sum_{k=1}^{K_1} \left\{ \sum_{i=1}^{M} \sqrt{E_{k,1}^{(i)}} b_{k,1}^{(i)} S_{k,1}^{(i)}(t) \right\} + n(t) \tag{2.4}$$

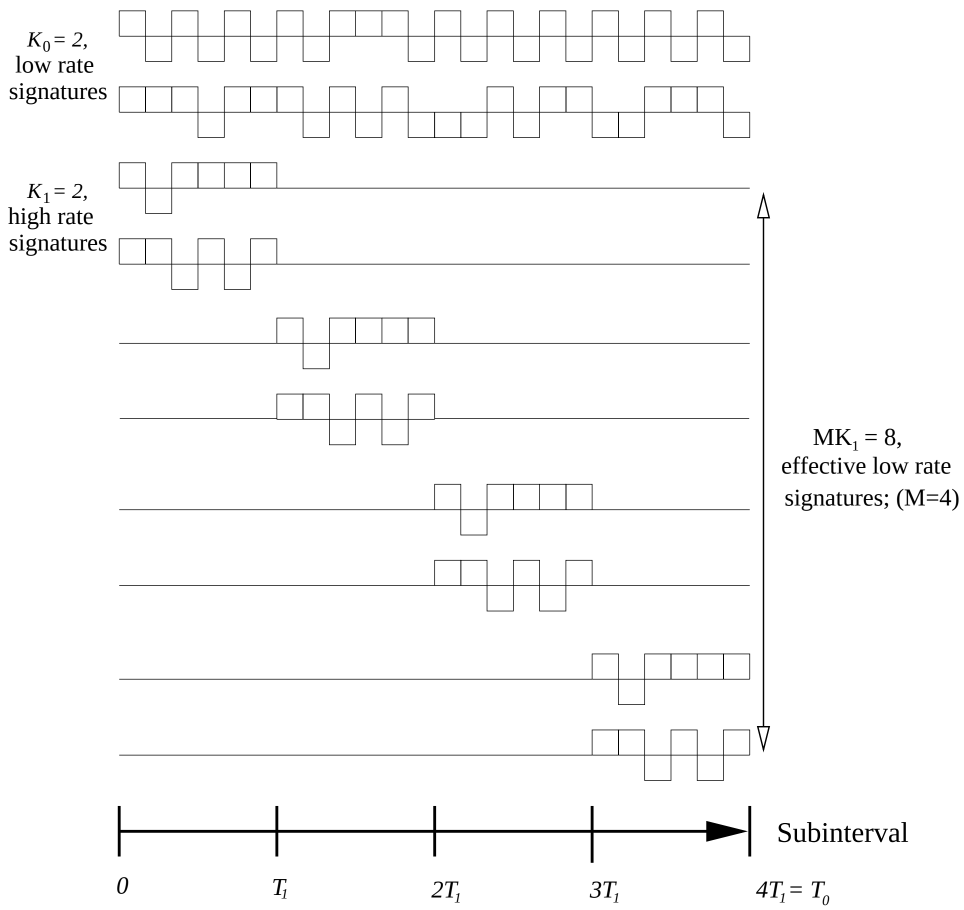

Figure 2.2: The figure depicts the $K_0 + MK_1$ signatures of the effective group 0 users for the interval $[0, T_0]$.

The $K = K_0 + MK_1$ bits transmitted in the interval $[0, T_0]$ can be written as the K bit vector $b = [b_1, b_2, \ldots, b_K]^\top$ where

$$b = [\overbrace{\underbrace{b_{1,0}, \ldots, b_{K_0,0}}_{\text{in } [0,T_0]}}^{\text{group 0 users}}, \overbrace{\underbrace{b_{1,1}^{(1)}, \ldots, b_{K_1,1}^{(1)}}_{\text{in } [0,T_1]}, \ldots \quad \ldots, \underbrace{b_{1,1}^{(M)}, \ldots, b_{K_1,1}^{(M)}}_{\text{in } [(M-1)T_1, MT_1]}}^{\text{group 1 users}}]^\top \tag{2.5}$$

This ordering defines an equivalent low rate system in which $K_0 + MK_1$ bits are transmitted in $[0, T_0]$. In the other words, a dual-rate system with K_0 low rate users and K_1 high rate users is equivalent to a single rate system of $K_0 + MK_1$ low rate users.

The bit of a group 1 user in the ith subinterval is transmitted using a short signature that is non-zero only in the ith subinterval. A depiction of this representation is provided in Figure 2.2. Note that for $n \leq K_0$, the bit b_n was transmitted by user n of group 0. Furthermore, examination of the above ordering will show that we can define functions $k_1(n)$ and $i_1(n)$ such that given $n > K_0$, we can identify that a group 1 user $k = k_1(n)$ transmitted bit b_n during subinterval $i = i_1(n)$. For the vector $b = [b_1, \ldots, b_K]^\top$, the bit b_n is transmitted with energy E_n using the signature waveform $s_n(t)$ where

$$s_n(t) = \begin{cases} S_{n,0}(t) & 1 \leq n \leq K_0 \\ S_{k_1(n),1}^{i_1(n)}(t) & n > K_0 \end{cases} \tag{2.6}$$

$$\sqrt{E_n} = \begin{cases} \sqrt{E_{n,0}} & 1 \leq n \leq K_0 \\ \sqrt{E_{k_1(n),1}^{i_1(n)}} & n > K_0 \end{cases} \tag{2.7}$$

In terms of the vector b, the received signal $r(t)$ from equation (2.4) can be written as

$$r(t) = \sum_{n=1}^{K} b_n \sqrt{E_n} s_n(t) + n(t) = S(t, b) + n(t) \tag{2.8}$$

2.3 Optimum Detection

Equation (2.8) is a representation of the dual rate system as an equivalent single rate system with $K = K_0 + K_1$ users. In the dual rate system, the optimum or maximum likelihood decision on b which maximizes the log-likelihood function [40, 59] is

$$b^* = \arg\left\{ \max_{b \in \{-1,1\}^K} \left[2\int_0^{T_0} r(t) S(t, b)\, dt - \int_0^{T_0} S^2(t, b)\, dt \right] \right\} \tag{2.9}$$

The sampled output of a bank of correlators for the signature waveforms $s_n(t)$ is the vector $r = [r_1, r_2, \ldots, r_K]^\top$ of sufficient statistics with

$$r_n = \int_0^{T_0} r(t) s_n(t)\, dt \qquad n = 1, \ldots, K \tag{2.10}$$

As a vector, r can be written as

$$r = \Gamma \Lambda b + N \tag{2.11}$$

where Λ is a diagonal matrix with $\Lambda_{n,n} = \sqrt{E_n}$ and Γ is the $K \times K$ cross-correlation matrix with (j, k)th element

$$[\Gamma]_{j,k} = \int_0^{T_0} s_j(t) s_k(t)\, dt \tag{2.12}$$

As in the single rate system [66], the optimum decisions can be written for the dual-rate system as

$$b^* = \arg \max_{b \in \{-1,1\}^K} \left[2r^\top \Lambda b - b^\top \Lambda \Gamma \Lambda b \right] \tag{2.13}$$

Similar to the single rate DS/CDMA system, the maximum likelihood receiver for the dual-rate DS/CDMA system is an NP-hard problem [64]. Thus, this thesis will explore the use of sub-optimum receivers for multi-rate DS/CDMA systems.

In the following section, we will discuss the performance measures which will be used in this thesis to analyze the performance of the proposed multi-rate multi-user detectors.

2.4 Performance Measures

In practice, the main performance measure of interest is the probability of bit error or bit error rate (BER). However, in several cases, such as for the matched filter and MMSE receivers, the bit error rate is hard to compute and analyze. In this situation, signal-to-interference ratio (SIR) can be used as an alternative performance measure. In the multi-user detection, several other performance measures, such as the *asymptotic efficiency* and the *near-far resistance* [28, 29, 65] are found useful. These performance measures are derived from the bit error rate of the multi-user detector.

Let us assume that under a multiuser detector, the bit error rate of user n of equation (2.8) is $q_n(\sigma)$. If $e_n(\sigma)$ denotes the energy that yields the same bit error rate $q_n(\sigma)$ in a single-user Gaussian channel with power spectral density σ^2, then the *asymptotic efficiency* [28, 29] of that multiuser detector for the nth user can be written as

$$\zeta_n = \lim_{\sigma \to 0} \frac{e_n(\sigma)}{E_n} \tag{2.14}$$

To quantify the robustness of a multi-user detector against the near-far problem, references [28, 29] derive another performance measure called the *near-far resistance.* The near-far resistance is the worst-case asymptotic efficiency over all interfering received energies. Using equation (2.14), we can write the near-far resistance of a multi-user receiver as

$$\bar{\zeta}_n = \inf_{\substack{E_j > 0 \\ j \neq n}} \zeta_n \tag{2.15}$$

Note that if the number of users in the system is one, or, if the signature of user n is orthogonal to the interfering signatures, then, for the conventional receiver, $\bar{\zeta}_n = 1$, otherwise, $\bar{\zeta}_n = 0$.

Chapter 3

Decorrelating Detectors for a Dual-rate Synchronous DS/CDMA System

3.1 Introduction

In this chapter, we investigate the decorrelating receiver structures for a dual rate synchronous DS/CDMA system. First we specify a receiver called the low rate decorrelator (LRD) for the dual-rate CDMA system that is simply the standard decorrelator of [28] applied to the equivalent low rate system. Applying the LRD to the interval of duration T_0 yields an M bit processing delay for high rate users and a computational complexity that grows with M. The complexity of the LRD leads us to consider a high rate decorrelator (HRD), in which during the bit interval of a high rate user, each low rate user is modeled as a high rate user. It provides bit decisions for each high rate user in every subinterval of duration T_0/M. To decode a low rate user, a soft decoding rule is used with M separate decorrelated outputs of each low rate user. We prove that the bit error rate of the standard decorrelator (LRD) is less than or equal to that of the soft decoding decorrelator (HRD). By evaluation, we show that for a small CDMA system where the signature sequences have good correlation properties, the HRD will perform nearly as well as the LRD. However, when the signature sequences have high correlations, then the LRD significantly outperforms the HRD.

We have seen that equation (2.8) is a representation of the received signal in the dual-rate system that is equivalent to a single rate system with $K = K_0 + MK_1$ group 0 users each transmitting 1 bit during $[0, T_0]$. In the next section, we use this representation to describe the working principle of the LRD.

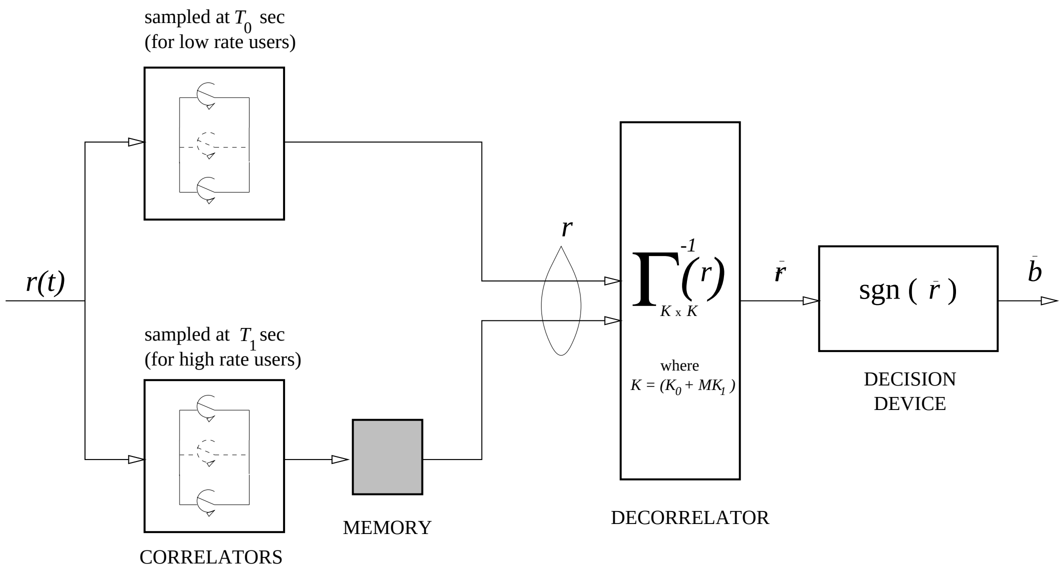

Figure 3.1: This is the block diagram of the low rate decorrelator or LRD.

3.2 The Low Rate Decorrelator, LRD

In a single rate CDMA system, the bit duration of each user is the same and the correlator outputs are sampled at every bit interval. The vector of decision statistics is then obtained after decorrelating the sampled outputs with the correlation matrix of signature waveforms. Finally, all users are decoded simultaneously. We can use the low rate representation of the dual-rate CDMA system to develop an equivalent decorrelator. In equation (2.11), each group 1 user has been replaced by M effective group 0 users with signature waveforms that are simply time shifted versions of one another. Further, each of these waveforms is non-zero in only one of the M sub-intervals corresponding to the appropriate group 1 users' bits; see Figure 2.2.

From equation (2.11), we decorrelate r by applying the transformation Γ^{-1} to yield

$$\bar{r} = \Gamma^{-1} r = \Lambda b + \bar{N} \tag{3.1}$$

where $\bar{N}$ is a zero mean Gaussian vector with the covariance matrix $\sigma^2 \Gamma^{-1}$. The decoding rule of the decorrelator is simply

$$\bar{b} = \mathrm{sgn}[\bar{r}] = \mathrm{sgn}\left[\Lambda b + \bar{N}\right] \tag{3.2}$$

The working principle of the LRD is presented in Figures 3.1 and 3.2. Since $\bar{N}_j$ has variance $\sigma^2 \left[\Gamma^{-1}\right]_{j,j}$, the probability that the jth input is decoded incorrectly can be

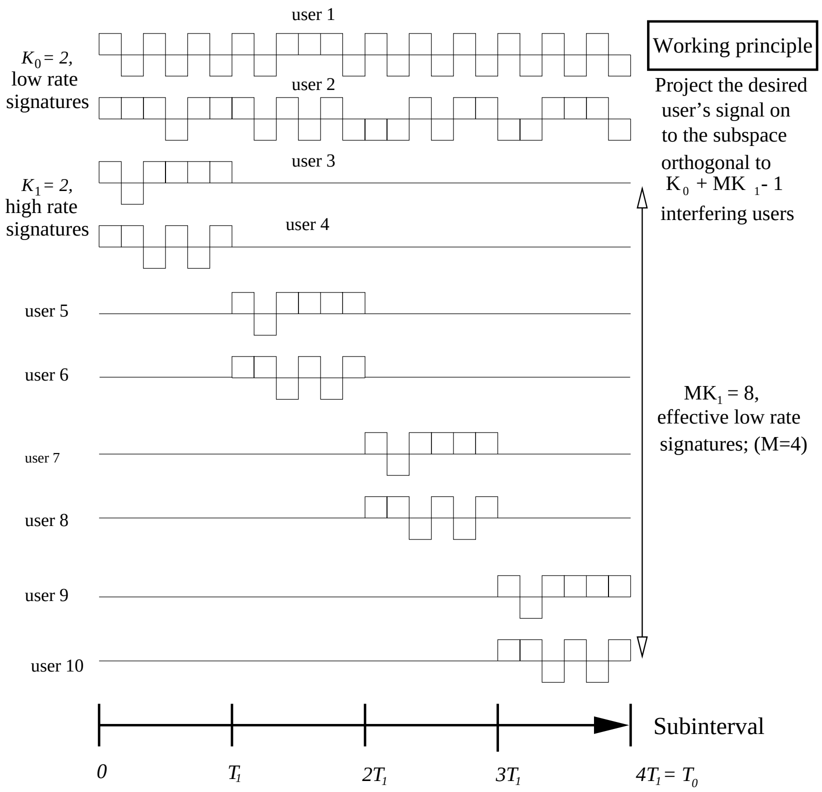

Figure 3.2: The figure depicts the working principle of the LRD for $K_0 = K_1 = 2$.

written as

$$q_j = Q\left[\sqrt{\frac{E_j}{\sigma^2\left[\Gamma^{-1}\right]_{j,j}}}\right] \tag{3.3}$$

where $Q[\cdot]$ denotes the standard normal complementary CDF. Using equation (2.14), the asymptotic efficiency of the LRD for the jth user can be written as

$$[\zeta_j]^L = 1/\left[\Gamma^{-1}\right]_{j,j} \tag{3.4}$$

If in the LRD system, $[\zeta_{n,0}]^L$ denotes the asymptotic efficiency for the nth group 0 user while $[\zeta_{k_1[n],1}^{(i_1[n])}]^L$ is the asymptotic efficiency for the ith bit of the nth group 1 user, then equation (3.4) becomes

$$[\zeta_n]^L = \begin{cases} [\zeta_{n,0}]^L & 1 \le n \le K_0 \\ \left[\zeta_{k_1[n],1}^{(i_1[n])}\right]^L & n > K_0 \end{cases} \tag{3.5}$$

Note that a standard decorrelator for a single rate system of $K = K_0 + MK_1$ users requires K correlators. By comparison, since the low rate decorrelator generates M

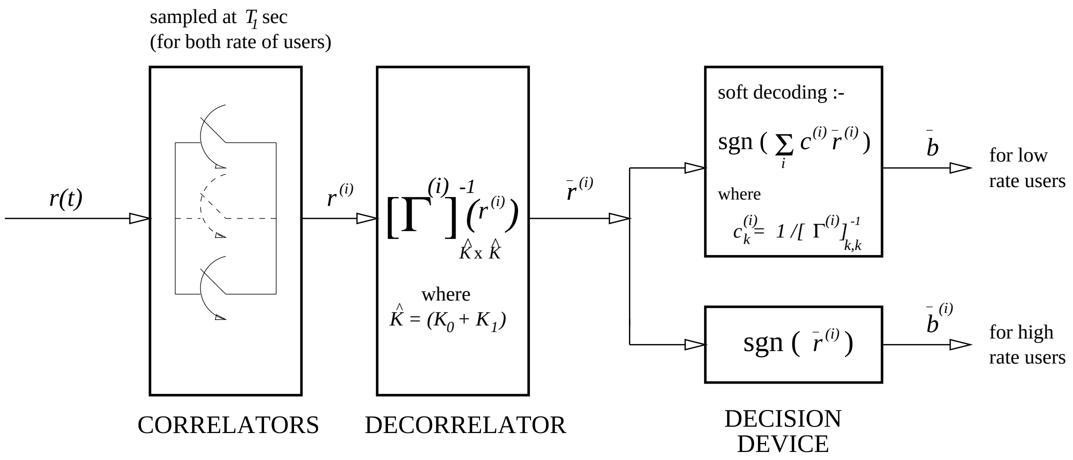

Figure 3.3: This is the block diagram of the high rate decorrelating detector or HRD.

effective group 0 users for each group 1 signature sequence, it requires only $K_0 + K_1$ correlators. However, the low rate decorrelator has certain disadvantages. First, the low rate decorrelator still requires inversion of the $K \times K$ matrix Γ. Although we will see that Γ has a sparse structure that makes computation of Γ^{-1} reasonably easy, the complexity of the low rate decorrelator grows with M. Second, for each high rate group 1 user, the M sampled correlator outputs in $[0, T_0]$ are stored and decoded simultaneously at time T_0 incurring an M bit processing delay; see Figure 3.1.

3.3 The High Rate Decorrelator, HRD

In this section, we describe a decorrelator in which decisions for the high rate users of group 1 are made every $T_1 = T_0/M$ units of time. In every subinterval $[(i-1)T_1, iT_1]$, there are K_1 group 1 users and K_0 group 0 users transmitting. Each high rate group 1 user k transmits one bit using the signature waveform $S_{k,1}(t)$. Each low rate group 0 user j transmits the ith segment of the signature waveform $S_{j,0}(t)$ denoted by

$$S_{j,0}^{(i)}(t) = \sum_{m=(i-1)L_1+1}^{iL_1} \left\{ a_{j,0}(m) \frac{1}{\sqrt{L_0}} p[t-(m-1)T_c] \right\} \tag{3.6}$$

At the receiver, the correlator outputs are sampled at the end of every subinterval of length T_1.

The high rate decorrelator, as shown in Figure 3.3, views the $K_0 + K_1$ transmitters as though they were $K_0 + K_1$ group 1 users each transmitting one bit in each subinterval;

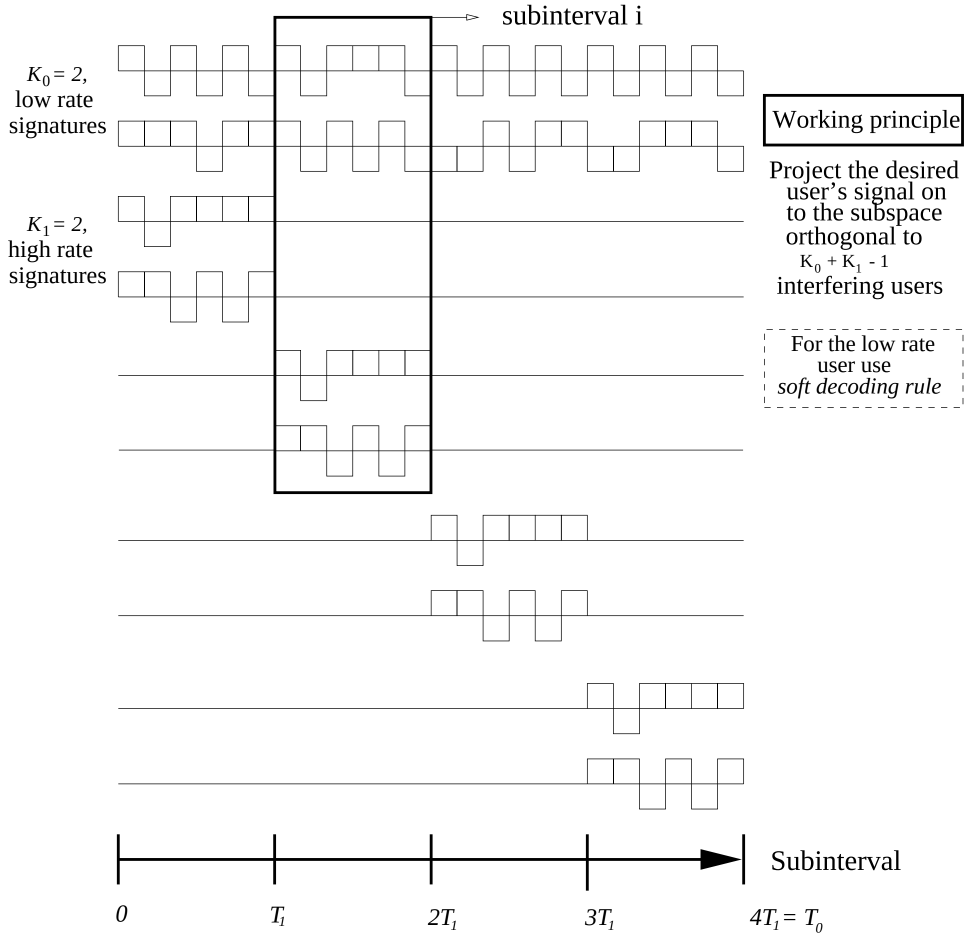

Figure 3.4: The figure depicts the working principle of the HRD for $K_0 = K_1 = 2$.

see also Figure 3.4. We enumerate these transmitting users such that the jth group 0 user is numbered j, $1 \leq j \leq K_0$, while the kth high rate user is numbered $(K_0 + k)$. For subinterval i, the input vector is $\hat{b}^{(i)} = \left[\hat{b}_1^{(i)}, \ldots, \hat{b}_{K_0}^{(i)}, \hat{b}_{(K_0+1)}^{(i)}, \ldots, \hat{b}_{K_0+K_1}^{(i)}\right]^\top$. The bit $\hat{b}_n^{(i)}$ is transmitted using the signature waveform

$$\hat{s}_n^{(i)}(t) = \begin{cases} S_{n,0}^{(i)}(t - (i-1)T_1) & 1 \leq n \leq K_0 \\ S_{n-K_0,1}(t) & K_0 < n \leq K_0 + K_1 \end{cases} \tag{3.7}$$

Note that for all i and n, $\hat{s}_n^{(i)}(t)$ is defined as a signature of duration T_1 on the interval $[0, T_1]$. In each subinterval i, each group 1 user k transmits with energy $E_{k,1}^{(i)}$; however, each group 0 user j transmits with a fraction of its total transmitted energy per bit. Since the signature waveform $S_{j,0}(t)$ is normalized to have unit energy over the interval $[0, T_0]$, the fraction of the bit energy that group 0 user j transmits in subinterval i is

$\int_{(i-1)T_1}^{iT_1} [S_{j,0}(t)]^2 dt = 1/M$.

The vector of correlator output samples at time iT_1 is

$$r^{(i)} = \Gamma^{(i)} \Lambda^{(i)} \hat{b}^{(i)} + N^{(i)} \tag{3.8}$$

where $\Gamma^{(i)}$ is the $(K_0 + K_1) \times (K_0 + K_1)$ cross-correlation matrix with j, kth element

$$\left[\Gamma^{(i)}\right]_{j,k} = \int_0^{T_1} \hat{s}_j^{(i)}(t) \hat{s}_k^{(i)}(t)\, dt \tag{3.9}$$

Furthermore, $\Lambda^{(i)}$ is a diagonal matrix with

$$\Lambda_{n,n}^{(i)} = \begin{cases} \sqrt{E_{n,0}} & 1 \le n \le K_0 \\ \sqrt{E_{n-K_0,1}^{(i)}} & K_0 < n \le K_0 + K_1 \end{cases} \tag{3.10}$$

and $N^{(i)}$ is a $K_0 + K_1$ element Gaussian noise vector with covariance matrix $\Gamma^{(i)}$. In order to recover the vector $\hat{b}^{(i)}$, we decorrelate $r^{(i)}$ using the cross-correlation matrix $\Gamma^{(i)}$. Specifically,

$$\bar{r}^{(i)} = \left[\Gamma^{(i)}\right]^{-1} r^{(i)} = \Lambda^{(i)} \hat{b}^{(i)} + \bar{N}^{(i)} \tag{3.11}$$

where $\bar{N}^{(i)}$ is a zero mean Gaussian noise vector with covariance matrix $\sigma^2 \left[\Gamma^{(i)}\right]^{-1}$.

Using equation (3.11), the decoding rule in subinterval i for a group 1 user $k = n - K_0 \ge 1$ is

$$\bar{b}_{k,1}^{(i)} = \operatorname{sgn}\left[\bar{r}_n^{(i)}\right] = \operatorname{sgn}\left[\Lambda_{n,n}^{(i)} \hat{b}_n^{(i)} + \bar{N}_n^{(i)}\right] \qquad K_0 < n \le K_0 + K_1 \tag{3.12}$$

The probability that a group 1 user k is decoded incorrectly in the ith subinterval equals the probability that bit $b_{k,1}^{(i)}$ is received in error which equals

$$\hat{q}_{k,1}^{(i)} = Q\left[\sqrt{\frac{E_{k,1}^{(i)}}{\sigma^2 \left[\Gamma^{(i)}\right]_{k+K_0,k+K_0}^{-1}}}\right] \tag{3.13}$$

and the asymptotic efficiency is

$$\left[\zeta_{k,1}^{(i)}\right]^H = 1/\left[\Gamma^{(i)}\right]_{k+K_0,k+K_0}^{-1} \tag{3.14}$$

For a group 0 user j, we obtain the decorrelated outputs

$$\bar{r}_j^{(i)} = \Lambda_{j,j}^{(i)} \hat{b}_j^{(i)} + \bar{N}_j^{(i)} = \sqrt{E_{j,0}}\, b_{j,0} + \bar{N}_j^{(i)} \qquad 1 \le j \le K_0 \tag{3.15}$$

To decode a group 0 user j, *maximal ratio combining* [3, 27] is used to combine the outputs of the M subintervals. Specifically, we implement the following *soft decoding* rule:

$$\bar{b}_{j,0} \quad = \quad \mathrm{sgn}\left[\sum_{i=1}^{M}\left(\frac{E_{j,0}}{\left[\Gamma^{(i)}\right]_{j,j}^{-1}}\right)\bar{r}_j^{(i)}\right] \qquad 1 \le j \le K_0 \tag{3.16}$$

From equation (3.16), we see that the soft decoding rule can be simplified to

$$\bar{b}_{j,0} \quad = \quad \mathrm{sgn}\left[\sum_{i=1}^{M}\left(\frac{1}{\left[\Gamma^{(i)}\right]_{j,j}^{-1}}\right)\bar{r}_j^{(i)}\right] \qquad 1 \le j \le K_0 \tag{3.17}$$

We see that in equation (3.17), the soft decoding rule does not require knowledge of the energies $E_{j,0}$ of the group 0 users. Under the soft decoding rule, the probability that the jth group 0 user is decoded incorrectly is

$$\hat{q}_{j,0} = Q\left[\sqrt{\frac{E_{j,0}}{\sigma^2}\sum_{i=1}^{M}\left(\frac{1}{\left[\Gamma^{(i)}\right]_{j,j}^{-1}}\right)}\right] \qquad 1 \le j \le K_0 \tag{3.18}$$

The corresponding asymptotic efficiency of the jth low rate user under the HRD is

$$[\zeta_{j,0}]^H \quad = \quad \sum_{i=1}^{M}\frac{1}{\left[\Gamma^{(i)}\right]_{j,j}^{-1}} \tag{3.19}$$

3.4 A Comparison of LRD and HRD

The performance of the low rate and high rate decorrelators is not the same simply because cross-correlation matrices are different in structure. Characterizing the performance differences between the low rate and high rate decorrelators requires study of the structure of the respective inverse correlation matrices.

3.4.1 The Low Rate Decorrelator

First, we identify the sparse structure of the low rate correlation matrix Γ. From equation (2.5), we can write the vector b of transmitted bits as

$$b^\top = \left[[\tilde{b}^{(0)}]^\top, [\tilde{b}^{(1)}]^\top, \ldots, [\tilde{b}^{(M)}]^\top\right] \tag{3.20}$$

where $\tilde{b}^{(0)}$ is the vector of bits transmitted by group 0 users over $[0, T_0]$ and $\tilde{b}^{(i)}$ is the vector of bits transmitted by group 1 users in subinterval i. Similarly, let $\tilde{s}^{(i)}(t)$ denote the vector of signature waveforms used to transmit the bit vector $\tilde{b}^{(i)}$. Note that each component of $\tilde{s}^{(0)}(t)$, is a signature of duration T_0. From equation (2.1), we can write

$$\tilde{s}^{(0)}(t) = [S_{1,0}(t), \cdots, S_{K_0,0}(t)] \tag{3.21}$$

For $i > 0$, each component of $\tilde{s}^{(i)}(t)$ is a signature that is nonzero only on the ith subinterval. In particular,

$$\tilde{s}^{(i)}(t) = \left[S_{1,1}^{(i)}(t), \cdots, S_{K_1,1}^{(i)}(t)\right] \qquad (i > 0) \tag{3.22}$$

Since each group 1 user applies the same signature in each subinterval,

$$\tilde{s}^{(i+1)}(t) = \tilde{s}^{(i)}(t - T_1) \qquad i \geq 1 \tag{3.23}$$

The LRD cross-correlation matrix Γ will be denoted by $\Gamma = \Gamma_M$ where for $k = 0, \ldots, M$, Γ_k is the block matrix

$$\Gamma_k = \begin{pmatrix} \Gamma_{00} & \Gamma_{01} & \Gamma_{02} & \cdots & \Gamma_{0k} \\ \Gamma_{10} & \Gamma_{11} & 0 & \cdots & 0 \\ \Gamma_{20} & 0 & \Gamma_{22} & & \vdots \\ \vdots & \vdots & & \ddots & 0 \\ \Gamma_{k0} & 0 & \cdots & 0 & \Gamma_{kk} \end{pmatrix} \tag{3.24}$$

Note that Γ_{ij} is the cross-correlation matrix generated from the signature vectors $\tilde{s}^{(i)}(t)$ and $\tilde{s}^{(j)}(t)$. That is, element m, n of Γ_{ij} is

$$[\Gamma_{ij}]_{m,n} = \int_0^{T_0} \tilde{s}_m^{(i)}(t)\tilde{s}_n^{(j)}(t)\, dt \tag{3.25}$$

As expected, $\Gamma_{ij} = \Gamma_{ji}^\top$. In addition, since the high rate users have the same signature in each subinterval, $\Gamma_{ii} = \Gamma_{kk}$ for all $i, k > 1$. The sparse structure of Γ arises because for $i, j > 0$ and $i \neq j$, the signature vector $\tilde{s}^{(i)}(t)$ is nonzero only in subinterval i while $\tilde{s}^{(j)}(t)$ is nonzero over the subinterval j. The inverse of Γ_k can be written in a corresponding block form:

$$\Gamma_k^{-1} = \begin{pmatrix} B_{00}^{(k)} & \cdots & B_{0M}^{(k)} \\ \vdots & \ddots & \vdots \\ B_{M0}^{(k)} & \cdots & B_{MM}^{(k)} \end{pmatrix} \tag{3.26}$$

The matrix elements of Γ_k^{-1} satisfy $B_{ij}^{(k)} = \left[B_{ji}^{(k)}\right]^\top$ and also the matrix equations

$$
\begin{aligned}
B_{00}^{(k)} &= \left(\Gamma_{00} - \sum_{i=1}^{k} \Gamma_{0i}\Gamma_{ii}^{-1}\Gamma_{i0}\right)^{-1} && (3.27)\\
B_{0i}^{(k)} &= -B_{00}^{(k)}\Gamma_{0i}\Gamma_{ii}^{-1} \qquad i > 0 && (3.28)\\
B_{ij}^{(k)} &= \Gamma_{ii}^{-1}\Gamma_{i0}B_{00}^{(k)}\Gamma_{0j}\Gamma_{jj}^{-1} \qquad i,j > 0, i \neq j && (3.29)\\
B_{ii}^{(k)} &= \Gamma_{ii}^{-1} + \Gamma_{ii}^{-1}\Gamma_{i0}B_{00}^{(k)}\Gamma_{0i}\Gamma_{ii}^{-1} \qquad i > 0 && (3.30)
\end{aligned}
$$

3.4.2 The High Rate Decorrelator

For the high rate decorrelator, we can view each group 0 user j as transmitting the same bit $b_{j,0}$ in each subinterval i using the signature $\hat{s}_j^{(i)}(t)$ which we recall is the segment of its actual signature $S_{j,0}(t)$ that occurs in subinterval i. Each group 1 user k transmits bit $b_{k,1}^{(i)}$ in subinterval i using the signature $S_{k,1}(t) = \hat{s}_{K_0+k}^{(i)}(t)$. Alternatively, we can view the group 0 users as transmitting a repetition of the vector $\tilde{b}^{(0)}$ while the group 1 users are transmitting $\tilde{b}^i$. The correlation matrix $\Gamma^{(i)}$ for the ith subinterval reflects the interaction of group 0 and group 1 users and can be written as

$$
\Gamma^{(i)} = \begin{pmatrix} \Gamma_{00}^{(i)} & \Gamma_{0i} \\ \Gamma_{i0} & \Gamma_{ii} \end{pmatrix} \tag{3.31}
$$

Note that Γ_{0i}, Γ_{i0} and Γ_{ii} are the same as in equations (3.24) and (3.25) for the low rate cross correlation matrix Γ. However, $\Gamma_{00}^{(i)} \neq \Gamma_{00}$ since $\Gamma_{00}^{(i)}$ represents the cross correlations of the group 0 users just in the ith subinterval while Γ_{00} describes the cross correlations of the group 0 users over $[0, T_0]$. For $\Gamma_{00}^{(i)}$, element m, n is

$$
\left[\Gamma_{00}^{(i)}\right]_{m,n} = \int_0^{T_1} S_{m,0}^{(i)}(t-(i-1)T_1)S_{n,0}^{(i)}(t-(i-1)T_1)\,dt \tag{3.32}
$$

We will repeatedly use the property that an invertible 2×2 block matrix has an inverse of the form

$$
\begin{pmatrix} A & B \\ C & D \end{pmatrix}^{-1} = \begin{pmatrix} (A-BD^{-1}C)^{-1} & -(A-BD^{-1}C)^{-1}BD^{-1} \\ -(D-CA^{-1}B)^{-1}CA^{-1} & (D-CA^{-1}B)^{-1} \end{pmatrix} \tag{3.33}
$$

Thus, by defining $L^{(i)}$ and $H^{(i)}$ as

$$
L^{(i)} = \left(\Gamma_{00}^{(i)} - \Gamma_{0i}\Gamma_{ii}^{-1}\Gamma_{i0}\right)^{-1} \qquad H^{(i)} = \left(\Gamma_{ii} - \Gamma_{i0}\left[\Gamma_{00}^{(i)}\right]^{-1}\Gamma_{0i}\right)^{-1} \tag{3.34}
$$

the inverse of the correlation matrix $\Gamma^{(i)}$ can be written as

$$\left[\Gamma^{(i)}\right]^{-1} = \begin{pmatrix} L^{(i)} & -L^{(i)}\Gamma_{0i}\Gamma_{ii}^{-1} \\ -H^{(i)}\Gamma_{i0}\left[\Gamma_{00}^{(i)}\right]^{-1} & H^{(i)} \end{pmatrix} \tag{3.35}$$

Using equations (3.26),(3.27) and (3.34), we will establish the following results.

Theorem 1 *For the group 0 user, the asymptotic efficiency of the LRD is greater than or equal to that of the HRD. Equality holds when the cross-correlation matrix of the HRD is the same in every subinterval i.*

Proof: For the LRD, the asymptotic efficiency of the jth group 0 user is

$$[\zeta_{j,0}]^L = \frac{1}{[\Gamma^{-1}]_{j,j}} = \frac{1}{\left[B_{00}^{(M)}\right]_{j,j}} \tag{3.36}$$

As $B_{00}^{(M)}$ is the upper left sub-matrix of the positive definite matrix Γ^{-1}, therefore, $B_{00}^{(M)}$ is also a positive definite matrix. In [28, Proposition 1], it is shown that when $B_{00}^{(M)}$ is a positive definite cross-correlation matrix with 1's on the diagonal, then $\frac{1}{\left[B_{00}^{(M)}\right]_{j,j}}$ can be expressed as a constrained minimization of the form

$$\frac{1}{\left[B_{00}^{(M)}\right]_{j,j}} = \min_{\substack{\vartheta\in R^{K_0} \\ \vartheta_j=1}} \vartheta^\top \left[B_{00}^{(M)}\right]^{-1} \vartheta \tag{3.37}$$

We have observed that this result holds for any positive definite matrix $B_{00}^{(M)}$. Therefore, we will write equation (3.36) as

$$[\zeta_{j,0}]^L = \min_{\substack{\vartheta\in R^{K_0} \\ \vartheta_j=1}} \vartheta^\top \left[B_{00}^{(M)}\right]^{-1} \vartheta \tag{3.38}$$

Since $\Gamma_{00} = \sum_{i=1}^{M} \Gamma_{00}^{(i)}$, equation (3.27) permits us to write

$$\left[B_{00}^{(M)}\right]^{-1} = \sum_{i=1}^{M} \left(\Gamma_{00}^{(i)} - \Gamma_{0i}\Gamma_{ii}^{-1}\Gamma_{i0}\right) = \sum_{i=1}^{M} \left[L^{(i)}\right]^{-1} \tag{3.39}$$

Suppose ϑ_o minimizes the objective function of equation (3.38), then equation (3.38) can be written as

$$\begin{aligned}[\zeta_{j,0}]^L &= \sum_{i=1}^{M}\left(\vartheta_o^\top\left[L^{(i)}\right]^{-1}\vartheta_o\right) && (3.40)\\ &\geq \sum_{i=1}^{M}\min_{\substack{\nu^{(i)}\in R^{K_0}\\ \nu_j^{(i)}=1}}\left(\left[\nu^{(i)}\right]^\top\left[L^{(i)}\right]^{-1}\nu^{(i)}\right) && (3.41)\\ &= \sum_{i=1}^{M}\frac{1}{\left[L^{(i)}\right]_{j,j}} && (3.42)\end{aligned}$$

From equation (3.35), we see that for $1 \leq j \leq K_0$, $\left[L^{(i)}\right]_{jj} = \left[\Gamma^{(i)}\right]_{jj}^{-1}$. Thus, by equation (3.19),

$$[\zeta_{j,0}]^L \geq \sum_{i=1}^{M}\frac{1}{\left[\Gamma^{(i)}\right]_{j,j}^{-1}} = [\zeta_{j,0}]^H \tag{3.43}$$

When the cross-correlation matrix of the HRD is the same for all i, then $L^{(i)} = L$, for all i, and the inequality (3.41) becomes an equality and $[\zeta_{j,0}]^L = [\zeta_{j,0}]^H$. □

Theorem 2 *For the group 1 user, the asymptotic efficiency of the LRD is greater than or equal to that of the HRD.*

Proof: To simplify the analysis, we will prove the above result for the Mth subinterval. We observe that our proof can be extended for any subinterval i.

Similar to equation (3.36), the asymptotic efficiency of the LRD for decoding the Mth transmitted bit of the nth group 1 customer is

$$\left[\zeta_{k_1[n],1}^{(M_1[n])}\right]^L = \frac{1}{\left[B_{MM}^{(M)}\right]_{n,n}} = \min_{\substack{\vartheta\in R^{K_1}\\ \vartheta_n=1}}\vartheta^\top\left[B_{MM}^{(M)}\right]^{-1}\vartheta \tag{3.44}$$

From equation (3.24), we can write the LRD cross correlation matrix $\Gamma = \Gamma_M$ in the 2×2 block form

$$\Gamma_M = \begin{pmatrix}\Gamma_{M-1} & \bar{\Gamma}\\ \bar{\Gamma}^\top & \Gamma_{MM}\end{pmatrix} \tag{3.45}$$

where $\bar{\Gamma}^\top = [\Gamma_{M0}, 0, \ldots, 0]$. By equations (3.26) and (3.33),

$$B_{MM}^{(M)} = \left(\Gamma_{MM} - \bar{\Gamma}^\top\Gamma_{M-1}^{-1}\bar{\Gamma}\right)^{-1} \tag{3.46}$$

Equations (3.26) and (3.27) imply

$$\bar{\Gamma}^\top \Gamma_{M-1}^{-1} \bar{\Gamma} = \Gamma_{M0} B_{00}^{(M-1)} \Gamma_{0M} = \Gamma_{M0} \left(\Gamma_{00} - \sum_{j=1}^{M-1} \Gamma_{0j} \Gamma_{jj}^{-1} \Gamma_{j0} \right)^{-1} \Gamma_{0M} \tag{3.47}$$

Since $\Gamma_{00} = \sum_{j=1}^{M} \Gamma_{00}^{(j)}$, combining equations (3.46) and (3.47) yields

$$\left[B_{MM}^{(M)}\right]^{-1} = \Gamma_{MM} - \Gamma_{M0} \left(\Gamma_{00}^{(M)} + \sum_{j=1}^{M-1} \left(\Gamma_{00}^{(j)} - \Gamma_{0j} \Gamma_{jj}^{-1} \Gamma_{j0} \right) \right)^{-1} \Gamma_{0M} \tag{3.48}$$

The HRD cross-correlation matrix $\Gamma^{(i)}$ is assumed to be a positive definite matrix; hence, the upper left sub-matrix of $\left[\Gamma^{(i)}\right]^{-1}$ or $L^{(i)}$ is also a positive definite matrix. By defining

$$\Upsilon = \sum_{j=1}^{M-1} \left(\Gamma_{00}^{(j)} - \Gamma_{0j} \Gamma_{jj}^{-1} \Gamma_{j0} \right) \tag{3.49}$$

$$A = \left(\Gamma_{00}^{(M)} \Upsilon^{-1} \Gamma_{00}^{(M)} + \Gamma_{00}^{(M)} \right)^{-1} \tag{3.50}$$

we can claim that A is also a positive definite matrix. Some algebra [24, page 656] will verify that

$$\left[B_{MM}^{(M)}\right]^{-1} = \Gamma_{MM} - \Gamma_{M0} \left(\left[\Gamma_{00}^{(M)}\right]^{-1} - A \right) \Gamma_{0M} \tag{3.51}$$

Using ϑ_o to denote the vector which minimizes the objective function of equation (3.44), equation (3.51) implies

$$\left[\zeta_{k_1[n],1}^{(M_1[n])}\right]^L = \vartheta_o^\top \left(\Gamma_{MM} - \Gamma_{M0} \left[\Gamma_{00}^{(M)}\right]^{-1} \Gamma_{0M} \right) \vartheta_o + \vartheta_o^\top \Gamma_{M0} A \Gamma_{0M} \vartheta_o \tag{3.52}$$

Since A is a positive definite matrix, $\vartheta_o^\top \Gamma_{M0} A \Gamma_{0M} \vartheta_o \geq 0$, implying

$$\left[\zeta_{k_1[n],1}^{(M_1[n])}\right]^L \geq \vartheta_o^\top \left(\Gamma_{MM} - \Gamma_{M0} \left[\Gamma_{00}^{(M)}\right]^{-1} \Gamma_{0M} \right) \vartheta_o = \vartheta_o^\top \left[H^{(M)}\right]^{-1} \vartheta_o \tag{3.53}$$

Thus,

$$\left[\zeta_{k_1[n],1}^{(M_1[n])}\right]^L \geq \min_{\substack{\nu \in R^{K_1} \\ \nu_n = 1}} \nu^\top \left[H^{(M)}\right]^{-1} \nu = \left[\zeta_{n,1}^{(M)}\right]^H \tag{3.54}$$

□

Equations (3.53) and (3.54) imply that equality holds when $\Gamma_{M0} = 0$. This occurs when the group 0 and group 1 users have uncorrelated signature sequences at the Mth subinterval.

Theorems 1 and 2 imply that the performance of the LRD is always superior to that of the HRD. These results can be argued by using the definition of the near-far resistance. The near-far resistance is the worst-case asymptotic efficiency over all interfering received energies; please see equation (2.15). Both the LRD and HRD are examples of linear orthogonal projection receivers in that the desired user's signal is projected onto a subspace orthogonal to the interfering signals. Since the asymptotic efficiency of an orthogonal projection receiver is independent of the interfering received energies, the near-far resistance of an orthogonal projection receiver is the same as its asymptotic efficiency. Results of [28, 29] imply that as the LRD is the standard decorrelator for the low rate system model, it achieves the optimum near-far resistance. On the other hand, the HRD is an arbitrary linear orthogonal projection receiver for the low rate system model and may have sub-optimum near-far resistance. Since the bit error rate of an orthogonal projection receiver is a decreasing function of its near-far resistance, it is expected that the HRD will never outperform the LRD. Chapter 4 will use a specific code construction for the low rate users such that in several cases, the LRD and HRD perform the same for the group 1 users. Generalizations of Theorems 1 and 2 for multi-rate decorrelators are given in [5].

3.5 Numerical Analysis

In Sections 3.2 and 3.3, we observed that in comparison to the HRD, the LRD has higher computational complexity which is an increasing function of M. On the other hand, without quantifying the difference in asymptotic efficiencies of the dual-rate decorrelators, Section 3.4 established that the LRD outperforms the HRD.

To compare the performance of the HRD with that of the LRD, we have evaluated numerically the bit error rate of both the dual rate decorrelators. We have seen that for a small CDMA system where the signature sequences had good correlation properties, then the HRD performed almost as well as the LRD. However, when the signature sequences had high correlations, then the HRD suffered in terms of performance.

First we considered a CDMA system which supported five users where $K_0 = 3$, and

$K_1 = 2$. A group 1 user transmitted $M = 8$ bits while a group 0 user transmitted one bit. The processing gain for the group 1 user was $L_1 = 31$, while the processing gain for the group 0 user was $L_0 = 8 \times 31 = 248$. Users 1, 2 and 3 were group 0 users, while users 4 and 5 were group 1. The SNR of the kth user of the system was $10\log(\frac{E_k}{\sigma^2})$.

We used $\log_2(L_1+1)$ or 5 shift registers to generate the signature sequences for both group of users. In each subinterval i, the signature sequences of the group 1 users were the maximum-length shift register sequences [7, 78] of length 31. It was assumed that each of the two group 1 users had fixed signature sequences over the time interval, $[0, T_0]$. We generated the group 0 signature sequences of length 248 by using using maximum-length shift register sequences of length 31 in each subinterval i; see Figure 3.5. Under the LRD as well as HRD system, the BER of a user is not only a function of its own received energy but also the cross-correlation of the signature sequences; see equations (3.3), (3.13) and (3.18). Therefore in order to provide balanced BERs among all the group 0 users, we assigned three signature sequences cyclically to the group 0 users over the time interval $[0, T_0]$. This cyclic assignment technique provided equal BERs to the group 1 users at every subinterval. Note that maximum-length shift register sequences of Figure 3.5 provided good correlation properties among the signature waveforms. In addition, the above signature sequence assignment strategies guaranteed the linear independence of the transmitted signature waveforms at each subinterval and as a result, the HRD as well as the LRD existed.

In Figure 3.6, the BER of group 0 user 1 is plotted as a function of its SNR. In this experiment, it was observed that the HRD performed as well as LRD. In the next experiment, the low rate and high rate decorrelators were compared to a conventional detector; please see Figure 3.7 where the BER of the group 0 user 1 is plotted as a function of the increasing SNR of the other users. Under the conventional receiver, the BER of the desired user drastically deteriorated as the interfering users increased their transmitted power, while the BER of the desired user was fixed for the decorrelators. As expected, both low rate and high rate decorrelators eliminated the near/far effect of the conventional detector. Figure 3.8 shows that for the group 1 users, the low rate decorrelator outperformed the high rate decorrelator although the improvement

Five Maximum-length Shift Register Sequences of Length 31	
s_1	+++++−−−++−+++−+−+−−−−+−−+−++−−
s_2	+++++−+−−−+−−+−+−++−−−−+++−−++−
s_3	+++++−++−−+++−−−−++−+−+−−+−−−+−
s_4	+++++−−++−+−−+−−−−+−+−+++−++−−−
s_5	+++++−−+−−++−−−−+−++−+−+−−−+++−

Signature Sequences of the users for the interval $[0, T_0]$		
User Number	Group	Cyclic Signature Assignment
1	0	$[s_1, s_2, s_3, s_1, s_2, s_3, s_1, s_2]$
2	0	$[s_2, s_3, s_1, s_2, s_3, s_1, s_2, s_3]$
3	0	$[s_3, s_1, s_2, s_3, s_1, s_2, s_3, s_1]$
4	1	$[s_4, s_4, s_4, s_4, s_4, s_4, s_4, s_4]$
5	1	$[s_5, s_5, s_5, s_5, s_5, s_5, s_5, s_5]$

Figure 3.5: The above signature sequences were used for the synchronous DS/CDMA system with five users. Note that + and − denote +1 and −1 respectively. The signature waveform of the low rate was normalized for the interval $[0, T_0]$ while the signature waveform of the high rate was normalized for the interval $[(i-1)T_1, iT_1]$.

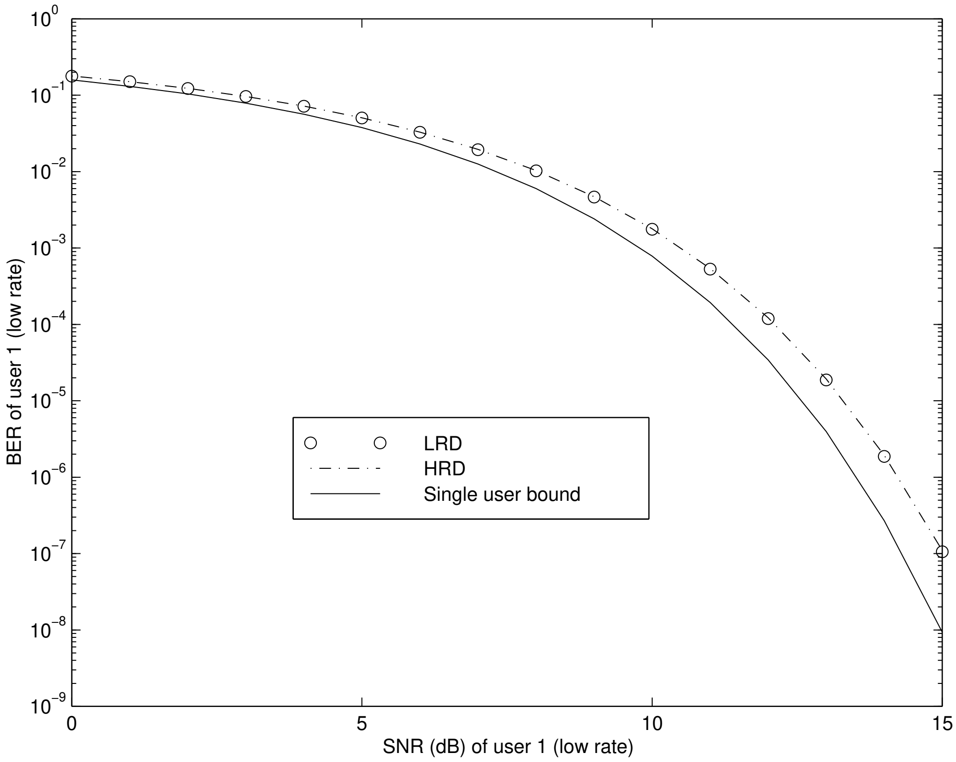

Figure 3.6: BER of the 1st group 0 user is plotted as a function of its SNR, when $K_0 = 3$, $K_1 = 2$, $L_0 = 248$ and $L_1 = 31$. In this experiment, maximum-length shift register sequences of Figure 3.5 were used to generate signature waveforms.

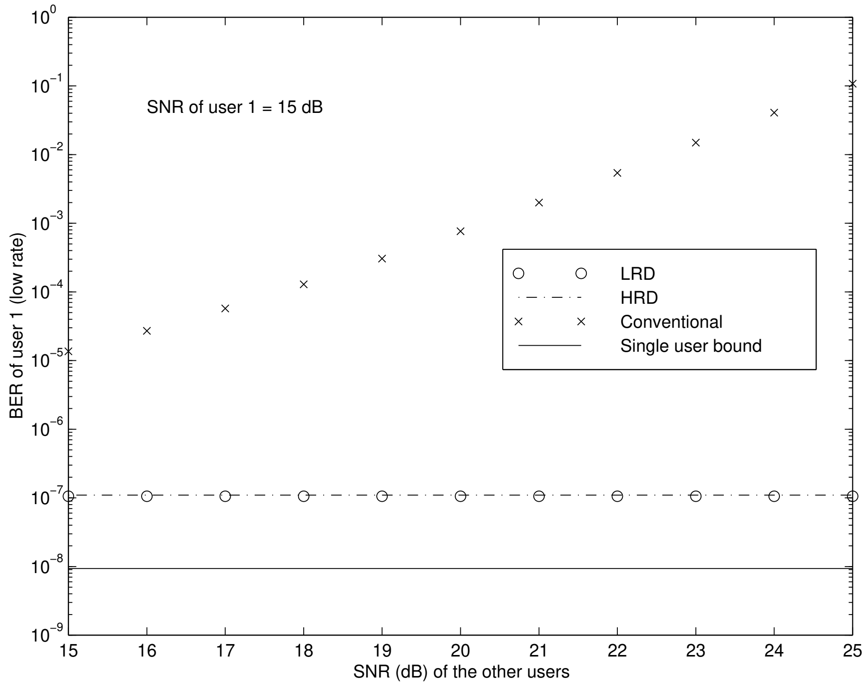

Figure 3.7: BER of the 1st group 0 user is shown as a function of the interfering users' SNR, when $K_0 = 3$, $K_1 = 2$, $L_0 = 248$ and $L_1 = 31$. In this experiment, maximum-length shift register sequences of Figure 3.5 were used to generate signature waveforms.

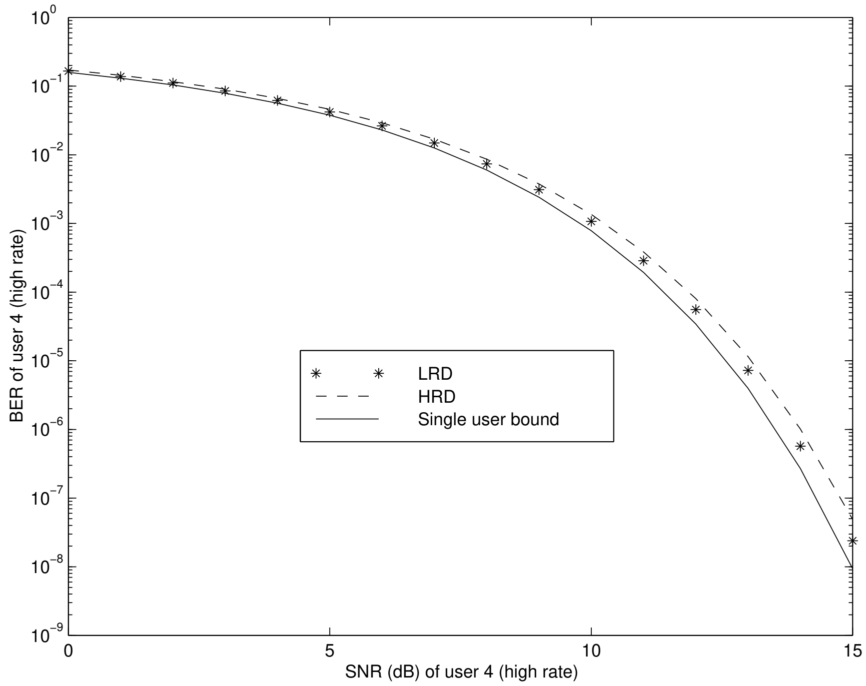

Figure 3.8: BER of the 1st group 1 user is shown as a function of its SNR, when $K_0 = 3$, $K_1 = 2$, $L_0 = 248$ and $L_1 = 31$. In this experiment, maximum-length shift register sequences of Figure 3.5 were used to generate signature waveforms.

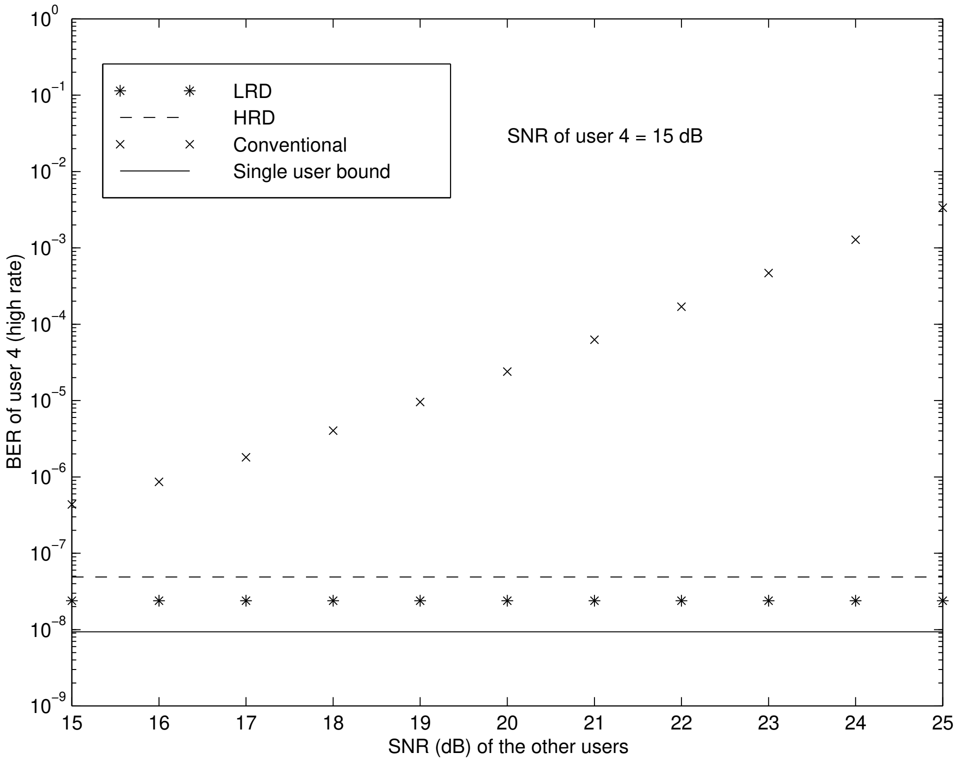

Figure 3.9: BER of the 1st group 1 user is plotted as a function of the interfering users' SNR, when $K_0 = 3$, $K_1 = 2$, $L_0 = 248$ and $L_1 = 31$. In this experiment, maximum-length shift register sequences of Figure 3.5 were used to generate signature waveforms.

was insignificant. The same result is also evident in Figure 3.9 where the performance of the decorrelators is compared to that of the conventional receiver. Since equations (3.3), (3.13) and (3.18) verify that the BER of each user is independent of the interfering users' energies, the energies of the interfering users are not mentioned in Figures 3.6 and 3.8.

To model a dual-rate DS/CDMA system with highly correlated signature waveforms, we used a set of signature waveforms derived from Gold sequences of length seven [8,62]; see Figure 3.10. Here, it was assumed that $K_0 = 2$, $K_1 = 2$, $L_0 = 56$ and $L_1 = 7$. Users 1 and 2 were group 0 users while users 3 and 4 were group 1 users. We also assumed that the group 0 users had the same signature sequences in every subinterval of duration of T_1. In this scenario, the LRD and HRD performed the same for each group 0 user; please see Theorem 1. However, for a high rate user performance degradation for the

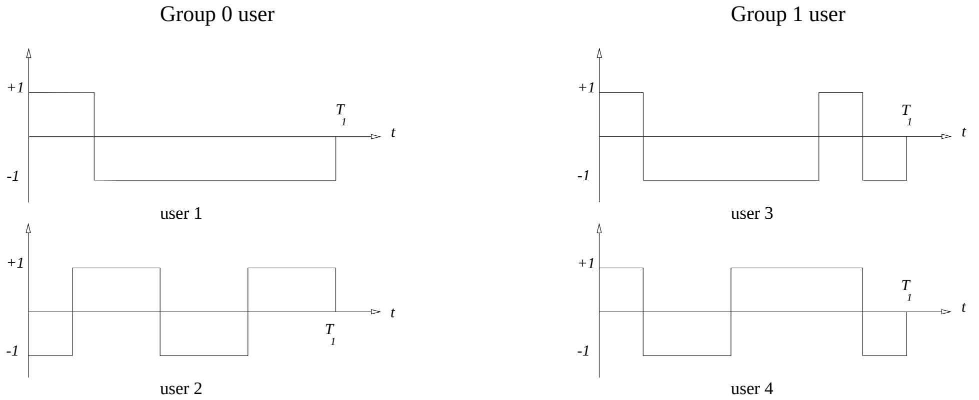

Figure 3.10: These Gold signature sequences were used for the synchronous DS/CDMA system with four users.

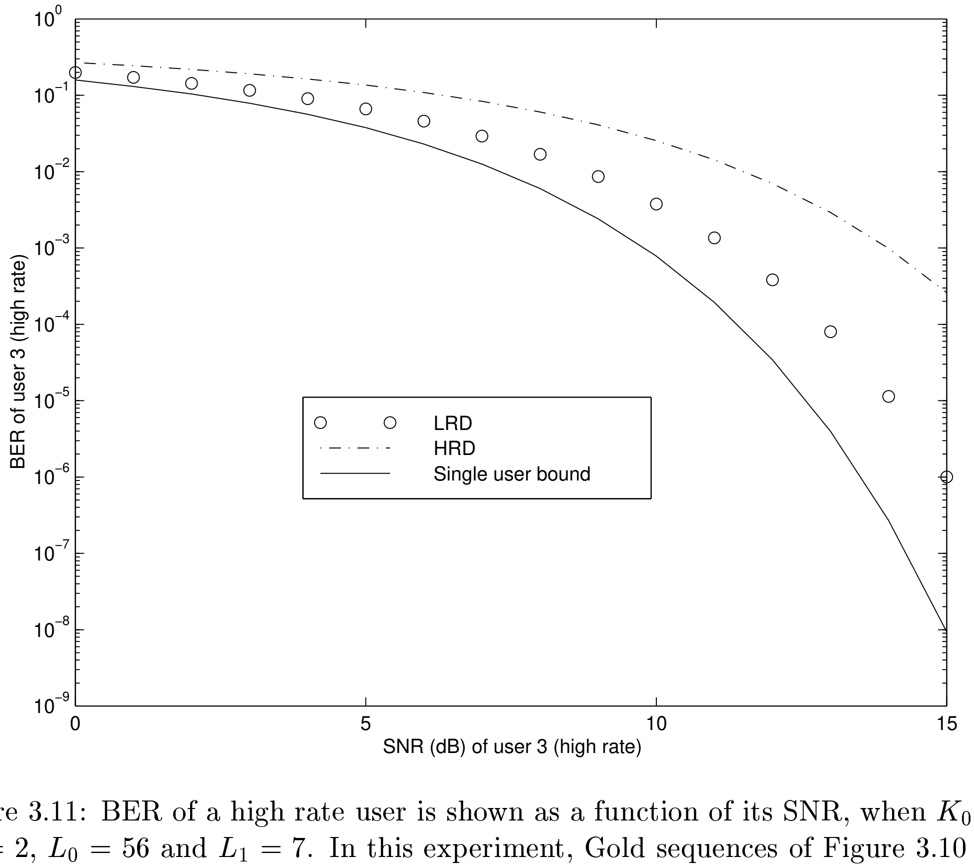

Figure 3.11: BER of a high rate user is shown as a function of its SNR, when $K_0 = 2$, $K_1 = 2$, $L_0 = 56$ and $L_1 = 7$. In this experiment, Gold sequences of Figure 3.10 were used to generate signature waveforms.

HRD versus the LRD was observed; please see Figure 3.11 where the BER of user 3 (high rate) is shown as a function of its SNR.

3.6 Chapter Summary

In a dual-rate synchronous DS/CDMA system, the low rate decorrelator introduces an M bit processing delay for the high rate users and has a complexity that grows with M. The high rate decorrelator eliminates the M bit processing delay of the high rate users and is significantly less complex than the low rate decorrelator. On the other hand, the low rate decorrelator yields lower bit error rate or higher asymptotic efficiency. To build the low rate decorrelator, it is necessary that $K_0 + MK_1 \leq L_0$, since otherwise, it will not be possible to find $K_0 + MK_1$ independent code words for the users of the equivalent single rate system. Thus for the low rate decorrelator, removing a group 1 user will permit us to add M group 0 users. On the other hand, for the high rate decorrelator, we must have $K_0 + K_1 \leq L_1$. In this case, removing one group 1 user permits us to carry only one additional group 0 user. Hence, the low rate decorrelator is more bandwidth efficient for the group 0 users. Alternatively, the high rate decorrelator wastes bandwidth to carry low rate users. Hence, it will be desirable to identify multi-rate detectors that are as bandwidth efficient as the low rate decorrelator while maintaining complexity comparable to the high rate decorrelator. In experiments, it was observed that when the signature sequences had good correlation properties, the HRD was found to perform nearly as well as the LRD while retaining the near-far resistance property. However, when there were many users in the system or the signature sequences did not possess good correlation properties, then the LRD significantly outperformed the HRD. As a solution to this problem, Chapter 5 proposes a bandwidth efficient decision feedback receiver for a dual-rate DS/CDMA system which retains the desirable properties of the HRD and outperforms the LRD.

Chapter 4

A Two Stage Decorrelator for a Dual-rate Synchronous DS/CDMA System

4.1 Introduction

This chapter proposes a signature assignment technique for a dual-rate DS/CDMA system. Under this new signature sequence assignment technique, M low rate users share the signature of a single high rate user without wasting bandwidth. Based on the signature assignment technique, a decorrelator that generates bit decisions for each high rate user in every subinterval of duration T_0/M is proposed. To decode a low rate user, a least squares technique is applied on M separate decorrelated outputs of each low rate user. We analyze, as well as evaluate, the performance of the proposed decorrelator and compare that with the performance of the LRD. It is found that similar to the HRD, the proposed decorrelator is outperformed by the LRD. However, in several cases, the proposed decorrelator achieves the performance of the LRD.

We will now describe the technique for M group 0 users to share one group 1 signature sequence. In other words, using a group 1 signature sequence of length L_1, we will generate M independent group 0 signature sequences of length $L_0 = ML_1$.

4.2 Signature Sequence Assignment

We denote the set of group 1 signature sequences as S_1, where $S_1 = \{S_{k,1} : 1 \leq k \leq G\}$, where $S_{k,1}$ denotes a group 1 signature sequence of length L_1 and G denotes the total number of group 1 signature sequences. We assume that each signature $S_{k,1}$, $1 \leq k \leq J$, is used to generate group 0 signature sequences, while, each signature sequence $S_{k,1}$, $J < k \leq J + K_1$ is used for the group 1 user $(k - J, 1)$. If we have G group 1 users, no

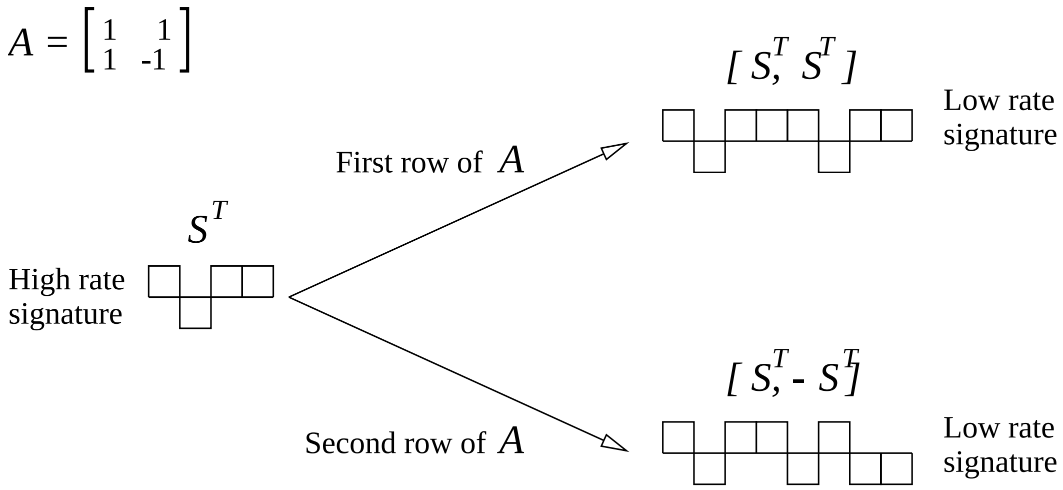

Figure 4.1: This figure shows how one can generate M low rate signatures from one high rate signature. Here $K_0 = 2$, $l_1 = 2$ and $M = 2$

group 0 users can be accommodated. With fewer than G group 1 users, each unused signature $S_{k,1} \in S_1$ can be shared by up to M group 0 users. How this sharing will be done will be explained shortly. We say the group 0 users that share the signature $S_{k,1}$, belong to a subgroup G_k. Thus, each group 0 user $(j, 0)$ belongs to a subgroup $G_{k'}$, for some k'. The jth user of the subgroup G_k is numbered $(j, k, 0)$. The number of group 0 users belonging to the subgroup G_k is l_k, where $\sum_{k=1}^{J} l_k = K_0$. We now explain how the group 0 users in subgroup G_k share the signature $S_{k,1}$. It is always possible to construct a full rank $M \times M$ matrix A_k, where $[A_k]_{j,i} \in \{1, -1\}$. Using the group 1 signature sequences $S_{k,1}$ of length L_1, for $1 \leq j \leq M$, we can generate M independent signature sequences of length $L_0 = ML_1$ as follows:

$$S_{j,k,0}^{\top} = \left\{ [A_k]_{j,1} S_{k,1}^{\top}, [A_k]_{j,2} S_{k,1}^{\top}, \ldots, [A_k]_{j,M} S_{k,1}^{\top} \right\} \tag{4.1}$$

For example, if $M = 2$ and A_k has jth row $[1, -1]$, then using equation (4.1), we can write $S_{j,k,0}^{\top} = \left\{ S_{k,1}^{\top}, -S_{k,1}^{\top} \right\}$; please see Figure 4.1. User $(j, k, 0)$ of subgroup G_k is assigned the signature $S_{j,k,0}$, where $1 \leq j \leq M$, for all $1 \leq k \leq J$. Note that the above signature sequence assignment strategy is similar to the sub-code concatenation scheme of [20] which generates additional orthogonal signature sequences for different bits of a high rate user.

Using equation (4.1), the received signal of equation (2.4) will be written as

$$r(t) = \sum_{i=1}^{M}\sum_{k=1}^{J}\left\{\sum_{j=1}^{l_k}[A_k]_{j,i}\sqrt{E_{j,k,0}}b_{j,k,0}\right\}S_{k,1}^{(i)}(t) + \sum_{i=1}^{M}\sum_{k=1}^{K_1}\left\{\sqrt{E_{k,1}^{(i)}}b_{k,1}^{(i)}S_{J+k,1}^{(i)}(t)\right\} + n(t) \tag{4.2}$$

If we denote

$$\epsilon_{k,0}^{(i)} = \left(\sum_{j=1}^{l_k}[A_k]_{j,i}\sqrt{E_{j,k,0}}b_{j,k,0}\right)^2$$

and

$$\beta_{k,0}^{(i)} = \operatorname{sgn}\left(\sum_{j=1}^{l_k}[A_k]_{j,i}\sqrt{E_{j,k,0}}b_{j,k,0}\right)$$

then we can rewrite equation (4.2) as

$$r(t) = \sum_{i=1}^{M}\left\{\sum_{k=1}^{J}\sqrt{\epsilon_{k,0}^{(i)}}\beta_{k,0}^{(i)}S_{k,1}^{(i)}(t) + \sum_{k=1}^{K_1}\sqrt{E_{k,1}^{(i)}}b_{k,1}^{(i)}S_{J+k,1}^{(i)}(t)\right\} + n(t) \tag{4.3}$$

4.3 Two Stage Decorrelator, 2SD

Based on the above signature sequence assignment technique, we will now develop the structure of a new high rate decorrelator which we call the two stage decorrelating detector (2SD). The 2SD exploits the fact that the subgroup G_k users use the same signature sequences and a group 0 user transmits the same bit during each subinterval i in which a group 1 user transmits one bit. Based on equation (4.3) as the representation of the received signal over the interval $[0, T_0]$, our proposed receiver will apply the following working principle.

1. At the end of subinterval $i < M$:
   (a) Examine the received signal over $[(i-1)T_1, iT_1]$.
   (b) Using the decorrelator, make bit decisions for the group 1 users in the subinterval i.
2. At the end of subinterval M:
   (a) For the group 1 user bits in $[(M-1)T_1, MT_1]$ follow 1(b). Applying a *least squares* technique on the M outputs of the decorrelator, decode the subgroup G_k user bits for the interval $[0, MT_1]$.

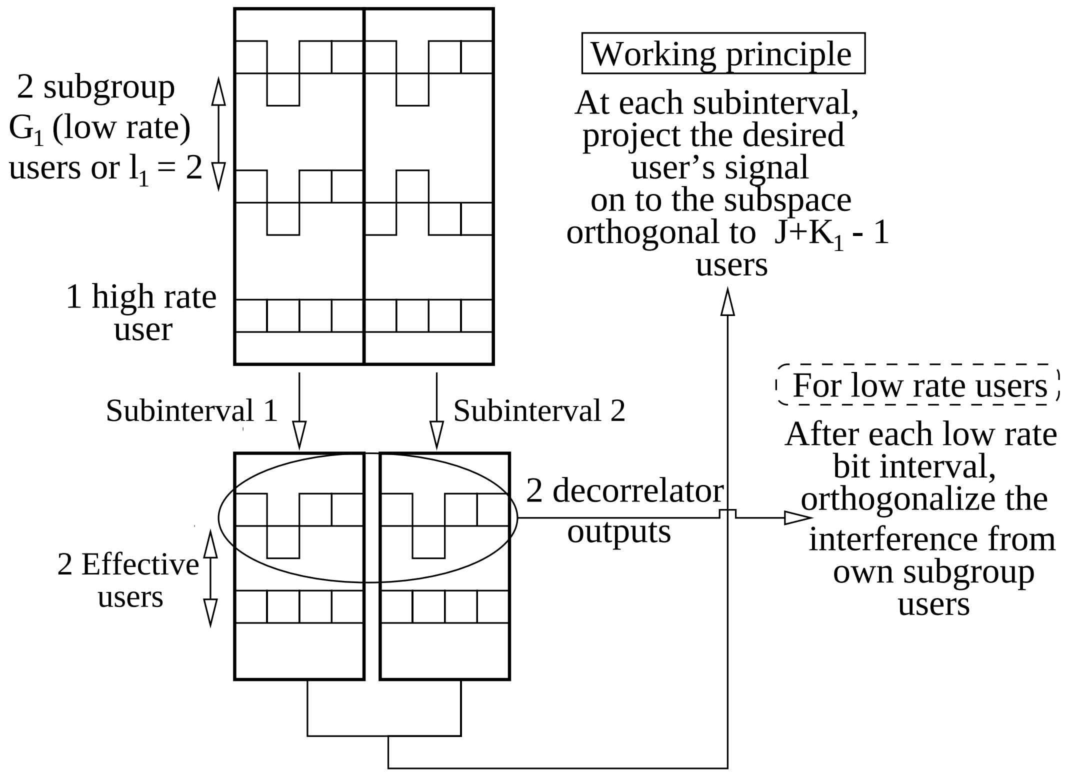

Figure 4.2: This figure depicts the working principle of the 2SD for $K_0 = 2$, $l_1 = 2$, $J = 1$, $K_1 = 1$ and $M = 2$.

In every subinterval i, the proposed high rate decorrelator, 2SD, views the $J+K_1$ transmitters as though they were K_0+K_1 users each transmitting one bit in each subinterval. For subinterval i, the input vector is $\hat{b}^{(i)} = \left[\hat{b}_1^{(i)}, \ldots, \hat{b}_J^{(i)}, \hat{b}_{(J+1)}^{(i)}, \ldots, \hat{b}_{J+K_1}^{(i)}\right]^\top$, where

$$\hat{b}_k^{(i)} = \begin{cases} \beta_{k,0}^{(i)} & 1 \leq k \leq J \\ b_{k-J,1}^{(i)} & J < k \leq J + K_1 \end{cases} \tag{4.4}$$

The bit $\hat{b}_k^{(i)}$ is transmitted using the signature waveform $S_{k,1}(t)$, $1 \leq k \leq J + K_1$. Note that for all i and k, $S_{k,1}(t)$ is defined as a signature of duration T_1 on the interval $[0, T_1]$. In each subinterval i, each group 1 user k transmits with energy $E_{k,1}^{(i)}$; however, each group 0 user j transmits with a fraction of its total transmitted energy per bit. Since the signature waveform $S_{j,0}(t)$ is normalized to have unit energy over the interval $[0, T_0]$, the fraction of the bit energy that group 0 user j transmits in subinterval i is $\int_0^{T_1} [S_{j,0}(t)]^2 dt = 1/M$. The vector of correlator output samples at time iT_1 is

$$r^{(i)} = \hat{\Gamma}\Lambda^{(i)}\hat{b}^{(i)} + N \tag{4.5}$$

where $\hat{\Gamma}$ is the $(J+K_1)\times(J+K_1)$ cross-correlation matrix with j,kth element $\hat{\Gamma}_{j,k} = \int_0^{T_1} S_{j,1}(t)S_{k,1}(t)\,dt$. Furthermore, $\Lambda^{(i)}$ is a diagonal matrix with

$$\Lambda^{(i)}_{k,k} = \begin{cases} \sqrt{\epsilon^{(i)}_{k,0}} & 1 \le k \le J \\ \sqrt{E^{(i)}_{k-J,1}} & J < k \le K_0 + K_1 \end{cases} \tag{4.6}$$

and N is a Gaussian noise vector with covariance matrix $\sigma^2\hat{\Gamma}$. In order to recover the vector $\hat{b}^{(i)}$, we decorrelate $r^{(i)}$ using the cross-correlation matrix $\hat{\Gamma}$. If $\bar{r}^{(i)}$ denotes the output vector of the decorrelator for the ith subinterval, then

$$\bar{r}^{(i)} = \hat{\Gamma}^{-1}r^{(i)} = \Lambda^{(i)}\hat{b}^{(i)} + \hat{N} \tag{4.7}$$

where $\hat{N}$ is a zero mean Gaussian noise vector with covariance matrix $\sigma^2\hat{\Gamma}^{-1}$. The working principle of the 2SD is depicted in Figure 4.2.

Using equation (4.7), the decoding rule in subinterval i for a group 1 user $k = n-J \ge 1$ is

$$\bar{b}^{(i)}_{k,1} = \mathrm{sgn}\left[\bar{r}^{(i)}_n\right] = \mathrm{sgn}\left[\Lambda^{(i)}_{n,n}\hat{b}^{(i)}_n + \hat{N}_n\right] \qquad J < n \le J + K_1 \tag{4.8}$$

The probability that a group 1 user k is decoded incorrectly in the ith subinterval equals the probability that bit $b^{(i)}_{k,1}$ is received in error which equals

$$q^{(i)}_{k,1} = Q\left[\sqrt{\frac{\zeta_{k,1}E^{(i)}_{k,1}}{\sigma^2}}\right] \tag{4.9}$$

where $\zeta_{k,1} = 1/\hat{\Gamma}^{-1}_{k+J,k+J}$ is the asymptotic efficiency of the 2SD for user $(k,1)$.

For the subgroup G_k users, we have M decorrelator outputs denoted by the vector $r_k = \left[\bar{r}^{(1)}_k, \ldots, \bar{r}^{(M)}_k\right]^\top$. We can write

$$r_k = \hat{A}_k\Lambda_k b_k + N_k \qquad 1 \le k \le J \tag{4.10}$$

where $\hat{A}_k$ is $M \times l_k$ matrix whose (h,j)th element is $[A_k]_{j,h}$ and Λ_k is a diagonal matrix with $[\Lambda_k]_{j,j} = \sqrt{E_{j,k,0}}$. The term b_k is a column vector of size l_k, where the jth element of b_k is $b_{j,k,0}$. The noise vector N_k is a zero mean Gaussian vector with the covariance matrix $\sigma^2\hat{\Gamma}^{-1}_{k,k}I$, where I is an $M \times M$ identity matrix. Since the matrix $\hat{A}_k$

has dimension $M \times l_k$, we solve for the least squares solution for b_k in equation (4.10) and

$$\bar{r}_k = \left[\hat{A}_k^\top \hat{A}_k\right]^{-1} \hat{A}_k^\top r_k = \Lambda_k b_k + \bar{N}_k \tag{4.11}$$

where the noise vector $\bar{N}_k$ is a zero mean Gaussian vector with the covariance matrix $\sigma^2 \hat{\Gamma}_{k,k}^{-1} \left[\hat{A}_k^\top \hat{A}_k\right]^{-1}$. Equation (4.11) corresponds to a second stage decorrelation of the subgroup G_k users. Using equation (4.11), the decoding rule for user $(j,k,0)$ is

$$\bar{b}_{j,k,0} = \operatorname{sgn}\left\{[\bar{r}_k]_j\right\} = \operatorname{sgn}\left\{[\Lambda_k]_{j,j}[b_k]_j + \left[\bar{N}_k\right]_j\right\} \tag{4.12}$$

where $1 \leq j \leq l_k$ and $1 \leq k \leq J$. The probability that the jth subgroup G_k user is decoded incorrectly is

$$q_{j,k,0} = Q\left[\sqrt{\frac{\zeta_{j,k,0} E_{j,k,0}}{\sigma^2}}\right] \tag{4.13}$$

where $\zeta_{j,k,0} = 1/(\hat{\Gamma}_{k,k}^{-1} \left[\hat{A}_k^\top \hat{A}_k\right]_{j,j}^{-1})$ is the asymptotic efficiency of the 2SD for user $(j,k,0)$.

4.4 Performance Analysis

In Chapter 6, we will prove that the performance of a multi-rate decorrelator improves monotonically with the length of the observation window. Compared to the LRD, the 2SD decodes users by employing a shorter observation window. We have observed that the result of Chapter 6 can be easily extended to show that the LRD will always outperform the 2SD. However, in several cases, the 2SD achieves the LRD performance. In this context, an example is given in the following theorem. The proof is given in Appendix A.

Theorem 3 *When $K_0 = MJ$ or $l_k = M$ for all $1 \leq k \leq J$, then for the group 1 user, the bit error rate or the asymptotic efficiency of the 2SD is equal to that of the LRD.*

Theorem 3 demonstrates that the two stage decorrelator decodes high rate users assuming all low rate signature sequences are in use or $l_k = M$ for all $1 \leq k \leq J$. This

Five Maximum-length Shift Register Sequences of Length 31	
s_1	+++++−−−++−+++−+−+−−−−+−−+−++−−
s_2	+++++−+−−−+−−+−+−++−−−−+++−−++−
s_3	+++++−++−−+++−−−−++−+−+−−+−−−+−
s_4	+++++−−++−+−−+−−−−+−+−+++−++−−−
s_5	+++++−−+−−++−−−−+−++−+−+−−−+++−

Signature Sequences for the group 1 bit interval		
User Number	Group	Signature Assignment
1-M	G_1	$[s_1]$
1	1	$[s_2]$
2	1	$[s_3]$
3	1	$[s_4]$
4	1	$[s_5]$

Figure 4.3: The above signature sequences were used for evaluating the performance of the 2SD. Note that + and − denote +1 and −1 respectively. The signature waveform of the low rate is normalized for the interval $[0, T_0]$ while the signature waveform of the high rate is normalized for the interval $[(i-1)T_1, iT_1]$.

result also explains why the HRD provides the high rate users higher bit error rate than the LRD; please see Theorem 2. To compare the performance of the 2SD with that of the LRD, we have evaluated numerically the bit error rate of both the 2SD and the LRD. We have seen that for a small CDMA system in which the signature sequences had good correlation properties, the 2SD performed nearly as well as the LRD.

In the experiments, we considered a dual-rate CDMA system where $1 \leq K_0 \leq M$, and $K_1 = 4$. A group 1 user transmitted $M = 7$ or 8 bits while a group 0 user transmitted one bit. The processing gain for the group 1 user was $L_1 = 31$, while the processing gain for the group 0 user was $L_0 = M \times 31$. The SNR of the kth user of the system was $10\log(\frac{E_k}{\sigma^2})$. We used $\log_2(L_1+1)$ or 5 shift registers to generate the signature sequences for both group of users. In each subinterval i, the signature sequences of the group 1 users were the maximum-length shift register sequences of length 31, see Figure 4.3. It was assumed that each of the four group 1 users had fixed signature sequences over the time interval, $[0, T_0]$. For $M = 7$, by shifting the following maximum-length shift register sequences of length 7, $[+++-+--]$, we generated the subgroup G_1 signature sequences of length 217. For $M = 8$, the Hadamard matrix of size 8×8 was used to generate the subgroup G_1 signature sequences of length 248.

In Figure 4.4, the bit error rate (BER) of low rate user $(1, 1, 0)$ is plotted as a function of its SNR with $l_1 = 2$ low rate users. In this experiment, it was observed that the 2SD performed as well as the LRD. In Figure 4.5, the BER of user $(1, 1, 0)$ is plotted as a function of the number l_1 of subgroup G_1 users. We observed for $M = 8$ and the selection of A_1 as a Hadamard matrix, that both the 2SD and the LRD were insensitive to l_1. For $M = 7$, the BER of user $(1, 1, 0)$ deteriorated as l_1 increased; however, the 2SD performed as well as the LRD.

In Figure 4.6, the BER of user (1,1) is shown by varying its SNR for $l_1 = 2$. In this experiment, we observed that for high rate user $(1, 1)$, the LRD insignificantly outperformed the 2SD. The behavior of the dual-rate decorrelators for decoding the high rate users was better understood, when the BER of user $(1, 1)$ was plotted as a function of l_1 for $M = 7$ and $M = 8$. In this experiment, it was observed that the performance of 2SD was insensitive to the increase of l_1 and M, whereas, the performance of the LRD deteriorated as l_1 increased; please see Figure 4.7. It was also noticed that when $l_1 = M$, the LRD had the same performance as the 2SD. This experimental result verified our theoretical result; see Theorem 3.

4.5 Chapter Summary

In this chapter, we have proposed a signature assignment technique for a dual-rate DS/CDMA system. Based on the signature assignment technique, a decorrelator that generates high rate bit decisions immediately after each high rate bit interval has been proposed. To decode a low rate user, an orthogonal projection is applied to separate decorrelated outputs of each low rate user. The proposed decorrelator significantly reduces the computational complexity of the standard decorrelator. Due to the structural simplicity, it suffers in terms of bit error rate. However, in several cases, the proposed decorrelator provides the performance of the low rate decorrelator.

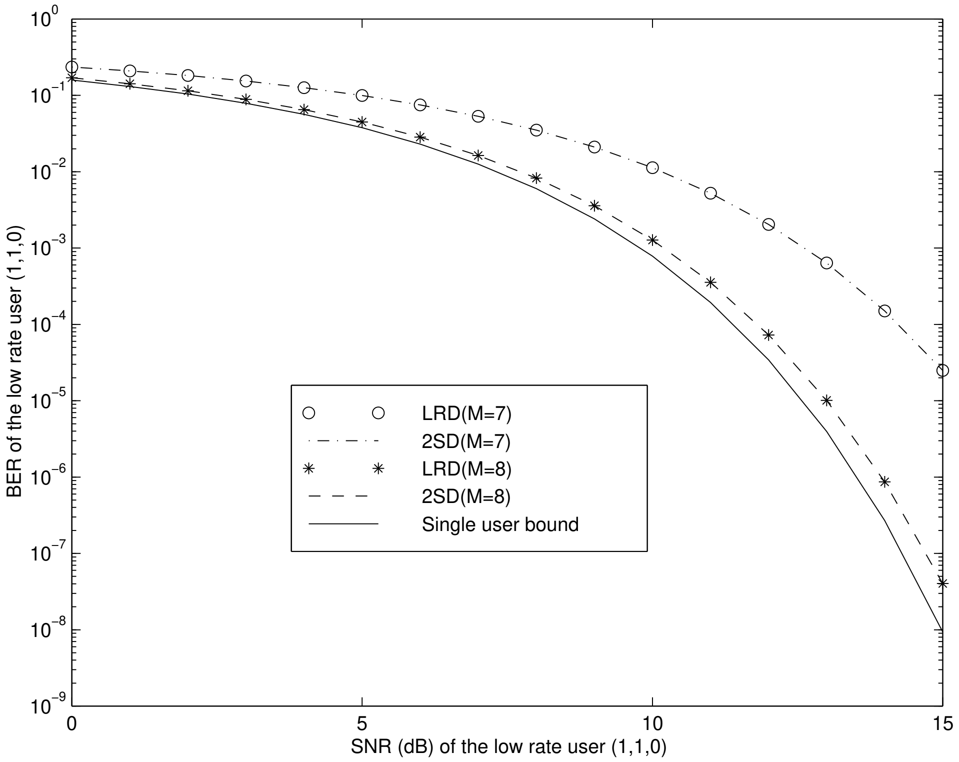

Figure 4.4: BER of user (1,1,0) is plotted as a function of its SNR.

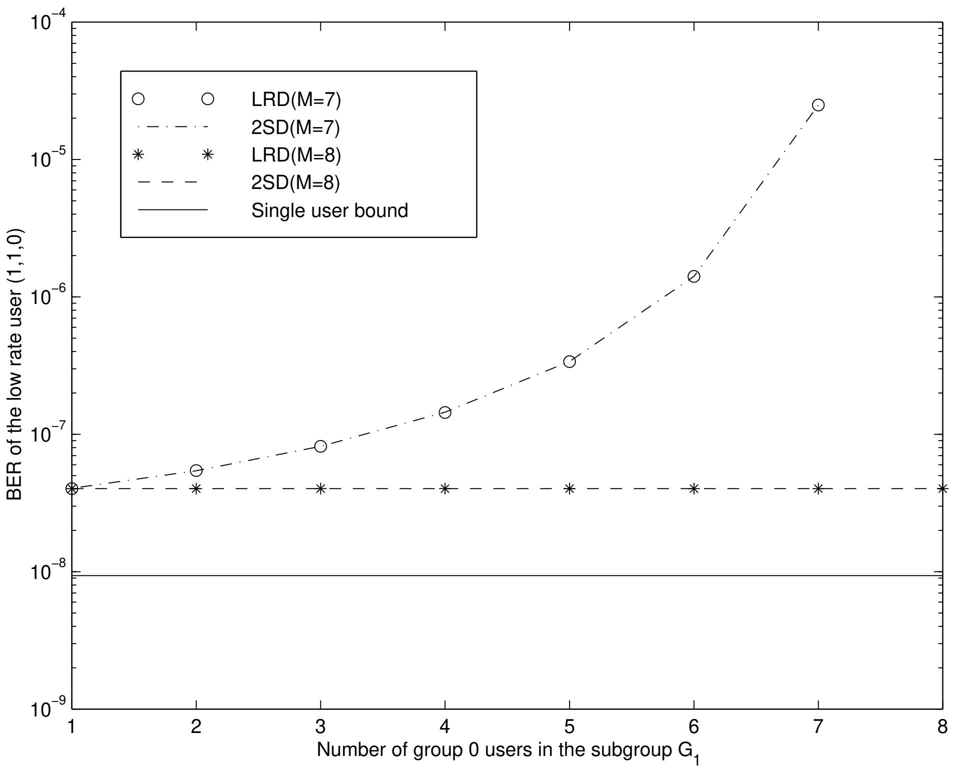

Figure 4.5: BER of user (1,1,0) is given by varying the number of users when the desired user's SNR = 15 dB.

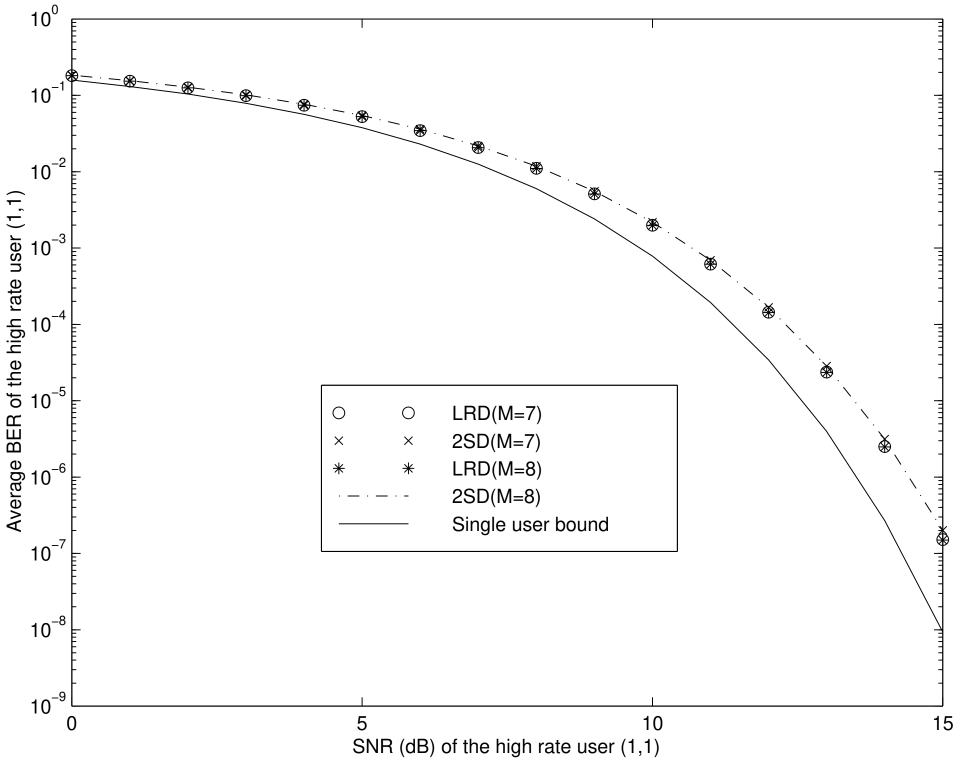

Figure 4.6: Average BER of user (1,1) is plotted as a function of its SNR.

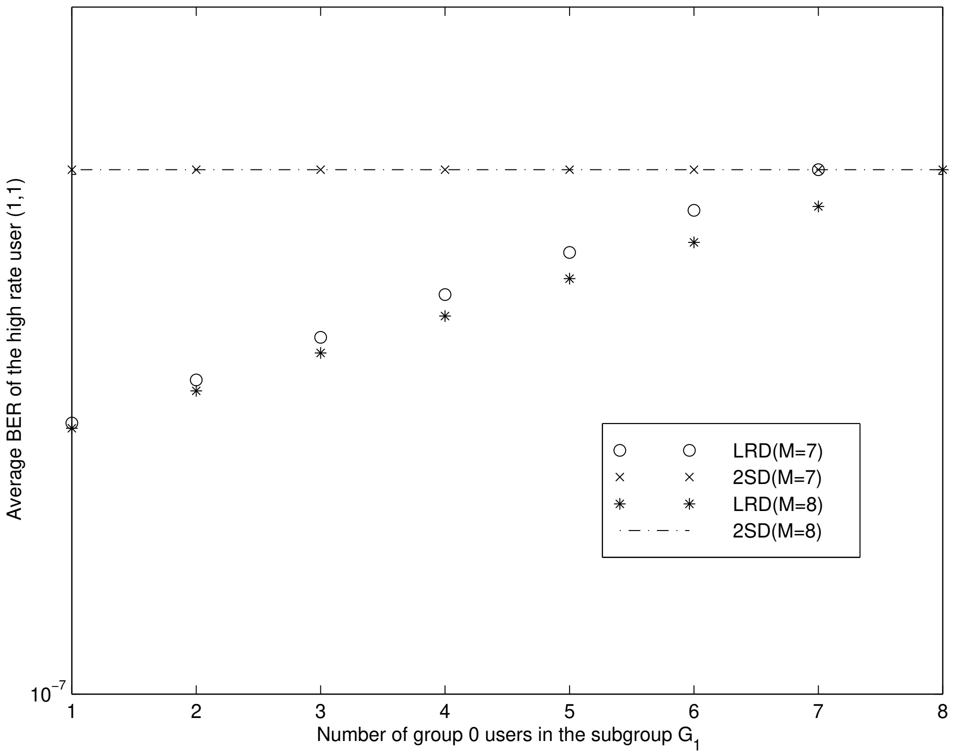

Figure 4.7: Average BER of user (1,1) is shown by varying the number of users when the desired user's SNR = 15 dB.

Chapter 5

A Decision Feedback Decorrelator for a Dual Rate Synchronous DS/CDMA System

5.1 Introduction

It is well known that the decorrelator does not require the knowledge of the received signal strengths. However, it eliminates the multiuser interference at the cost of increased noise variance. A somewhat more complex receiver is the decorrelating decision-feedback detector [8]. The decision feedback receiver achieves better performance by utilizing bit decisions and the knowledge of the received signal strengths of the stronger users to reduce multiuser interference for the weaker users.

Motivated by the decision feedback detector of the single rate system [8], in this chapter, we develop a decision feedback decorrelating detector for the dual rate synchronous CDMA system. This proposed receiver is called the *high rate decision feedback decorrelator* or *HRDF*. The HRDF initiates the bit decision process at the end of the high rate bit interval. Each bit is decoded by utilizing the decisions of all previously decoded users. This chapter will study the performance of the HRDF and compare that with the performance of the dual rate decorrelators (LRD and HRD).

5.2 Modified Correlator

Linear multiuser receivers, such as the decorrelator [28,29] or MMSE detector [31], can be implemented in a decentralized fashion by modifying the correlator signal; see Figures 5.1 and 5.2. Reference [65] shows that the modified correlators of a decorrelator can be found as a product of the inverted cross-correlation matrix and the transpose of the signature sequences or by applying the Gram-Schmidt orthogonalization on the

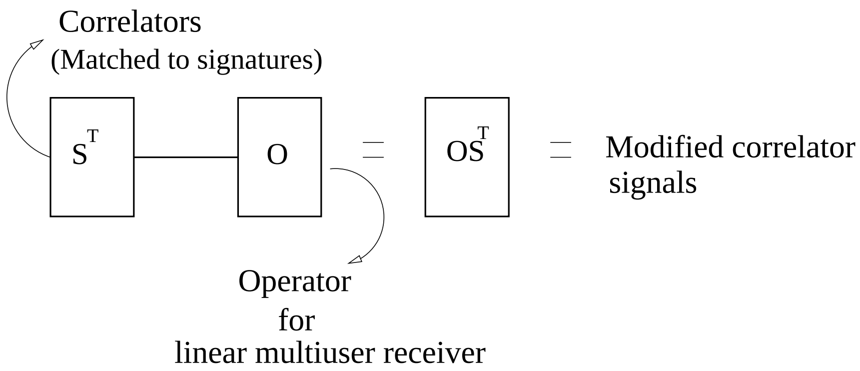

Figure 5.1: The figure shows how one can generate modified correlators for a linear multi-user receiver.

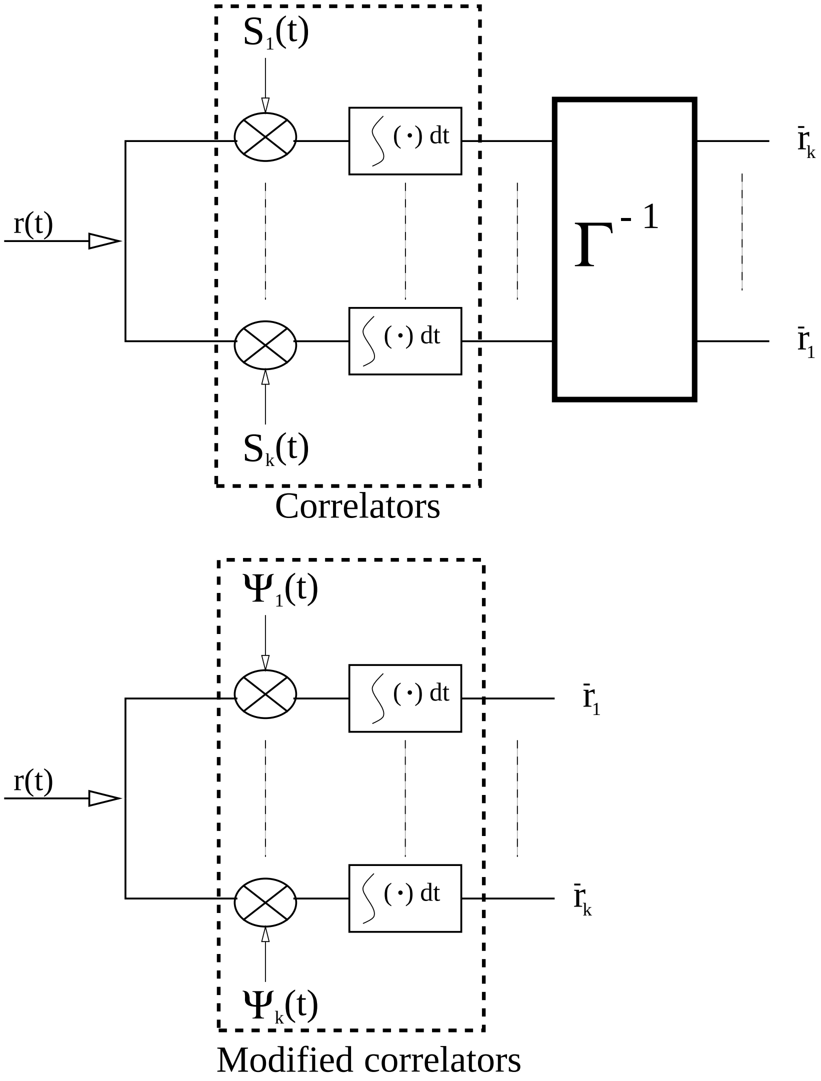

Figure 5.2: First or upper part of this figure shows the traditional implementation of a decorrelator. Second or lower part of the figure depicts the implementation of a decorrelator by modified correlators.

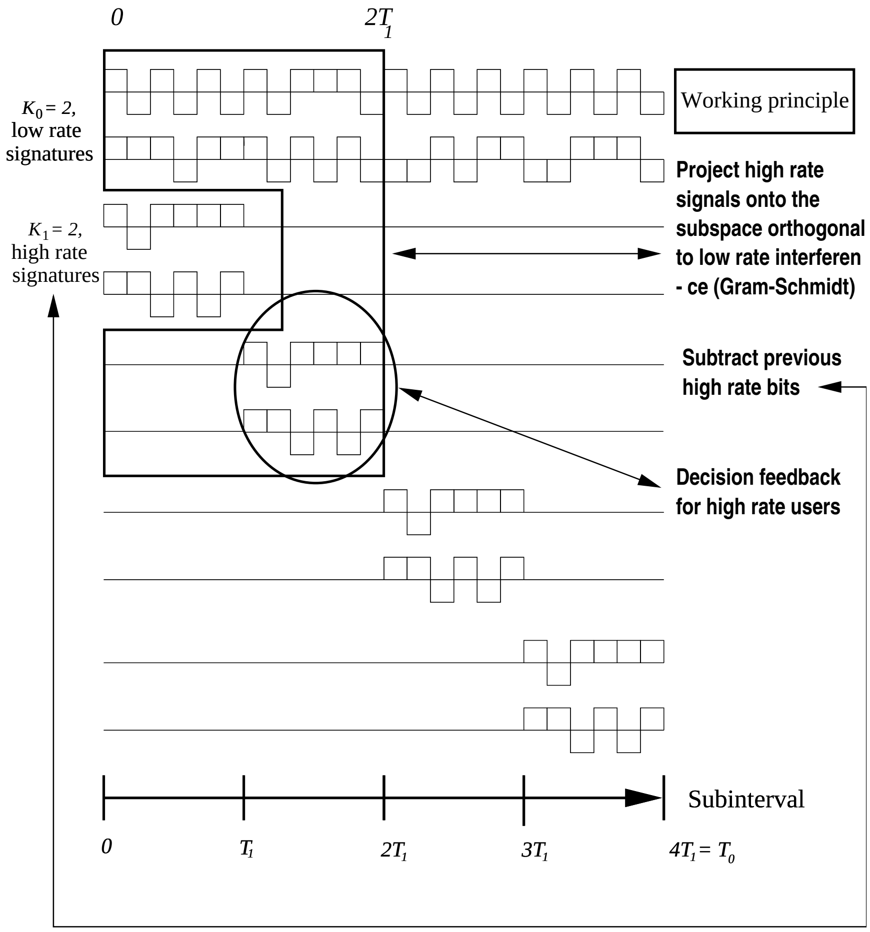

Figure 5.3: The figure depicts the working principle of the HRDF.

interfering users' signature sequences; please see Figure 5.2. In this study, we will concentrate our attention on the the Gram-Schmidt procedure to build modified correlators for implementing the HRDF.

5.3 High Rate Decision Feedback Decorrelator, HRDF

We will see that the HRDF is bandwidth efficient, retains all the desirable properties of the HRD and outperforms the LRD. The HRDF exploits the fact that a group 0 user transmits the same bit during each subinterval i in which a group 1 user transmits one bit. The working principles of this receiver are as follows.

1. At the end of each subinterval $i < M$:

    (a) Decorrelate the partial signature sequences of the group 0 users over $[0, iT_1]$.

(b) For $i > 1$, subtract away group 1 users for the interval $[0, (i-1)T_1]$ based on bit decisions in each of the $(i-1)$ subintervals.

(c) Using decision feedback, make bit decisions for the group 1 users in the subinterval $[(i-1)T_1, iT_1]$.

Steps 1(a) - 1(c) are depicted in Figure 5.3.

2. At the end of subinterval M:

(a) Repeat step 1(b) and use decision feedback to decode the group 0 user bits in $[0, MT_1]$ together with the group 1 user bits in $[(M-1)T_1, MT_1]$.

5.3.1 Structure of the HRDF

Recall that during the ith subinterval, the jth group 0 user has transmitted using the signature segment $S_{j,0}^{(i)}(t)$ as given by equation (3.6). Furthermore, over the interval $[0, iT_1]$, the jth group 0 user has transmitted using the *partial signature*

$$\tilde{S}_{j,0}^{(i)}(t) = \sum_{m=1}^{i} S_{j,0}^{(m)}(t) \qquad j = 1, \ldots, K_0 \tag{5.1}$$

Using equation (5.1), the baseband signal which is received during the interval $[0, iT_1]$ can be written as

$$r^{(i)}(t) = \sum_{j=1}^{K_0} \sqrt{E_{j,0}}\, b_{j,0} \tilde{S}_{j,0}^{(i)}(t) + \sum_{k=1}^{K_1} \left\{ \sum_{m=1}^{i} \sqrt{E_{k,1}^{(m)}}\, b_{k,1}^{(m)} S_{k,1}^{(m)}(t) \right\} + n(t) \tag{5.2}$$

The group 0 users' partial signatures segments transmitted during the interval $[0, iT_1]$, where $i < M$, are not normalized and may not be linearly independent. Therefore, we generate the effective group 0 users from the actual group 0 users by applying the Gram-Schmidt procedure to the group 0 partial signatures of equation (5.1).

Let us assume that the Gram-Schmidt procedure on the partial signatures of the group 0 users in the interval $[0, iT_1]$, where $i < M$, yields $K_0^{(i)}$ basis functions,

$$\left\{ \Psi_{j,0}^{(i)}(t) : j = 1, \ldots, K_0^{(i)} \right\}$$

where $\Psi_{j,0}^{(i)}(t)$ is normalized to have unit energy on the interval $[0, iT_1]$. Using these basis functions, we can write each low rate partial signature as a linear combination

$$\tilde{S}_{j,0}^{(i)}(t) = \sum_{j'=1}^{K_0^{(i)}} a_{jj'}^{(i)} \Psi_{j',0}^{(i)}(t)$$

Thus, the received signal during the interval $[0, iT_1]$, where $i < M$, can be written

$$r^{(i)}(t) = \sum_{j'=1}^{K_0^{(i)}} \sqrt{\epsilon_{j',0}^{(i)}} \beta_{j',0}^{(i)} \Psi_{j',0}^{(i)}(t) + \sum_{k=1}^{K_1} \left\{ \sum_{m=1}^{i} \sqrt{E_{k,1}^{(m)}} b_{k,1}^{(m)} S_{k,1}^{(m)}(t) \right\} + n(t) \quad (5.3)$$

where

$$\begin{aligned} \epsilon_{j',0}^{(i)} &= \left(\sum_{j=1}^{K_0} a_{jj'}^{(i)} \sqrt{E_{j,0}} b_{j,0} \right)^2 \\ \beta_{j',0}^{(i)} &= \operatorname{sgn} \left(\sum_{j=1}^{K_0} a_{jj'}^{(i)} \sqrt{E_{j,0}} b_{j,0} \right) \end{aligned}$$

Effectively, we have reduced K_0 group 0 users with possibly dependent partial signatures to $K_0^{(i)}$ effective group 0 users with orthogonal signatures. Each effective group 0 user transmits one bit $\beta_{j,0}^{(i)}$ with energy $\epsilon_{j,0}^{(i)}$ in the interval $[0, iT_1]$, where $i < M$. We observe that the energy $\epsilon_{j,0}^{(i)}$ of a group 0 effective user depends on the bits transmitted by the group 0 users and also on the projections of the partial signatures on the basis function $\Psi_{j,0}^{(i)}$. Thus, the energies of the group 0 effective users are not known.

Let us denote $k_1^{(i)}[n] = n - K_0^{(i)}$ if $n > K_0^{(i)}$, $i < M$ and redefine the $K^{(i)} = K_0^{(i)} + K_1$ effective users' signature waveforms, energies and transmitted bits of equation (5.3) as follows:

$$s_n^{(i)}(t) = \begin{cases} \Psi_{n,0}^{(i)}(t) & 1 \le n \le K_0^{(i)} \\ S_{k_1^{(i)}[n],1}^{(i)}(t) & K_0^{(i)} < n \le K^{(i)} \end{cases} \quad (5.4)$$

$$\sqrt{E_n^{(i)}} = \begin{cases} \sqrt{\epsilon_{n,0}^{(i)}} & 1 \le n \le K_0^{(i)} \\ \sqrt{E_{k_1^{(i)}[n],1}^{(i)}} & K_0^{(i)} < n \le K^{(i)} \end{cases} \quad (5.5)$$

$$b_n^{(i)} = \begin{cases} \beta_{n,0}^{(i)} & 1 \le n \le K_0^{(i)} \\ b_{k_1^{(i)}[n],1}^{(i)} & K_0^{(i)} < n \le K^{(i)} \end{cases} \quad (5.6)$$

Using equations (5.4)-(5.6), equation (5.3) can be written as

$$r^{(i)}(t) = \sum_{n=1}^{K^{(i)}} \sqrt{E_n^{(i)}} b_n^{(i)} s_n^{(i)}(t) + \sum_{m=1}^{i-1} \left\{ \sum_{k=1}^{K_1} \sqrt{E_{k,1}^{(m)}} b_{k,1}^{(m)} S_{k,1}^{(m)}(t) \right\} + n(t) \qquad t \in [0, iT_1] \tag{5.7}$$

The proposed receiver of Figure 5.4 will decode each group 1 bit after the end of its transmission. We see in equation (5.7) that the received signal $r^{(i)}(t)$ over the interval $[0, iT_1]$ is the sum of the following three components, i) the baseband signals due to the $K^{(i)}$ effective users, ii) cumulative interference from group 1 bits of the previous subintervals and iii) the additive Gaussian noise.

At the end of the subinterval M, the group 0 bits of the interval $[0, MT_1]$ and group 1 bits of the subinterval $[(M-1)T_1, MT_1]$ will be jointly decoded. At this time, this joint decoding will use the actual signature waveform, energy, transmitted bit of each group 0 user. In this case, the effective number of users $K^{(M)}$ equals the actual number of users $K_0 + K_1$. In this regard, it is assumed that during the interval $[0, MT_1]$, the $K^{(M)}$ signature waveforms of the effective users will be linearly independent.

Let us assume that the Gram-Schmidt procedure on the signature waveforms $\left\{ s_n^{(i)}(t) \right\}$ given in equation (5.4) yields the set of basis functions

$$\left\{ \Psi_j^{(i)}(t) : 1 \le j \le K^{(i)} \right\}$$

where

$$\Psi_j^{(i)}(t) \quad = \quad \Psi_{j,0}^{(i)}(t) \qquad \text{for } 1 \le j \le K_0^{(i)}$$

i.e., for the effective group 0 users. Now let us modify the correlators so that the received signal will be correlated with $\left\{ \Psi_j^{(i)}(t) \right\}$. However, in the subinterval $i < M$, as we want to decode the group 1 bits only, thus, we shall correlate the received signal with $\left\{ \Psi_j^{(i)}(t); K_0^{(i)} < j \le K^{(i)} \right\}$, whereas, for $i = M$, the group 0 users will be decoded together with the group 1 users and the complete set of basis functions $\left\{ \Psi_j^{(i)}(t) \right\}$ will be used in the correlators. For $i < M$, the HRDF can be viewed as a partial decision feedback multiuser detector for the dual-rate synchronous DS/CDMA system. A partial decision feedback multiuser detector for the asynchronous single rate DS/CDMA system is proposed in [9].

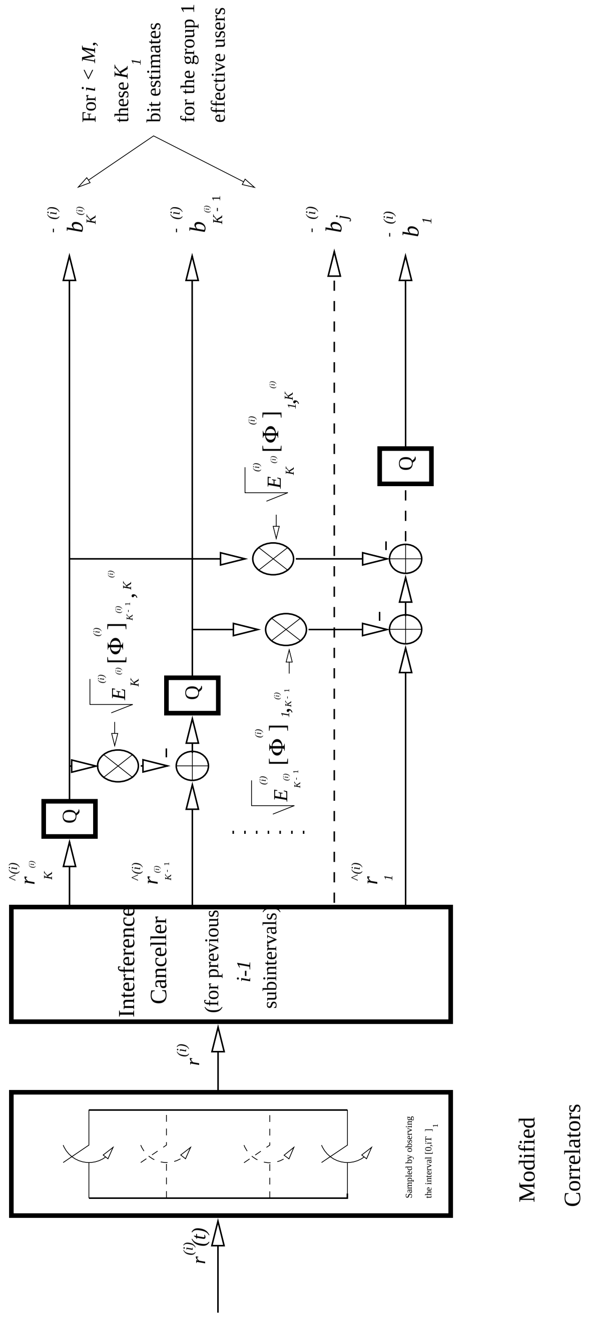

Figure 5.4: This diagram shows the operational principles of the high rate decision feedback decorrelating detector, HRDF. The "Interference Canceller" estimates $\Upsilon^{(i)}$ of equation (5.8) and subtracts from the outputs of the modified correlators.

We now examine the decision feedback receiver over subintervals $i < M$. The sampled output of the bank of modified correlators at subinterval $i < M$ is the vector $r^{(i)}$, where

$$r^{(i)} = \Phi^{(i)}\Lambda^{(i)}b^{(i)} + \Upsilon^{(i)} + n^{(i)} \tag{5.8}$$

where $\Phi^{(i)}$ is an upper triangular matrix of size $K_1 \times K_1$, the (j,n)th component of $\Phi^{(i)}$ is

$$\Phi^{(i)}_{j,n} = \begin{cases} 0 & j > n \\ \int_0^{iT_1} s^{(i)}_{j+K_0^{(i)}}(t)\Psi^{(i)}_{n+K_0^{(i)}}(t)\,dt & j \leq n \end{cases} \tag{5.9}$$

Note that, $\Phi^{(i)}$ is an the upper triangular matrix because of Gram-Schmidt orthogonalization on the signature waveforms $\left\{s^{(i)}_n(t)\right\}$ given in equation (5.4). The term $\Lambda^{(i)}$ is a $K_1 \times K_1$ diagonal matrix with $\Lambda^{(i)}_{n,n} = \sqrt{E^{(i)}_{n+K_0^{(i)}}}$ for $i < M$ and $n^{(i)}$ is a Gaussian noise vector of size K_1 with cross-correlation matrix $\sigma^2 I$, where I is an identity matrix of size $K_1 \times K_1$. The term $\Upsilon^{(i)}$, is a $K_1 \times 1$ column vector which is the residual multiuser interference resulting from the group 1 users of the previous $i-1$ subintervals. The nth component of $\Upsilon^{(i)}$ is

$$\Upsilon^{(i)}_n = \begin{cases} 0 & i = 1 \\ \sum_{m=1}^{i-1}\left[\sum_{j=1}^{K_1}\phi^{(mi)}_{j,n}\sqrt{E^{(m)}_{j,1}}\,b^{(m)}_{j,1}\right] & 1 \leq i \leq M-1 \end{cases} \tag{5.10}$$

where

$$\phi^{(mi)}_{j,n} = \int_0^{iT_1} S^{(m)}_{j,1}(t)\Psi^{(i)}_{n+K_0^{(i)}}(t)\,dt \tag{5.11}$$

In subinterval M, the complete set of basis functions $\left\{\Psi^{(M)}_j(t)\right\}$ will be used in the correlators and the dimension of the sampled output of bank of modified correlators of equation (5.8), $r^{(M)}$ will be $K^{(M)} \times 1$, where, the corresponding upper triangular matrix $\Phi^{(M)}$ and the diagonal matrix $\Lambda^{(M)}$ are $K^{(M)} \times K^{(M)}$. The residual multiuser interference vector $\Upsilon^{(M)}$ and the independent Gaussian noise vector $n^{(M)}$ are $K^{(M)} \times 1$.

In general, for any subinterval i $(1 \leq i \leq M)$, the kth element of the vector $r^{(i)}$ will be

$$r_k^{(i)} = [\Phi^{(i)}]_{k,k}\sqrt{E_k^{(i)}}b_k^{(i)} + \sum_{j=k+1}^{K^{(i)}} \left\{[\Phi^{(i)}]_{k,j}\sqrt{E_j^{(i)}}b_j^{(i)}\right\} + \Upsilon_k^{(i)} + n_k^{(i)} \tag{5.12}$$

Note that in equation (5.4), for $n > K_0^{(i)}$, $s_n^{(i)}(t)$ denotes a signature waveform that is nonzero only over the ith subinterval and has zero cross-correlation with $S_{k,1}^{(m)}(t)$ for $m < i$. However, as we have used modified correlator signals of duration $[0, iT_1]$, therefore, the transmitted signal of group 1 users in previous $i-1$ subintervals will have an effect on the group 1 bit decisions at the ith subinterval.

We have assumed that we know the actual bit energies $E_{j,0}$ and $E_{k,1}$ of each group 0 user j and group 1 user k. At the receiver end, the users will be ordered and decoded sequentially in a decreasing order. The bit decision process will exploit previous decisions to decode the current user. In subinterval i, given the group 1 bit decisions, $\bar{b}_{j,1}^{(m)}$ from the previous $(i-1)$ subintervals, if we have already made bit decisions $\bar{b}_{k+1}^{(i)}, \dots, \bar{b}_{K^{(i)}}^{(i)}$ in the ith subinterval, then we can write the decision statistic for user k as

$$\bar{r}_k^{(i)} = r_k^{(i)} - \sum_{m=1}^{i-1}\left[\sum_{j=1}^{K_1}\phi_{j,k}^{(mi)}\sqrt{E_{j,1}^{(m)}}\bar{b}_{j,1}^{(m)}\right] - \sum_{j=k+1}^{K^{(i)}}[\Phi^{(i)}]_{k,j}\sqrt{E_j^{(i)}}\bar{b}_j^{(i)} \tag{5.13}$$

The corresponding decoding rule is

$$\bar{b}_k^{(i)} = \mathrm{sgn}[\bar{r}_k^{(i)}] \tag{5.14}$$

5.3.2 Ranking Procedure for Users

References [8, 39, 62] have observed that the feedback in the receiver of the single rate CDMA system is primarily beneficial if the interfering users are stronger. Therefore, these receivers rank and decode the users according to nondecreasing strengths of received energies. However, this ranking is not necessarily the only way to order users. In our receiver design, we propose a novel approach to rank the $K^{(i)}$ users as follows.

We define the *orthogonal energy*, or *OE*, of a user as the fraction of its received energy associated with the subspace orthogonal to the interfering users. We write the orthogonal energy as

$$\mathrm{OE}_n^{(i)} = E_n^{(i)} / \left(\bar{\Gamma}^{(i)}\right)^{-1}_{n,n} \tag{5.15}$$

where $\Gamma^{(i)}$ denotes $K^{(i)} \times K^{(i)}$ cross-correlation matrix of equation (5.4). For the interval $[0, iT_1]$, where $i < M$, we order the K_1 group 1 users such that $\mathrm{OE}_n^{(i)}$ is increasing in n. However, for $i = M$, group 0 users will be decoded together with group 1 users. In particular, without classifying the user by its rate, all $K^{(M)} = K_0 + K_1$ users will be ranked according to nondecreasing OEs.

This heuristic ordering procedure is motivated by the known performance of the decorrelator. For the very last user, i.e. the first user decoded, there is no feedback and a decision feedback receiver is equivalent to a decorrelator. In a bandwidth efficient CDMA system with many users, the signature waveforms may have high cross-correlations which could lead to erroneous decisions to the earlier ranked users. From equations (3.3), (3.13) and (3.18), it is seen that the bit error rate of the decorrelator is a decreasing function of OE. Therefore, we rank the users by their decreasing OEs rather than their energies in order to reduce the likelihood of early decision feedback errors which have an impact on the decoding of lower ordered users.

5.3.3 Alternative Implementations of the HRDF

The implementation of the HRDF requires $K_0 + MK_1$ modified correlators and two interference cancellers. We can implement the HRDF by using $\sum_{i=1}^{M} K_0^{(i)} + K_1$ correlators matched to the effective signature waveforms rather than using $K_0 + MK_1$ modified correlators. However, this technique requires an additional linear transformation $([\Phi^{(i)}]^\top)^{-1}$ at the outputs of the correlators. Note that this alternative method is used in the decision feedback receiver of the single rate system [8]. In order to process the current bit decision, the first interference canceller cancels out the multiuser interference caused by the high rate bits of the previous subintervals and the second one subtracts the multiuser interference caused by the previously decoded users of the current subinterval. Every step of the bit decision process is executed by measuring the cross-correlation among the current modified correlator signal and the signature waveforms corresponding to the bits which are decoded previously. However, these operations of interference cancellers can be observed by adapting the following method applied in [39]. At the end of each bit decision, the corresponding baseband signal will be regenerated and subtracted from the received signal, and then, this new signal will be correlated with the correlator corresponding to the bit which will be decoded next.

5.3.4 Bandwidth Efficiency of the HRDF

In Chapter 3, it has been observed that to build the LRD, it is necessary that $K_0 + MK_1 \leq L_0$. Thus, for the LRD, removing a group 1 user will permit adding M group 0 users. On the other hand, for the HRD, we must have $K_0 + K_1 \leq L_1$. In this case, removing one group 1 user permits us to carry only one additional group 0 user. Hence, the LRD is more bandwidth efficient for the group 0 users. Similar to the LRD system, the HRDF system model allows us to support M group 0 users by using one group 1 signature sequence, hence it is more bandwidth efficient than the HRD.

5.4 Performance Measures

To observe the performance of the proposed decision feedback receiver, we simulated a HRDF system. In the simulations, we used a set of signature waveforms derived from Gold sequences of length seven [8, 62]; see Figure 3.10. These Gold sequences were assumed as the group 1 signature sequences. As the HRDF system model permits us to use group 1 signature sequences to support group 0 users, we used the signature sequences of Figure 3.10 to support the group 1 users as well group 0 users. Here we assumed four users were active. Among the four users, there were $K_0 = 2$ group 0 users, and $K_1 = 2$ group 1 users. Users 1 and 2 were group 0 users while users 3 and 4 were group 1 users. It was also assumed that the group 0 users had the same signature sequences in every subinterval i. In an interval of T_0, a group 1 user transmitted $M = 8$ bits while a group 0 user transmitted one bit. The SNR of the kth user of the system was $10\log(\frac{E_k}{\sigma^2})$ and it was assumed that the received energies of group 1 users did not vary from bit to bit.

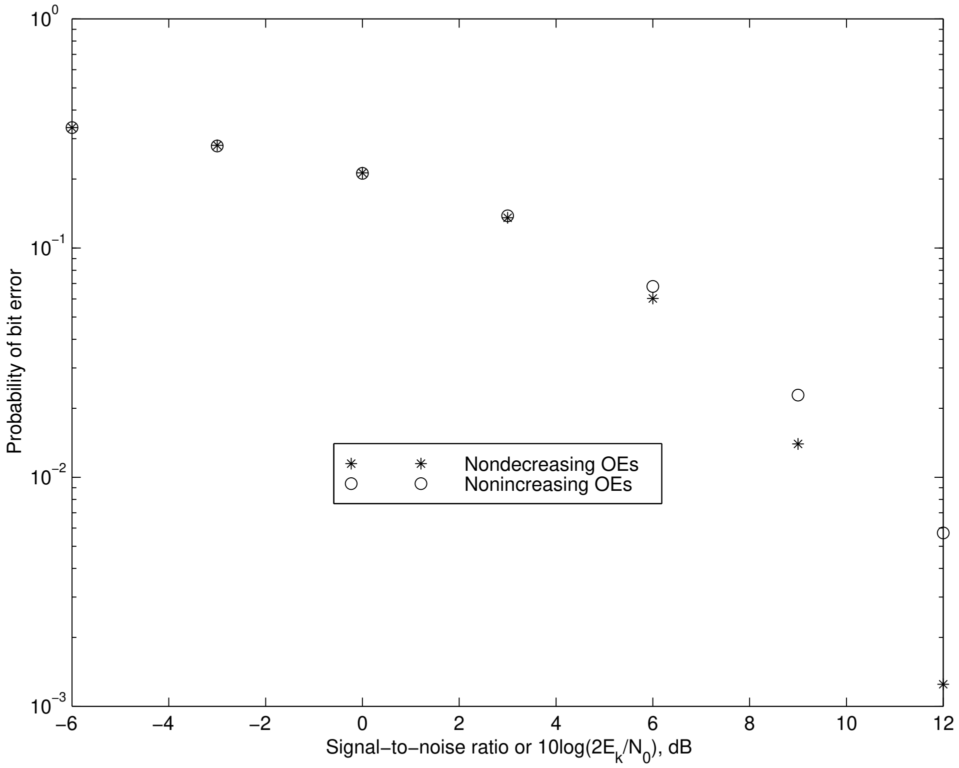

Figure 5.5: This figure depicts the performance of the HRDF, when users were ranked according to nondecreasing and nonincreasing OEs.

Instead of ranking users according to nondecreasing received energies, we have proposed to rank users according to nondecreasing OEs in order to implement the HRDF; see section 5.3. The motivation behind this ordering technique was to reduce the likelihood of early decision feedback errors which have an impact on the decoding of lower ordered users. To observe the effect of this proposed ordering technique on the performance of the HRDF, we simulated the HRDF system, when users were ranked according to nondecreasing and nonincreasing OEs. In this experiment, it was assumed that all users had the same SNR. By varying the SNRs from -6 dB to 12 dB, we measured the probability that the HRDF made a error decoding an arbitrary bit of a randomly chosen user. Our experimental results showed that when the SNRs were small (less than 2 dB) the HRDF exhibited similar performance under the both ordering techniques; see Figure 5.5. However, when the SNRs were greater than 2 dB, our proposed technique that ordered users according to nondecreasing OEs outperformed significantly the technique that ordered users according to nonincreasing OEs.

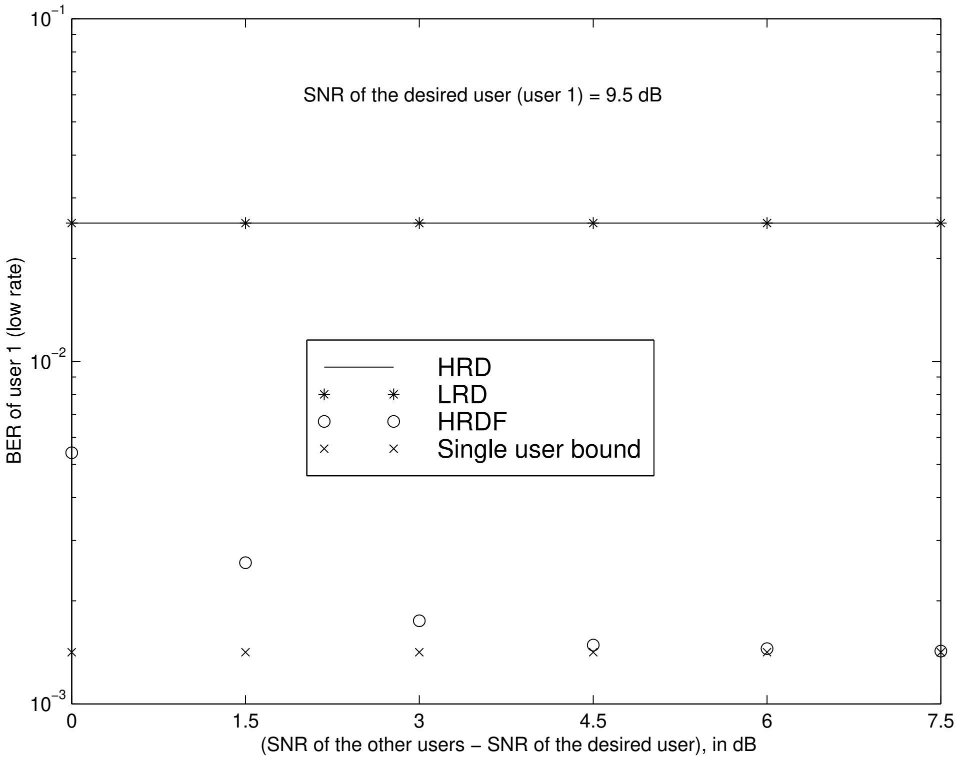

Figure 5.6: Bit error rate of user 1 (group 0) is shown for $K_0 = 2$, $K_1 = 2$, $L_0 = 56$ and $L_1 = 7$.

In the following experiments, the performance of the simulated HRDF system was compared to the evaluated performance of the LRD and HRD. First we observed the bit error rate (BER) of the group 0 user 1 as a function of the SNR of the other users, while the SNR of the desired group 0 user was fixed at 9.5 dB; see Figure 5.6. In this experiment, it was found that the proposed receiver, HRDF, significantly outperforms the LRD and HRD. As the other users become stronger relative to the desired user, the feedback data for decoding the desired user became more accurate. As a consequence, the BER of user 1 approached the single user bound; see Figure 5.6. Note that the high rate and low rate decorrelators yielded the same bit error probability for the group 0 user. This was observed in Theorem 1 to be a consequence of using the same cross-correlation matrix in every subinterval i. From Figure 5.6, we see that the HRDF performs better than either of the dual rate decorrelators of Chapter 3 for all operating points we have considered.

Until the Mth subinterval, the group 1 users were decoded by decorrelating the

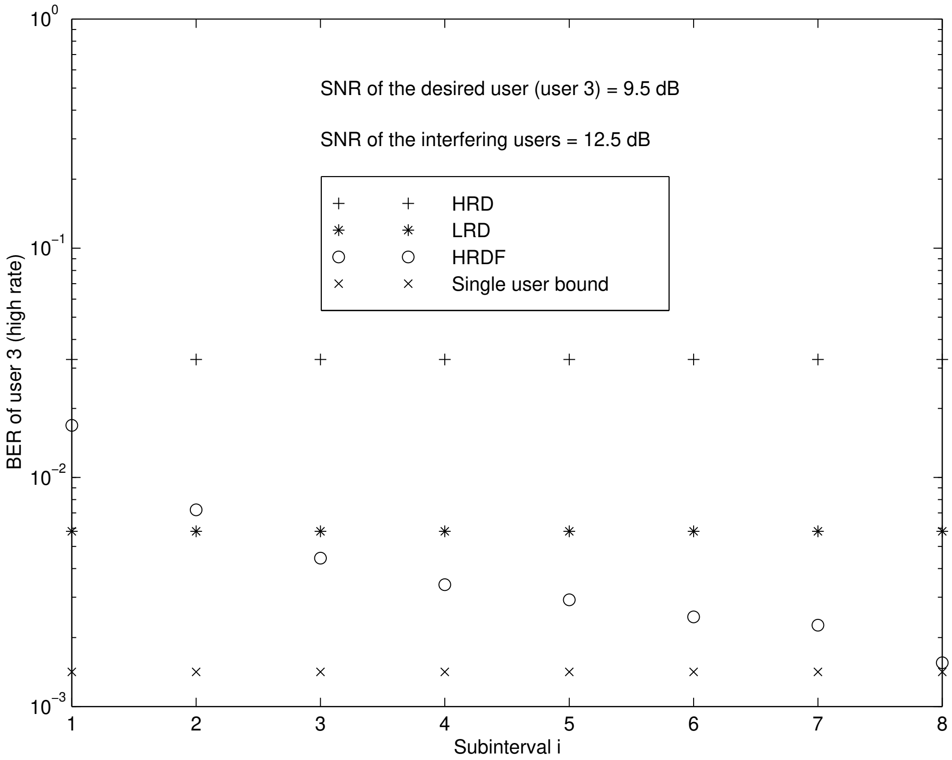

Figure 5.7: Bit error rate of user 3 (group 1) is plotted for $K_0 = 2$, $K_1 = 2$, $L_0 = 56$ and $L_1 = 7$.

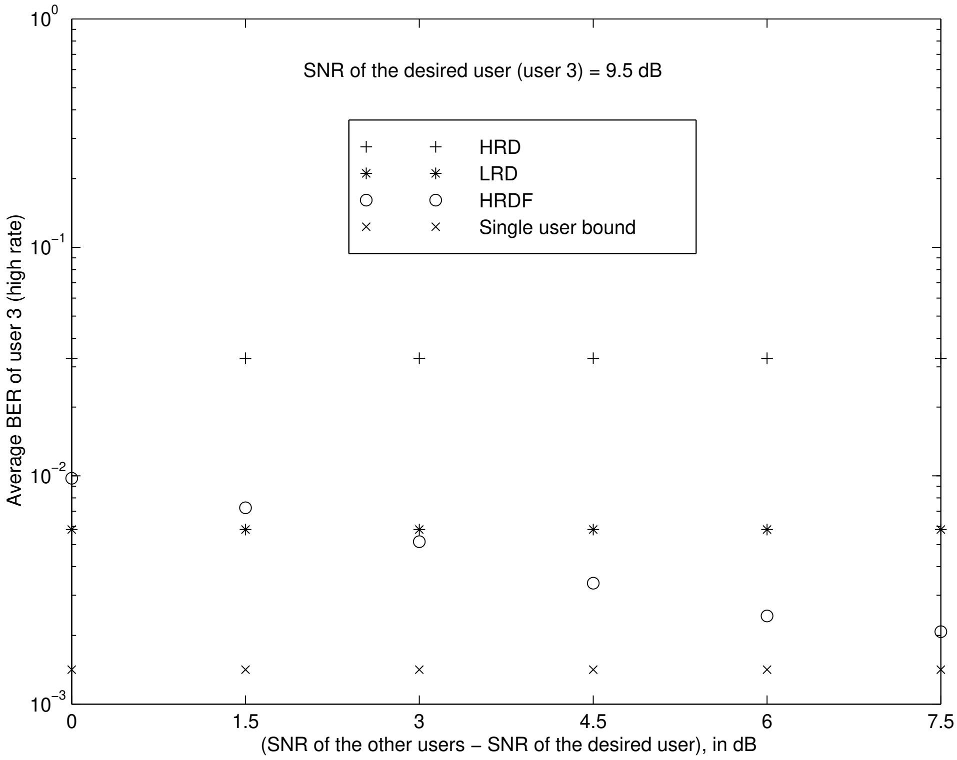

Figure 5.8: Average bit error rate of user 3 (group 1) is shown for $K_0 = 2$, $K_1 = 2$, $L_0 = 56$ and $L_1 = 7$.

group 0 users which enhanced the noise variance of the group 1 users. However, in this specific example (using the signature sequences shown in Figure 3.10), the enhancement of the noise variance became smaller as i increased. In other words, in successive subintervals, the group 1 user experienced less multi-user interference from group 0 users and hence decreasing BER; see Figure 5.7. In this experiment, the BER of user 3 (a group 1 user) in different subintervals, i, was observed when the SNR of the other users was 12.5 dB and the SNR of the desired group 1 user was fixed at 9.5 dB. Here, it was also noted that user 3 observed sharp improvement in the BER at the Mth subinterval compared to the $(M-1)$th subinterval. This result showed the gain from using decision feedback for the group 0 users over decorrelating the group 0 users at the Mth subinterval.

In order to quantify the relative performance of the HRDF with respect to the HRD and the LRD for decoding the group 1 user, we defined the *average BER* of the kth group 1 user as

$$\bar{P}_{k,1} = \frac{1}{M}\sum_{i=1}^{M} P_{k,1}^{(i)}$$

where $P_{k,1}^{(i)}$ denoted the BER of the kth group 1 user at the ith subinterval under the HRDF system. Since, interference cancellation was done in the HRDF system by increasing the observation window from $i = 1$ to M, the above performance measure yielded a composite performance metric for the entire window. In Figure 5.8, we have plotted the average BER of user 3 as a function of the SNR of the interfering users. In this experiment, it was observed that as the interfering users became stronger, the performance of the HRDF approached to the single user bound.

5.5 Chapter Summary

We have found that similar to the high rate decorrelator, HRD, our proposed high rate decision feedback decorrelating detector, HRDF, eliminates the bit processing delay of the low rate decorrelator, LRD and outperforms both the LRD and the HRD. Our experimental results showed that as the interfering users grew stronger, the bit error rate of the weaker user approached the single user bound. In addition, we have also observed that HRDF system is as bandwidth efficient as the LRD system.

Chapter 6

An Asynchronous Multi-rate Decorrelator

6.1 Introduction

In [29], the asynchronous decorrelator for a single rate DS/CDMA system was proposed. This decorrelator achieves the optimum near-far resistance [28, 29] by extending the observation window to infinity. However, only the decorrelator with a finite observation window, the *truncated* or *finite window decorrelator* [22,68] can be implemented. On the other hand, the truncated window decorrelator may perform poorly or may not even be feasible. Naturally, the existence of a decorrelator hinges on the linear independence of the transmitted signature waveforms within the observation window. References [22,23] showed by example that a decorrelator with a moderate observation window length asymptotically achieves the performance of the infinite window decorrelator. Within a signal processing framework, reference [56] studied finite window decorrelators for an asynchronous system with multipath. This work investigated the existence of FIR decorrelating receivers.

For a single rate asynchronous system, a sliding window decorrelator (SLWA) was proposed in [71] to improve the decorrelator's performance. However, the SLWA works only with coded DS/CDMA systems. The paper [77] suggested the insertion of isolated bits into the information streams before modulation in order to realize a finite window decorrelator. This technique reduces the effective throughput of the system. Alternative solutions to the infinite window decorrelator can also be found in [2, 12] which consider asynchronous DS/CDMA systems supporting users transmitting at the same bit rate. Reference [38] designed a decorrelator employing finite precision sequences for despreading. To improve the performance of the HRD for decoding the high rate users, a sliding window decorrelator was proposed in [5]. The performance improvement is achieved by sliding the observation window and estimating the high rate bits several times.

Generalizing the synchronous dual-rate system model of Chapter 2, this chapter derives an asynchronous multi-rate DS/CDMA system. For the asynchronous multi-rate DS/CDMA system, we will propose a decentralized, truncated window decorrelator called the *asynchronous multi-rate decorrelator* or *AMD*. The AMD will decode bits of a user by employing a set of modified correlators. Due to the decentralization of our decorrelator, each user will be able to suppress the multiuser interference as long as that user has non-zero asymptotic efficiency [28,29] over its observation window. In this chapter, we prove that the performance of any truncated window decorrelator improves monotonically with the observation window length. However, a longer observation window yields greater computational complexity. Therefore, in order to implement the AMD, a user should only extend the observation window over reasonable number of bits. For a given observation window, we will derive upper and lower bounds on the performance of the infinite window decorrelator. These bounds are functions of the observation window length and follow naturally from the implementation of the AMD. These bounds help us to characterize practical window sizes. Our experimental results show that as the window size increases, the bounds converge rapidly to the performance of the infinite window decorrelator. In addition, analyzing these bounds one can obtain significant insights into the performance of a truncated window decorrelator.

6.2 Asynchronous Multi-rate System

Similar to the synchronous dual-rate system of Chapter 2, in our asynchronous multi-rate DS/CDMA system model, each bit results in the baseband transmission of a sequence of pulses, $p[t]$. Each pulse has a duration of one chip period T_c. These pulses are sent over an additive white Gaussian noise channel in which the noise $n(t)$ has power spectral density σ^2.

For a system with K users, the transmission rate of user j is denoted by $R_j = M_j R$ for an integer $M_j \geq 1$, where R denotes the system base rate. The bit transmission time of user j is $T_j = 1/R_j$ and the processing gain is $L_j = T_j/T_c$. The jth user has signature waveform

$$S_j(t) = \sum_{m=1}^{L_j} \{a_j(m) \frac{1}{\sqrt{L_j}} p[t - (m-1)T_c]\} \qquad t \in [0, T_j] \tag{6.1}$$

where $a_j(m) \in \{-1, 1\}$ denotes the signature sequence of user j. The energy of the pulse $p[t]$ is normalized so that for all j,

$$\int_0^{T_j} S_j^2(t)\, dt = 1 \tag{6.2}$$

Let us denote Δ_j as the delay of the jth user. In the asynchronous channel, the received signal due to the jth user is given by

$$r_j(t) = \sum_{i=-\infty}^{+\infty} b_j^{(i)} \sqrt{E_j^{(i)}} S_j(t - iT_j - \Delta_j) \qquad 1 \le j \le K \tag{6.3}$$

where $b_j^{(i)} \in \{-1, +1\}$ is the ith bit and $E_j^{(i)}$ is the received energy of the jth user.

We assume that the receiver knows the time delay Δ_j for each user j and the received signal is

$$r(t) = \sum_{k=1}^{K} r_k(t) + n(t) \tag{6.4}$$

Without loss of generality, rest of the chapter will consider user j of equation (6.3) as the user of interest. As a consequence, we will concentrate on decoding the ith bit $b_j^{(i)}$, $0 \le i \le M_j - 1$ of user j. In order to decode $b_j^{(i)}$, we assume $\Delta_j = 0$ and that the other Δ_k are computed relative to $\Delta_j = 0$. It may be desirable for different bits to be processed using different window sizes. The bit $b_j^{(i)}$ will be decoded by processing the following windowed received signal

$$R_j^{(i)}(t) = r(t)\left[u\left(t - [i - n_j^{(i)}]T_j\right) - u\left(t - [i + 1 + d_j^{(i)}]T_j\right)\right] \tag{6.5}$$

where $u(t)$ is the unit step function. With respect to bit $b_j^{(i)}$, the window of $R_j^{(i)}(t)$ extends $n_j^{(i)}$ bits into the past and $d_j^{(i)}$ bits into the future. As a result, the length of the ith observation window becomes $n_j^{(i)} + d_j^{(i)} + 1$ bits.

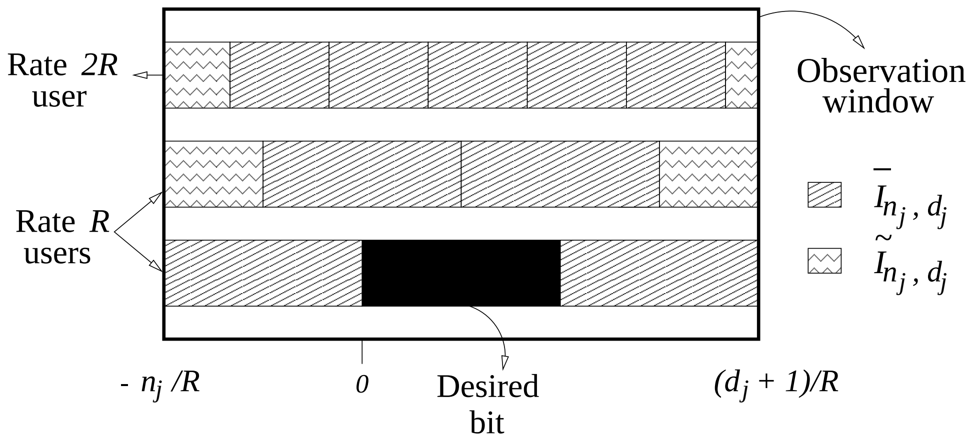

Figure 6.1: This figure depicts two types of interfering signatures (non-zero portions only) when the desired user j is a rate R user.

6.3 The Asynchronous Multi-rate Decorrelator AMD

In this work, to implement the AMD, we focus our attention on the Gram-Schmidt orthogonalization. We make repeated use of a well known property of the Gram-Schmidt procedure. Let us assume two sets of functions $S_1 \subset S_2$ that are defined over the time interval $\left[-\bar{T}, \hat{T}\right]$. Gram-Schmidt orthogonalization on the set S_i, $i = 1, 2$, generates l_i normalized basis functions. Let V_i denote the orthonormal set of basis functions corresponding to the set S_i. For a function $v(t)$ with unit energy on $\left[-\bar{T}, \hat{T}\right]$, let $v_{i,m}$ denotes the projection of $v(t)$ on the mth basis function of the set V_i, then

$$1 - \sum_{m=1}^{l_1} v_{1,m}^2 \geq 1 - \sum_{m=1}^{l_2} v_{2,m}^2 \tag{6.6}$$

In the following section, we will see that Gram-Schmidt orthogonalization on the interfering users' signature waveforms is equivalent to solving a functional constrained maximization problem.

6.3.1 The Modified Correlator Signal

Among the M_j bits of user j, now we will concentrate on the bit $b_j^{(0)}$ that was transmitted using the signature sequence $S_j(t)$ of equation (6.1). For the sake of simplicity, the superscript which denotes the bit number will be ignored. We denote I_{n_j,d_j} as a set of signature waveforms that are generated by the interfering users' within the observation window $[-n_jT_j, (d_j+1)T_j]$. The size of the set I_{n_j,d_j} is L_{n_j,d_j}.

We decompose I_{n_j,d_j} into the disjoint union

$$I_{n_j,d_j} = \bar{I}_{n_j,d_j} \cup \tilde{I}_{n_j,d_j}$$

where, $\bar{I}_{n_j,d_j}$ is the set of normalized interfering signatures corresponding to complete bit transmissions within the observation window. The term $\tilde{I}_{n_j,d_j}$ is the set of interfering partial signature waveforms. Each signature in $\tilde{I}_{n_j,d_j}$ is truncated either at the left boundary $-n_jT_j$ or the right boundary $(d_j+1)\,T_j$ of the observation window and hence, it is not normalized. Note that other bits of user j within the window $[-n_jT_j, (d_j+1)T_j]$ are included in $\bar{I}_{n_j,d_j}$. The sets $\bar{I}_{n_j,d_j}$ and $\tilde{I}_{n_j,d_j}$ are depicted in Figure 6.1. In the set I_{n_j,d_j}, we order the subset $\bar{I}_{n_j,d_j}$ first.

Let us assume that the Gram-Schmidt procedure on the set I_{n_j,d_j} yields $l_{n_j,d_j} \leq L_{n_j,d_j}$ orthonormal basis functions. This set of basis function is denoted as

$$\Psi_{n_j,d_j} = \left\{\Psi_m(t) : m = 1, \ldots, l_{n_j,d_j}\right\} \tag{6.7}$$

Among the l_{n_j,d_j} basis functions, the first $\bar{l}_{n_j,d_j}$ basis functions are generated by the subset $\bar{I}_{n_j,d_j}$. Let us define the set

$$Q_j = I_{n_j,d_j} \cup \{S_j(t)\}$$

We also assume that $S_j(t)$ is numbered $(l_{n_j,d_j}+1)$ in the signal set Q_j. If the projection of $S_j(t)$ onto the subspace orthogonal to the set I_{n_j,d_j} is non-zero, then the Gram-Schmidt procedure on the set Q_j will yield a new non-zero normalized basis function

$$\Phi_0(t) = \Psi_{l_{n_j,d_j}+1}(t) \tag{6.8}$$

in addition to the set Ψ_{n_j,d_j} of equation (6.7). We will find that the following property of $\Phi_0(t)$ will prove useful.

Theorem 4 *The Gram-Schmidt orthonormal basis function $\Phi_0(t)$ of equation (6.8) is the solution to the following optimization problem:*

$$\begin{array}{rll} \sqrt{\zeta_{n_j,d_j}} = max_{\Phi(t)} & \int_{-n_jT_j}^{(d_j+1)T_j} \Phi(t)S_j(t)\,dt & \\ subject\ to & \int_{-n_jT_j}^{(d_j+1)T_j} \Phi(t)I_m(t)\,dt = 0 & I_m(t) \in I_{n_j,d_j} \\ & \int_{-n_jT_j}^{(d_j+1)T_j} \Phi^2(t)\,dt = 1 & \end{array} \tag{6.9}$$

Proof: By definition of $\Psi_{l_{n_j,d_j}+1}(t)$,

$$S_j(t) = \sum_{m=1}^{l_{n_j,d_j}+1} \psi_m \Psi_m(t) \tag{6.10}$$

where

$$\psi_m = \int_{-n_j T_j}^{(d_j+1)T_j} \Psi_m(t) S_j(t)\, dt \tag{6.11}$$

Note that the coefficient $\psi_{l_{n_j,d_j}+1}$ satisfies

$$\psi_{l_{n_j,d_j}+1} = \left\{ 1 - \sum_{m=1}^{l_{n_j,d_j}} \psi_m^2 \right\}^{\frac{1}{2}} > 0 \tag{6.12}$$

Let us assume that $\hat{\Phi}(t)$ is a feasible solution to equation (6.9). This implies that $\hat{\Phi}(t)$ is orthogonal to each $I_m(t) \in I_{n_j,d_j}$. Thus, $\hat{\Phi}(t)$ is orthogonal to each orthonormal basis function, $\Psi_m(t) \in \Psi_{n_j,d_j}$. Hence, by equation (6.10),

$$\begin{aligned}
\int_{-n_j T_j}^{(d_j+1)T_j} \hat{\Phi}(t) S_j(t)\, dt &= \sum_{m=1}^{l_{n_j,d_j}+1} \psi_m \int_{-n_j T_j}^{(d_j+1)T_j} \hat{\Phi}(t) \Psi_m(t)\, dt && (6.13)\\
&= \psi_{l_{n_j,d_j}+1} \int_{-n_j T_j}^{(d_j+1)T_j} \hat{\Phi}(t) \Psi_{l_{n_j,d_j}+1}(t)\, dt && (6.14)\\
&\leq \psi_{l_{n_j,d_j}+1} && (6.15)
\end{aligned}$$

The inequality of equation (6.15) is simply the Schwarz Inequality

$$\int_{-n_j T_j}^{(d_j+1)T_j} \hat{\Phi}(t) \Psi_{l_{n_j,d_j}+1}(t)\, dt \leq \left[\int_{-n_j T_j}^{(d_j+1)T_j} \hat{\Phi}^2(t)\, dt \right]^{\frac{1}{2}} \left[\int_{-n_j T_j}^{(d_j+1)T_j} \Psi^2_{l_{n_j,d_j}+1}(t)\, dt \right]^{\frac{1}{2}} \tag{6.16}$$

and equality holds iff

$$\hat{\Phi}(t) = \Psi_{l_{n_j,d_j}+1}(t) = \Phi_0(t) \tag{6.17}$$

□

Note that the solution to the maximization problem (6.9) is equivalent to the decorrelator; please see [38]. Also in [56], the decorrelator was observed as a solution to a constrained minimization problem.

We will use the basis function $\Phi_0(t)$ as the modified correlator signal to decode the bit b_j. Since $\Phi_0(t)$ is orthogonal to all interfering signatures $I_m(t) \in I_{n_j,d_j}$, the output of the desired modified correlator is

$$r_j = \int_{-n_jT_j}^{(d_j+1)T_j} R_j(t)\Phi_0(t)\,dt = \psi_{l_{n_j,d_j}+1}\sqrt{E_j}b_j + N_j \tag{6.18}$$

where N_j is a Gaussian random variable with mean zero and variance σ^2. The corresponding decoding rule will be

$$\bar{b}_j = \operatorname{sgn}(r_j) \tag{6.19}$$

The probability that the bit b_j is decoded incorrectly is

$$q_{n_j,d_j} = Q\left(\sqrt{\frac{\zeta_{n_j,d_j}E_j}{\sigma^2}}\right) \tag{6.20}$$

where $Q(\cdot)$ is the standard normal complementary CDF and

$$\zeta_{n_j,d_j} = \psi^2_{l_{n_j,d_j}+1} = \left\{\int_{-n_jT_j}^{(d_j+1)T_j} \Phi_0(t)S_j(t)\,dt\right\}^2 \tag{6.21}$$

The term ζ_{n_j,d_j} is the asymptotic efficiency [28,29] of the AMD for decoding the bit b_j in the observation window $[-n_jT_j,(d_j+1)T_j]$. In equation (6.20), E_j/σ^2 is independent of n_j and d_j. Therefore analyzing the bit error q_{n_j,d_j} as a function of both n_j and d_j is equivalent to analyzing the asymptotic efficiency ζ_{n_j,d_j} as a function of both n_j and d_j. For the AMD, we will use the asymptotic efficiency ζ_{n_j,d_j} as the performance measure.

We now establish that it is always possible to improve the performance of the AMD by increasing the length of the observation window.

Theorem 5 *The asymptotic efficiency, ζ_{n_j,d_j} is an increasing function of both n_j and d_j.*

Proof: For $\delta \geq 0$, let $n'_j = n_j + \delta$. We will show that $\zeta_{n_j,d_j} \leq \zeta_{n'_j,d_j}$. A similar argument will hold when we increase d_j.

Theorem 4 implies that for the observation window of size $n'_j + d_j + 1$, the modified correlator signal $\Theta_0(t)$ is the solution to the following optimization problem.

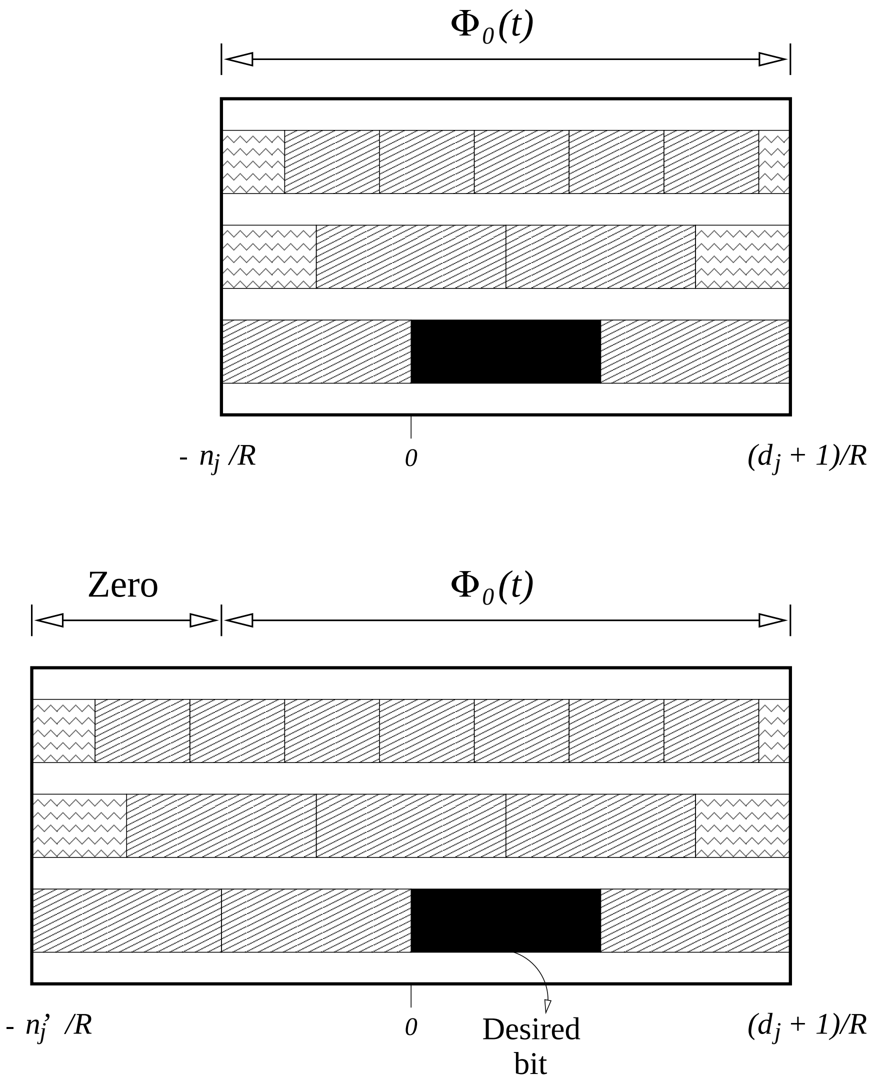

Figure 6.2: This figure depicts how $\Phi_0(t)$ is orthogonal to each signal $I_m(t) \in I_{n'_j,d_j}$. Here the desired user j is a rate R user.

$$\begin{array}{rll} \sqrt{\zeta_{n'_j,d_j}} = \max_{\Theta(t)} & \int_{-n'_jT_j}^{(d_j+1)T_j} \Theta(t)S_j(t)\,dt & \\ \text{subject to} & \int_{-n'_jT_j}^{(d_j+1)T_j} \Theta(t)I_m(t)\,dt = 0 \qquad I_m(t) \in I_{n'_j,d_j} & \\ & \int_{-n'_jT_j}^{(d_j+1)T_j} \Theta^2(t)\,dt = 1 & \end{array} \tag{6.22}$$

Now we will verify that the solution to equation (6.9), $\Phi_0(t)$ satisfies the constraint (6.22) and thus it will be a feasible solution to the optimization problem. The signature waveforms of the set $I_{n'_j,d_j}$ will be partitioned as $I_{n'_j,d_j} = I'_{n'_j,d_j} \cup I''_{n'_j,d_j}$. We define $I'_{n'_j,d_j}$ and $I''_{n'_j,d_j}$ as follows.

- $I'_{n'_j,d_j} = \hat{I}_{n'_j,d_j} \cup \bar{I}_{n_j,d_j}$, where each $I'_m(t) \in \hat{I}_{n'_j,d_j}$ is the result of extending the partial signature $I_m(t) \in \tilde{I}_{n_j,d_j}$ over the new observation window. Theorem 4 implies that the signal $\Phi_0(t)$ is orthogonal to each $I_m(t) \in I_{n_j,d_j}$. Since $\Phi_0(t)$ is non-zero only for $t \in [-n_jT_j, (d_j+1)T_j]$, for each $I'_m(t) \in \hat{I}_{n'_j,d_j}$, we can write

$$\int_{-n'_jT_j}^{(d_j+1)T_j} \Phi_0(t)I'_m(t)\,dt = \int_{-n_jT_j}^{(d_j+1)T_j} \Phi_0(t)I_m(t)\,dt = 0 \tag{6.23}$$

  Again, as $\bar{I}_{n_j,d_j} \subset I_{n_j,d_j}$, $\Phi_0(t)$ is orthogonal to each $I_m(t) \in \bar{I}_{n_j,d_j}$. These observations can be easily verified by Figure 6.2.

- $I''_{n'_j,d_j}$ is the subset of signatures which are zero over $[-n_jT_j, (d_j+1)T_j]$. Once again, since $\Phi_0(t)$ is non-zero only for $t \in [-n_jT_j, (d_j+1)T_j]$, the signal set $I''_{n'_j,d_j}$ is orthogonal to $\Phi_0(t)$; please see Figure 6.2.

The above observations imply that $\Phi_0(t)$ is orthogonal to each $I_m(t) \in I_{n'_j,d_j}$. Thus, the function $\Phi_0(t)$ of equation (6.9) is feasible with respect to the constraint (6.22), however, it may be or may not be the optimal solution. Hence $\zeta_{n_j,d_j} \leq \zeta_{n'_j,d_j}$. □

Theorem 5 implies that in a multi-rate asynchronous channel, the infinite window decorrelator performs better than any truncated window decorrelator. In Chapter 3 , we have proposed two types of decorrelators, called the low rate decorrelator (LRD) and the high rate decorrelator (HRD), for a dual rate synchronous DS/CDMA system. The LRD decodes bits using a window size of one low rate bit, whereas, the HRD decodes bits using a window size of one high rate bit. As the HRD is a truncated window decorrelator for a dual-rate synchronous DS/CDMA system, Theorem 5 implies that the LRD always outperforms the HRD. This result has been proven in Chapter 3 by studying the structures of the LRD and HRD cross-correlation matrices; please see Theorems 1 and 2.

Theorem 5 encourages the receiver designer to extend the observation window for improved receiver performance. However, further extension of the observation window may provide a negligible performance gain compared to the increase in receiver complexity. Therefore, based on the asymptotic efficiency of the truncated window decorrelator, we will develop a simple upper bound on the performance of the infinite

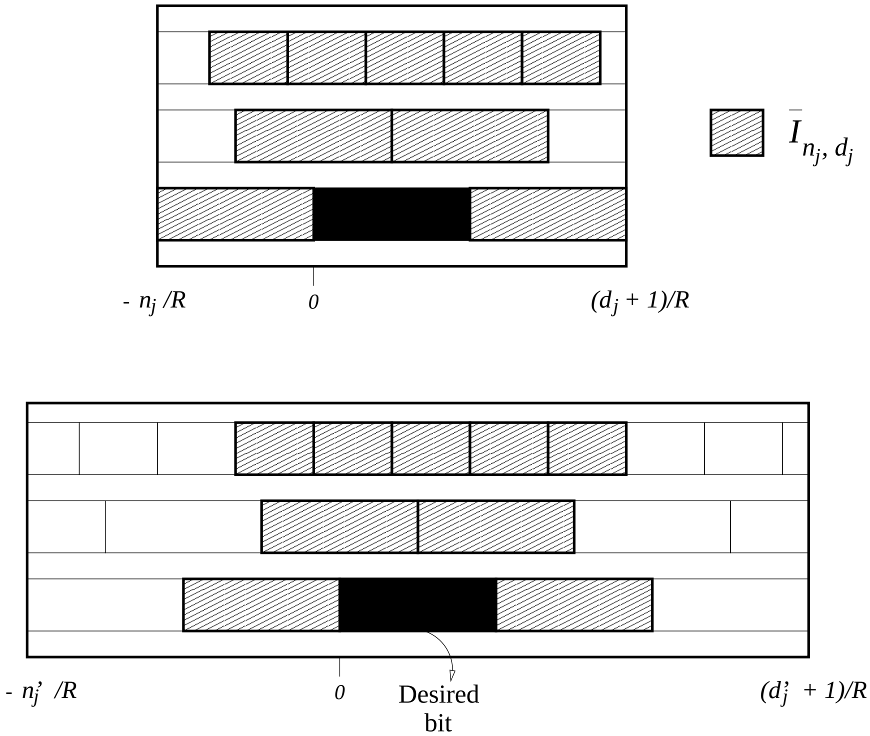

Figure 6.3: This figure shows that $\bar{I}_{n_j,d_j} = I_{n_j,d_j} \cap I_{n'_j,d'_j}$.

window decorrelator. This upper bound will indicate whether the observation window should be extended. We will see that this upper bound can be determined easily from the construction of the modified correlator.

Using equation (6.11), we define $\bar{\zeta}_{n_j,d_j}$ as

$$\bar{\zeta}_{n_j,d_j} = 1 - \sum_{m=1}^{\bar{l}_{n_j,d_j}} \psi_m^2 \tag{6.24}$$

Recall that first $\bar{l}_{n_j,d_j}$ basis functions of the set Ψ_{n_j,d_j} of equation (6.7) are generated by the subset $\bar{I}_{n_j,d_j}$. In equation (6.24), the term $\sum_{m=1}^{\bar{l}_{n_j,d_j}} \psi_m^2$ or $\left(1 - \bar{\zeta}_{n_j,d_j}\right)$ denotes the energy of the desired signature waveform which is projected on the subspace spanned by $\bar{I}_{n_j,d_j}$. Note that $\bar{\zeta}_{n_j,d_j}$ would be the asymptotic efficiency if it were only necessary to decorrelate against the complete signatures in the observation window $[-n_jT_j, (d_j+1)T_j]$. Now we will derive the upper bound on the performance of the infinite window decorrelator by proving the following theorem.

Theorem 6 *For any observation window of duration* $\left[-n'_jT_j, (d'_j+1)T_j\right]$, *where* $n'_j \geq$

n_j and $d'_j \geq d_j$, the asymptotic efficiency $\zeta_{n'_j,d'_j}$ will be bounded by

$$\zeta_{n_j,d_j} \leq \zeta_{n'_j,d'_j} \leq \bar{\zeta}_{n_j,d_j} \tag{6.25}$$

and $\bar{\zeta}_{n_j,d_j}$ is a decreasing function of both n_j and d_j.

Proof: Theorem 5 implies that $\zeta_{n_j,d_j} \leq \zeta_{n'_j,d'_j}$. Recall that the subset $\bar{I}_{n_j,d_j}$ consists of complete signature waveforms. The observation window $\left[-n'_jT_j, (d'_j+1)T_j\right]$ contains all the complete signature waveforms of the observation window $[-n_jT_j, (d_j+1)T_j]$ or $\bar{I}_{n_j,d_j} \subset \bar{I}_{n'_j,d'_j}$; please see Figure 6.3. However, $\bar{I}_{n'_j,d'_j} \subset I_{n'_j,d'_j}$. Therefore, using equation (6.6), we will write

$$\zeta_{n'_j,d'_j} \leq \bar{\zeta}_{n_j,d_j} \tag{6.26}$$

Since $\bar{I}_{n_j,d_j} \subset \bar{I}_{n'_j,d'_j}$, the result of equation (6.6) also implies

$$\bar{\zeta}_{n'_j,d'_j} \leq \bar{\zeta}_{n_j,d_j} \tag{6.27}$$

□

The above theorem remains true as n'_j and d'_j approach infinity. Thus the asymptotic efficiency of the infinite window decorrelator is always lower bounded by ζ_{n_j,d_j} which is a monotonic increasing function of both n_j and d_j and upper bounded by $\bar{\zeta}_{n_j,d_j}$ which is a monotonic decreasing function of both n_j and d_j.

We observe that Theorems 5 and 6 remain true when different bits of a user are processed with different signature waveforms such as random CDMA (R-CDMA) [63]. Furthermore, Theorems 5 and 6 hold for any nonnegative increment of the observation window. However, in order to implement the AMD, we will assume that the increment of the observation window is a non-negative integer number of the desired user's bits.

The proposed receiver has the following features. The timing of all users must be acquired. The AMD will be able to decode a user by suppressing the multiuser interference as long as the desired user has non-zero asymptotic efficiency. We have mentioned earlier that, in the observation window $[-n_jT_j, (d_j+1)T_j]$, the first $\bar{l}_{n_j,d_j}$ basis functions are generated by orthogonalizing the sub-set $\bar{I}_{n_j,d_j} = I_{n_j,d_j} \cap I_{n'_j,d'_j}$.

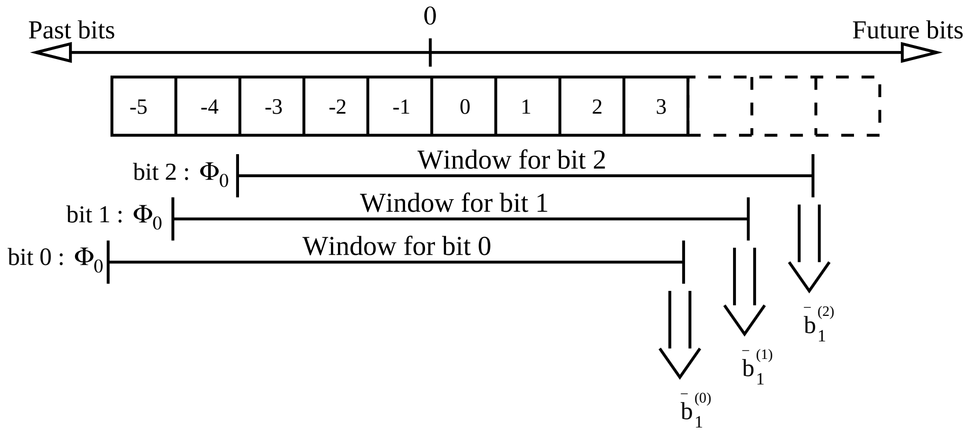

Figure 6.4: Here we have assumed that user j is a rate R user and $n_j^{(0)} = 5$ and $d_j^{(0)} = 3$. This picture depicts operation of the correlators which decode $b_j^{(0)}, b_j^{(1)}$ and $b_j^{(2)}$. The modified correlator signals are time shifted versions of one another.

These $\bar{l}_{n_j,d_j}$ basis functions can be used directly in the longer observation window $\left[-n_j'T_j, (d_j'+1)T_j\right]$. We have shown the decoding technique of the 0th bit. Similarly, modified correlators will be generated for decoding the ith bit of user j, where $i = 1, \ldots, M_j - 1$. In this case, the origin of the observation window slides by an additional T_j for each subsequent bit decoded. After each M_j bits, user j will observe the same pattern of signature waveforms from the other interfering users. Thus, the receiver dedicated to the user j needs to know the specifications of M_j modified correlators; see Figure 6.4. Furthermore, the user j will experience M_j different asymptotic efficiencies or BERs.

6.4 Empirical Results

In our experiments, we modeled a dual-rate asynchronous DS/CDMA system. The processing gain of the low rate users was 64 and the processing gain of the high rate users was 8. The signature waveforms were generated using random signature sequences. The time offsets of different users were also randomly generated. To simplify the computations, we assumed that the time offsets were multiples of the chip duration. The desired bit was decoded by employing a symmetric observation window with $n_j = d_j$.

First, we considered an asynchronous dual-rate system with five low rate and five high rate users. For a low rate user, Figure 6.5 shows upper and lower bounds of

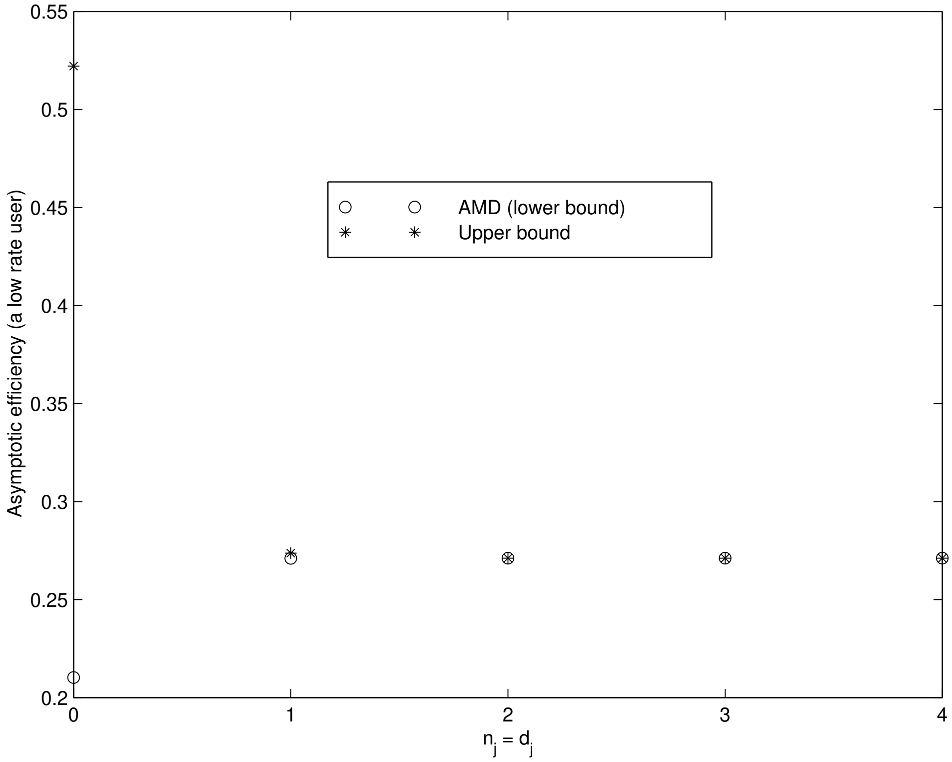

Figure 6.5: For a dual-rate CDMA system, the asymptotic efficiency of a low rate bit is plotted as a function of $n_j = d_j$ for an observation window of length $n_j + d_j + 1$.

Theorem 6 as a function of n_j, when $n_j = d_j$. Note that for each low rate user j, $M_j = 1$. Thus in each sliding window of fixed n_j and d_j, the low rate user saw the same interfering signatures. This implies that for fixed n_j and d_j, each bit of the low rate user experienced the same asymptotic efficiency. When $n_j = d_j = 0$, for the desired low rate user, the AMD was equivalent to the one shot decorrelator of [68]. The performance of the AMD or the lower bound of Theorem 6 improved dramatically when n_j and d_j were increased by one. At $n_j = d_j = 1$, the difference between the upper bound and lower bound was insignificant. This fact coupled with Theorem 6, indicated that a further increase of the observation window would not yield any significant performance gain. This observation was verified by our experimental results; see Figure 6.5.

For the same experiment, similar results were observed for the 0th bit of a high rate user; see Figure 6.6 where asymptotic efficiency of the desired bit is plotted as a function of n_j and d_j, where $n_j = d_j = 0, \ldots, 20$. In this example, the AMD did not

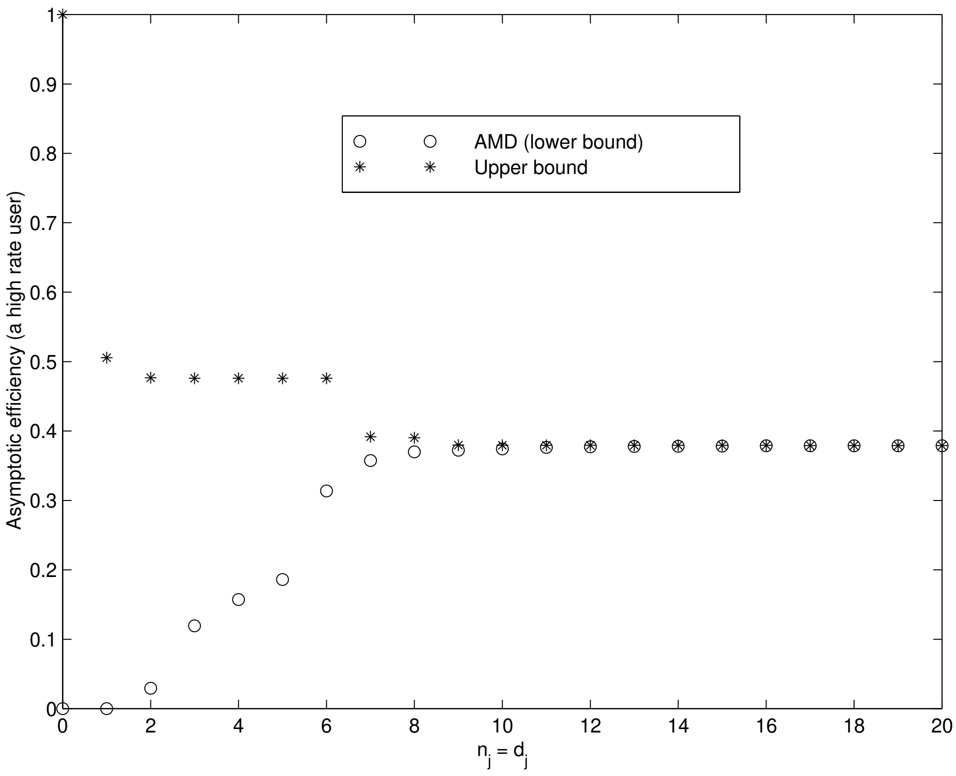

Figure 6.6: For a dual-rate CDMA system, the asymptotic efficiency of a high rate bit is given as a function of $n_j = d_j$ for an observation window of length $n_j + d_j + 1$.

provide the desired bit non-zero asymptotic efficiency at $n_j = d_j = 0, 1$; however, further increment of the observation window provided the desired bit a non-zero asymptotic efficiency. Here we noticed that the AMD performed closely to the upper bound at $n_j = d_j = 7$. In this example along with the example of Figure 6.5 at $n_j = d_j = 1$, when the observation window covered the interfering signatures which had non-zero cross correlations with the desired signature, the AMD performed very closely to the infinite window decorrelator.

It is desirable to characterize practical window sizes as a function of the cross-correlations of the users and the number of users in the system. Therefore, in the next experiment, as a function of the number of users in the system, we found the minimum length of the observation window which guaranteed a high rate user with at least 90% of the maximum asymptotic efficiency, $\zeta_{\infty,\infty}$. This quality of service (QoS) objective was met by satisfying $\zeta_{n_j,d_j} \geq 0.9\bar{\zeta}_{n_j,d_j}$; see Theorem 6. To observe the effect of the

Number of users		Trial 1			Trial 2		
Low rate	High rate	LB	UB	W	LB	UB	W
1	1	1.00000	1.00000	1	0.90909	1.00000	3
2	2	0.90651	0.96825	5	0.90653	0.96825	3
3	3	0.67676	0.68046	15	0.56567	0.60897	3
4	4	0.48395	0.50117	15	0.37066	0.37572	13
5	5	0.35731	0.39171	15	0.22128	0.23156	13
6	6	0.08026	0.08994	21	0.19628	0.20905	19

Figure 6.7: In this experiment, we determined the minimum window size that guaranteed a high rate bit with at least 90% of the maximum asymptotic efficiency. Here $LB = \zeta_{n_j,d_j}$ and $UB = \bar{\zeta}_{n_j,d_j}$ are the lower and upper bounds on the infinite asymptotic efficiency and $W = n_j + d_j + 1$ is the window size.

cross-correlations of the users on practical window sizes, we performed this experiment for two different sets of signatures and time offsets. Our experimental results are shown in Figure 6.7. In each experimental trial, we started with one low rate and one high rate user and then sequentially added a pair of users, one low rate and one high rate. The signatures and time offsets were randomly generated. Here the experimental results showed that increasing the number of users resulted in smaller values of $\zeta_{\infty,\infty}$ which required longer observation windows. As expected, when the number of users in each group is fixed, different sets of users' cross-correlations yielded different window sizes.

In the above experiments, it was observed that the bounds of Theorem 6 converged quickly as the length of the observation window increased. When the infinite window decorrelator did not suffer from poor performance, we obtained ζ_{n_j,d_j} very close to $\zeta_{\infty,\infty}$ by extending the observation window over the interfering signatures which had non-zero cross-correlations with the desired signature. For a user with bit rate M_jR, this required $n_j = d_j = M_j$.

6.4.1 Implementation of the Gram-Schmidt Procedure

In our experiments, we used the classical Gram-Schmidt procedure (CGSP) from [14, page 218] or [41, page 159] for computing the orthonormal basis functions $\{\Psi_k(t)\}$. Often the CGSP suffers from poor numerical properties in that there is a loss of orthogonality among the computed orthonormal basis vectors. In theory, if at any step

m, the current signature $q_m(t) \in Q_j = I_{n_j,d_j} \cup \{S_j(t)\}$ is a linear combination of the previously generated orthonormal basis vectors, then step m of the CGSP will yield a zero vector. In practice, however, due to numerical errors, we might not have a zero vector from a signature $q_m(t)$, even though, it is a linear combination of the previously generated orthonormal basis vectors. As a result, there may be a loss of orthogonality among the computed orthonormal basis vectors. In our experiments, we alleviated this problem using the following technique.

Let us assume that at the end of step $m-1$ of the CGSP, there are m' orthonormal basis vectors, $\{\Psi_k(t); 1 \leq k \leq m'\}$, where $m' \leq m-1$. At step m, the signature $q_m(t)$ will yield orthonormal basis vector $m'+1$, if

$$\int_{-n_jT_j}^{(d_j+1)T_j} q_m^2(t)\,dt - \sum_{k=1}^{m'} \left\{ \int_{-n_jT_j}^{(d_j+1)T_j} q_m(t)\Psi_k(t)\,dt \right\}^2 \leq 10^{-20}$$

Otherwise, we assume that $q_m(t)$ is a linear combination of the previous m' orthonormal basis vectors. Using this approach, there will be some occasions for which the decorrelator will exist, however, our Gram-Schmidt procedure generates a zero function for the modified correlator. In this case, the ideal decorrelator will have a bit error rate less than a half, whereas our modified correlator will have a bit error rate of a half. As a result, the performance we achieve is upper bounded by the performance of the truncated window decorrelator that is not subject to finite precision.

An alternative procedure to overcome the shortcomings of the CGSP is the modified Gram-Schmidt procedure (MGSP) [14, page 218]. However, the complexity of the MGSP is higher than that of the CGSP.

6.5 Chapter Summary

In this chapter, we have studied a decentralized, truncated window decorrelator for an asynchronous DS/CDMA system which supports users of different bit rates. The decorrelator is implemented via a set of modified correlators whose signals are generated by applying the Gram-Schmidt procedure on the interfering signature set. It is proven that the performance of any truncated window decorrelator improves monotonically with the observation window length. To account for the complexity associated with long observation windows, the proposed decorrelator decodes a user by employing an observation window which is extended over a reasonable number of its bits. We have used the implementation of the truncated window decorrelator to develop upper and lower bounds on the performance of the infinite window decorrelator. These bounds are functions of the observation window length and can be used to compare the performance of the proposed decorrelator with the infinite window decorrelator. Numerical results showed that as the length of the observation window increased, the upper and lower bounds converged quickly to the performance of the infinite window decorrelator.

Chapter 7

Quality of Service for an Asynchronous Multi-rate Decorrelator

7.1 Introduction

Recently, several studies [25, 57, 60] have been performed in order to integrate power control with multiuser detectors. The motivation of these works was to achieve a performance gain over multiuser detection by providing power control for multiuser detection. References [25, 57] addressed power control for the linear MMSE multiuser receiver in a single-rate system. The proposed schemes are synchronous and require SIR (signal-to-interference ratio) measurements for the power updates.

In this chapter, a class of QoS objectives for the AMD are proposed. The choice of a QoS objective will dictate a corresponding power control algorithm. The criterion that is used for power control is minimize the total transmitted power while at the same time guaranteeing each user's QoS requirement. In this study, we consider the following QoS objectives.

- For each bit of a user, meet a bit error rate (BER) objective.
- Using a fixed transmitted power, provide an individual user with an average BER.
- Using a fixed transmitted power, guarantee a target BER to the bit with the lowest asymptotic efficiency or the worst BER.

If the uplink channel gain of the mobile is known then it is simple to provide each user its QoS objective. In practice, however, the measurement of the channel gain is non-trivial and neglects the stochastic behavior of the channel. This practical situation leads us to use stochastic approximation methods [44] to develop an asynchronous,

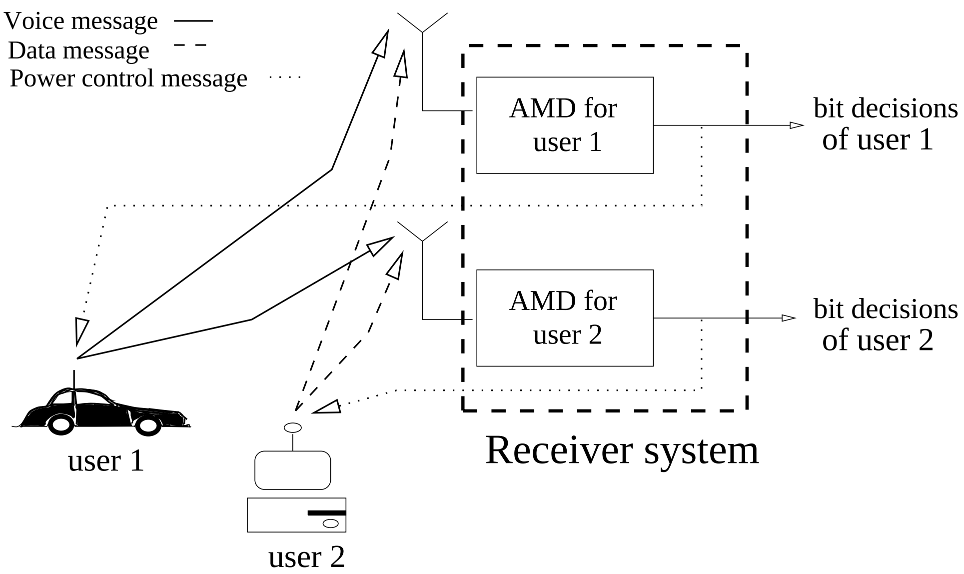

Figure 7.1: This figure depicts the working principle of the proposed stochastic power control algorithm for the asynchronous multi-rate decorrelator (AMD).

distributed, iterative power control algorithm for the AMD that finds the correct powers without knowledge of the uplink gain. In this stochastic power control algorithm, a mobile needs to know only the output of the AMD to update its transmitted power in order to achieve its QoS objective; please see Figure 7.1. The proposed power control algorithm is feasible as long as asymptotic efficiencies of the bits of the desired user are nonzero. In this case, the algorithm converges in the mean square sense to an optimal power at which the user achieves its QoS requirement.

The power control algorithm in this work is fundamentally different from power control algorithms that have been presented in the literature, for example [11,16,75,76]. These works have assumed the availability of perfect measurements of deterministic quantities such as the SIR, received power, or interference in order to prove that the transmitter powers converge deterministically to an optimum power vector. In practice, however, these quantities cannot be estimated perfectly and deterministic convergence results are invalid when these deterministic variables are replaced with their random estimates. Consequently, we adopt the term *stochastic power control* for algorithms that use actual random measurements to converge stochastically to the optimal transmitter power vector. For conventional matched filter receivers, [58] has studied stochastic power control for matched filter receivers where each user aims for a target SIR using its matched filter output. However, [58] required each user to estimate its uplink channel gain to its assigned base station. Following the approach of [58], this work also uses stochastic measurements at each user's filter output to derive stochastic mean square convergence results. Unlike [58] however, this work exploits the decorrelator's effective orthogonality of users at the receiver to develop an algorithm that does not require a user to know its uplink channel gain.

7.2 Quality of Service for the AMD

Since the transmitted power is proportional to the received energy, we will refer to $E_j^{(i)}$ of equation (6.3) as power. In this study, the asymptotic efficiency of the AMD for decoding the bit $b_j^{(i)}$ will be redefined as $\zeta_j^{(i)}$. Let us denote the uplink channel gain of user j by h_j and its transmitted power in the ith slot by $P_j^{(i)}$. Then the received power at the ith slot becomes $E_j^{(i)} = h_j P_j^{(i)}$.

We will now propose a class of QoS objectives for the AMD. The criterion that is used for power control is to guarantee each user's link quality objective or QoS requirement. We will consider the following link quality objectives.

- *The fixed BER (FB) objective:* Provide each bit of user j with a target probability of error q_j^*. Mathematically, we must choose a set of transmitter powers $P_j^{(i)}$, $i = 0, \ldots, M_j - 1$, such that

$$Q\left(\sqrt{\frac{\zeta_j^{(i)} h_j P_j^{(i)}}{\sigma^2}}\right) = q_j^* \qquad i = 0, \ldots, M_j - 1 \tag{7.1}$$

Note that the FB objective requires that the transmitter power of user j be adjusted from bit to bit. When the target BER q_j^* is low, then small variations in $\zeta_j^{(i)}$ will significantly change the transmitted power. Thus it may not be possible for user j to adjust the transmitter power quickly enough. This situation leads us to propose the following link quality objective.

- *Average BER (AB) objective:* Using a fixed transmitted power, guarantee user j an average bit error target q_j^* over M_j transmitted bits. Here $P_j^{(i)} = P_j$, for each bit $b_j^{(i)}$ and the link quality objective of user j is

$$\frac{1}{M_j}\sum_{i=0}^{M_j-1} Q\left(\sqrt{\frac{\zeta_j^{(i)} h_j P_j}{\sigma^2}}\right) = q_j^* \tag{7.2}$$

We observe that the AB objective achieves the same average BER as the FB objective by the use of a fixed transmitter power. The AB objective yields different BERs for different bits. The bit with the lowest asymptotic efficiency will experience the highest BER. In an asynchronous multi-rate channel, several bits of user j may experience significantly lower asymptotic efficiencies than others. In this case, user j may prefer to protect those bits which are suffering from low asymptotic efficiencies. To handle this situation, we propose the following link quality objective.

- *Worst case BER (WB) objective:* Using a fixed transmitted power, provide target BER q_j^* to the bit with the lowest asymptotic efficiency. That is, we choose P_j such that

$$\max_i Q\left(\sqrt{\frac{\zeta_j^{(i)} h_j P_j}{\sigma^2}}\right) = q_j^* \tag{7.3}$$

Compared to the AB objective, the WB objective will demand higher transmitted power from the mobile. We will see that the same power control algorithm can be used to achieve either the AB or WB objective. For either objective, user j will have a target received power E_j^* that guarantees the corresponding link QoS. Of course, E_j^* will depend on whether user j desires the AB or WB objective. Since $Q(\cdot)$ is a monotone decreasing function, a straightforward offline calculation can determine E_j^* for either objective. If the uplink channel gain h_j is known, then the target transmitted power P_j^* is simply E_j^*/h_j.

In practice, the uplink channel gain is often difficult to measure. The base station may require training sequences from the mobile in order to measure h_j. We develop a stochastic approximation method [44] that uses the AMD outputs to iteratively converge to a target received power E_j^* without the knowledge of the uplink channel gain h_j. Let us refer this stochastic approximation method as the *target power* or *TP* algorithm.

Based on the value of E_j^*, the TP algorithm will achieve the AB or WB objective. In the TP algorithm, the base station will use the modified correlator outputs to estimate the average received power and the mobile uses this estimated average received power to update its transmitted power in order to meet the link quality objective. It is easy to verify that the TP algorithm is feasible as long as the asymptotic efficiencies of user j are nonzero.

In the TP algorithm, we assume that both in the uplink (from the mobile to the base) and the downlink (from the base to the mobile), bits are transmitted in packets. It is also assumed that the base station measures J modified correlator outputs and estimates the average received power over J bits. Let us concentrate on the J modified correlators which are used to decode the bits numbered from 0 through $J-1$. From equation (6.18), the output for the ith bit of user j is $r_j^{(i)}$ then

$$r_j^{(i)} = \sqrt{\zeta_j^{(i)} h_j P_j} b_j^{(i)} + N_j^{(i)} \tag{7.4}$$

Under the transmitted power P_j, the power of user j, averaged over the outputs of J modified correlators of user j is

$$\overline{Y}_j(P_j) = \frac{h_j P_j}{J} \sum_{i=0}^{J-1} \zeta_j^{(i)} + \sigma^2 \tag{7.5}$$

In equation (7.5), we see that $P_j = P_j^*$ iff $\overline{Y}_j(P_j) = \overline{Y}_j(P_j^*) = Y_j^*$. Therefore, the target power P_j^* will be achieved if the average power at the output of modified correlators equals Y_j^*. In the TP algorithm, the base station will transmit the average of the squared values of the J modified correlator outputs to user j and user j will use this value to update its transmitted power in order to achieve the target average power, Y_j^*.

Squaring equation (7.4), we get

$$\left(r_j^{(i)}\right)^2 = \zeta_j^{(i)} h_j P_j + 2\sqrt{\zeta_j^{(i)} h_j P_j} b_j^{(i)} N_j^{(i)} + \left(N_j^{(i)}\right)^2 \tag{7.6}$$

The noise components at the J modified correlator outputs can be represented by the noise vector

$$\mathbf{N_j} = \left[N_j^{(0)}, \ldots, N_j^{(J-1)}\right] \tag{7.7}$$

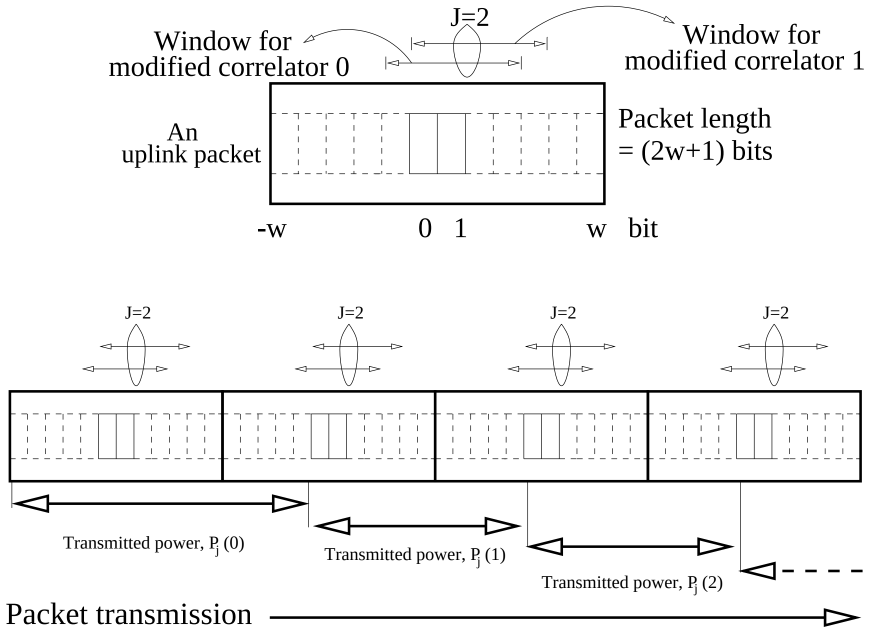

Figure 7.2: The modified correlators whose outputs are used in different power control iterations operate over different time intervals. Therefore, random noise vectors $\mathbf{N_j}(m)$, $m = 1, 2, \ldots$, are identically distributed and statistically independent or i.i.d.

Note that the autocorrelation matrix of the noise vector $\mathbf{N_j}$ will be a function of the cross-correlations of the J modified correlators. Using m to denote the number of power control iterations, we will need to assume that the AMD and the mobile terminal are synchronized such a way that random noise vectors $\mathbf{N_j}(m)$, $m = 1, 2, \ldots$, are independent and identically distributed (iid). A set of iid noise vectors $\mathbf{N_j}(m)$, $m = 1, 2, \ldots$, can be obtained by carefully choosing the J bits used for power control. One such choice of J bits is depicted in Figure 7.2. The number of outputs, J will depend on the lengths of the uplink and downlink packets, the length of modified correlators and the quantization levels of the modified correlator outputs.

Using equations (7.6) and (7.7), let us denote the sample mean of the average power at the outputs of modified correlators as $Y_j[P_j, \mathbf{N_j}]$ where

$$Y_j[P_j, \mathbf{N_j}] = \frac{1}{J} \sum_{i=0}^{J-1} \left\{ \zeta_j^{(i)} h_j P_j + 2\sqrt{\zeta_j^{(i)} h_j P_j}\, b_j^{(i)} N_j^{(i)} + \left(N_j^{(i)} \right)^2 \right\} \tag{7.8}$$

Taking the conditional expectation on both sides of equation (7.8), we can write the average power at the outputs of modified correlators as

$$E[Y_j[P_j, \mathbf{N_j}] | P_j = \xi] = \frac{h_j \xi}{J} \sum_{i=0}^{J-1} \zeta_j^{(i)} + \sigma^2 = \overline{Y}_j(\xi) \tag{7.9}$$

When $\xi = P_j^*$, we obtain the target average power, Y_j^* at the outputs of modified correlators. We have mentioned earlier that in the TP algorithm, our goal is to obtain $\overline{Y}_j(\xi) = Y_j^*$ to guarantee user j the target power P_j^*. Using $Y_j[P_j, \mathbf{N_j}]$ and Y_j^*, the TP algorithm for user j implements the stochastic approximation method

$$P_j(m+1) = P_j(m) - a_m \left(Y_j[P_j(m), \mathbf{N_j}(m)] - Y_j^* \right) \tag{7.10}$$

Note that a_m may be a constant or a function of the iteration index m. The properties of a_m that are necessary for the convergence of the proposed equation (7.10) will be discussed shortly.

Either AB or WB objectives can be achieved by appropriately setting the target average received power Y_j^* or $\left(E_j^*/J\right) \sum_{i=0}^{J-1} \zeta_j^{(i)} + \sigma^2$ in equation (7.10). Notice that the TP algorithm requires the knowledge of asymptotic efficiencies $\left\{\zeta_j^{(i)}\right\}$, the noise power or variance σ^2 and the target received power E_j^*. Measurement of $\left\{\zeta_j^{(i)}\right\}$ simply follows from the construction of the modified correlators. We assume that the base station knows σ^2 perfectly. Calculation of E_j^* for the WB objective needs to invert the Q function. A simple iterative numerical method that calculates E_j^* for the AB objective is given in Appendix C.

7.3 Convergence of the TP Algorithm

Let us denote the *mean square error* of the transmitter power at the mth iteration by

$$\Theta_m = E\left[\left[P_j(m) - P_j^* \right]^2 \right] \tag{7.11}$$

Our goal will be to verify that the TP algorithm converges by showing that

$$\lim_{m \to \infty} \Theta_m = 0 \tag{7.12}$$

The evolution of the stochastic power control algorithm is dictated by the received power error

$$X_j(m) = Y_j[P_j(m), \mathbf{N_j}(m)] - Y_j^* \tag{7.13}$$

We will use upper bounds on the first and second conditional moments of $X_j(m)$ given $P_j(m)$ in order to prove convergence. Using $\mu_k(\xi) = E\left[X_j^k(m)|P_j(m) = \xi\right]$ to denote the kth conditional moment, we prove the following lemmas in Appendix B.

Lemma 1 *There exists a positive constant c_0 such that*

$$\mu_1(\xi) = E[X_j(m)|P_j(m) = \xi] = c_0\left(\xi - P_j^*\right) \tag{7.14}$$

Lemma 2 *There exists positive constants c_1 and c_2 such that*

$$\mu_2(\xi) = E\left[X_j^2(m)|P_j(m) = \xi\right] \leq c_1\left(\xi - P_j^*\right)^2 + c_2 \tag{7.15}$$

To prove the convergence of $\Theta(m)$, the following intermediate result will be used.

Theorem 7 *The mean square error at the $m+1$th iteration, Θ_{m+1} satisfies the upper bound*

$$\Theta_{m+1} \leq \left(1 - 2a_m c_0 + a_m^2 c_1\right)\Theta_m + a_m^2 c_2 \tag{7.16}$$

Proof of Theorem 7 can be found in Appendix B. Theorem 7 implies that the limit (7.12) will hold if

$$\lim_{m\to\infty}\left[\left(1 - 2a_m c_0 + a_m^2 c_1\right)\Theta_m + a_m^2 c_2\right] = 0 \tag{7.17}$$

In this study, we will establish the limit (7.12) by proving the convergence of (7.17). In the following section, we will study the convergence of the TP algorithm for a fixed a_m.

7.3.1 Convergence of the TP Algorithm for a fixed a_m

To study the convergence of the TP algorithm for a fixed a_m, we need to prove the following theorem. The proof is given in Appendix B.

Theorem 8 *If $a_m = a$ and $|1 - 2ac_0 + a^2c_1| \leq 1$, then*

$$\lim_{m\to\infty} \Theta_m \leq \frac{ac_2}{2c_0 - ac_1} \tag{7.18}$$

Note that $|1-2ac_0+a^2c_1| \leq 1$ implies $2c_0 \geq ac_1$ and thus, the upper bound of Theorem 8 is always positive. Equation (7.18) implies that choosing an arbitrarily small a, we can obtain $\frac{ac_2}{2c_0-ac_1} \approx 0$. However, as a approaches zero, $|1 - 2ac_0 + a^2c_1|$ approaches 1 and the convergence speed slows down. This problem also arises when c_0 and c_1 are very small. In this case, we need to choose a very large a to achieve $|1 - 2ac_0 + a^2c_1| < 1$. Suitable selection of a requires the knowledge of c_0, c_1 and c_2. As c_0 and c_1 are functions of the uplink channel gain h_j, thus, the selection of a is as difficult as the measurement of h_j. This practical situation leads us to search a coefficient sequence a_m which will always guarantee $\lim_{m\to\infty} \Theta_m = 0$.

7.3.2 Convergence of the TP Algorithm for $a_m = f(m)$

In the following theorem, we show that if a_m satisfies two simple conditions, then $\lim_{m\to\infty} \Theta_m = 0$.

Theorem 9 *If the sequence a_m satisfies*

$$\sum_{m=1}^{\infty} a_m = \infty \qquad \sum_{m=1}^{\infty} a_m^2 < \infty \tag{7.19}$$

then

$$\lim_{m\to\infty} \Theta_m = \lim_{m\to\infty} E\left[\left(P_j(m) - P_j^*\right)^2\right] = 0 \tag{7.20}$$

Note that

$$a_m = a/m \tag{7.21}$$

meets the conditions (7.19). The proof of Theorem 9 follows Sakrison's procedure [44, pages 60-61]; see Appendix B.

Although the TP algorithm will converge, a number of issues must be resolved in order to implement the algorithm. In practice, the uplink channel gain h_j and the noise variance σ^2 are very small. Therefore, the received power measurement $Y_j[P_j, \mathbf{N_j}(m)]$ and the target received power Y_j^* in equation (7.10) will be very small. The TP algorithm uses these small values to update the transmitted power which typically is several orders of magnitude larger. If the initial transmitted power varies significantly from P_j^*, then the convergence speed of the TP algorithm will be extremely slow. For fast convergence, we need to choose a sufficiently large. A heuristic procedure for the selection of a will be presented in the following section.

A second practical concern is that the channel gain h_j, the time offsets of equation (6.3), and the asymptotic efficiencies of user j can vary with time. Therefore, to track these variations, we would initialize the TP algorithm using $a_m = a/m$. When a_m becomes small, we would use a small fixed value for a_m. For constructing the blind MMSE receiver, a similar technique is also used in [17].

7.4 Empirical Results

We modeled a circular single cell of a dual-rate rate asynchronous DS/CDMA system. The radius of the cell was chosen to be $r_0 = 1000$ meters. It was assumed that the mobiles were uniformly distributed in the cell. This assumption yielded a probability density function $f(r) = 2r/r_0^2$ for the distance of a user from the base station. We used a path loss exponent $\alpha = 4$. The height of the base station was 30 meters so that the uplink channel gain of user j, h_j was $1/\left(r^2 + 30^2\right)^{\alpha/2}$. It was assumed that there were five low rate and five high rate users in the system. The processing gain of the low rate users was 64 and the processing gain of the high rate users was 8. The signature waveforms were generated using random signature sequences. The time offsets of different users were randomly generated. We assumed that the time offsets were multiples of the chip duration. The Gaussian noise had power spectral density 6×10^{-14} W/Hz.

In the experiment, user j was a high rate customer. The length of the observation window was $(n_j + d_j + 1)$, where n_j denoted the number of desired users' bits into the past and d_j is the number of its bits into the future and $n_j = d_j = 7$. After an interval of 8 bits, user j observed the same pattern of the signature waveforms from the other interfering users. Thus, the receiver dedicated to user j needed to know the specifications of 8 modified correlators and as a result, user j experienced 8 different asymptotic efficiencies. In our experiments, the following asymptotic efficiencies were used

$$\left\{\zeta_j^{(i)} | 0 \leq i \leq 7\right\} = \left\{0.3573 \;\; 0.3319 \;\; 0.3392 \;\; 0.3782 \;\; 0.4543 \;\; 0.3298 \;\; 0.3329 \;\; 0.2765\right\}$$

We assumed that the user j applied the AB link quality objective. The target average BER q_j^* was 10^{-2} and the corresponding target received power E_j^* was 9.5356×10^{-13}. The technique presented in Figure 7.2 was used to satisfy the requirement of iid noise vectors $\mathbf{N_j}(m)$, $m = 1, 2, \ldots$,.

In the first experiment, the average BER was determined as a function of the number of power control iterations for fixed a_m as well as $a_m = 10^{13}/m$; see Figure 7.3. Here in each iteration, the output of modified correlator 0 was used to update the transmitted power or $J = 1$. The mobile initialized the transmitted power from zero or $P_j(0) = 0$. The empirical results showed that for $a_m = 10^{13}/m$, the mobile achieved its QoS objective quickly compared to the fixed a_m of 10^{10}, or 10^{11}. These large values of a were needed, because the $|Y_j[P_j, \mathbf{N_j}(m)] - Y_j^*|$ of equation (7.10) were very small and $P_j^* \gg P_j(0)$. In this experiment, we found that in the case of fixed a_m, smaller values of a_m suffered from slow convergence, as suggested by the discussion in Section 7.3.1. In the following experiments, we only studied the sequence $a_m = a/m$.

In Figure 7.4, we plot the average BER as a function of the number power control iterations for $J = 1, 8, 16$, where $a = 10^{13}$ and $P_j(0) = 0$. As expected, in this experiment, we observed that for $J = 16$, the TP algorithm converged quickly. However, for both $J = 8$ and $J = 16$, the mobile increased the transmitted power uniformly to achieve q_j^*. Similar results were also observed in [58] where the stochastic power control algorithm for the matched filter receiver was studied.

Figure 7.5 describes the effect of a on the convergence when $J = 8$ and $P_j(0) = 0$.

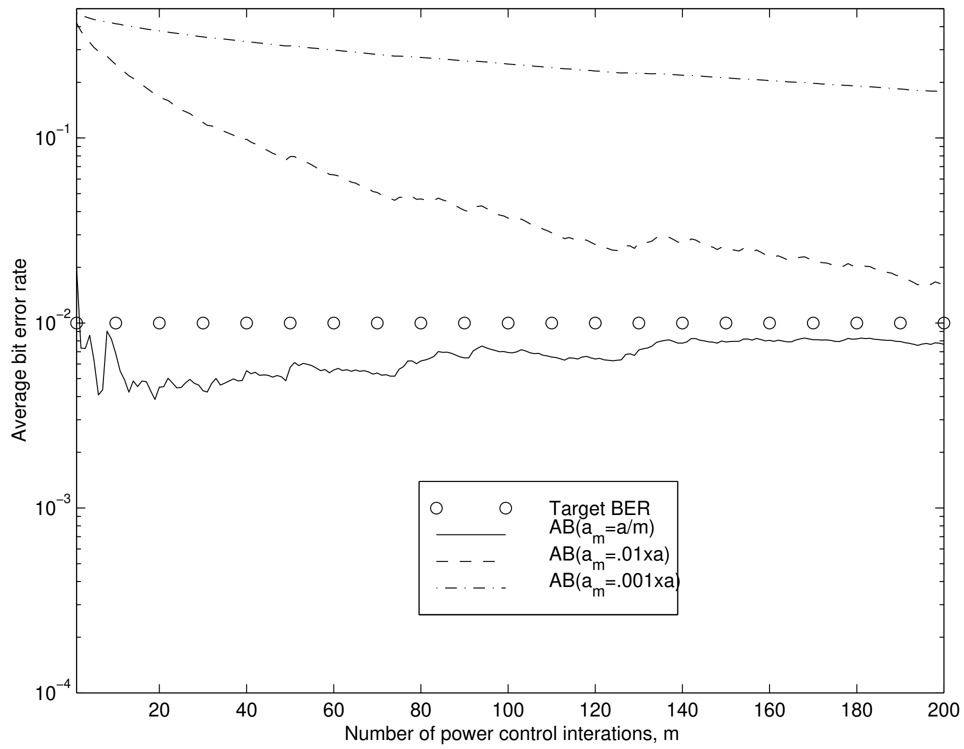

Figure 7.3: The average BER is plotted as a function of the number of power control iterations for fixed a_m as well as $a_m = a/m$. Here $J = 1$, $a = 10^{13}$ and $P_j(0) = 0$.

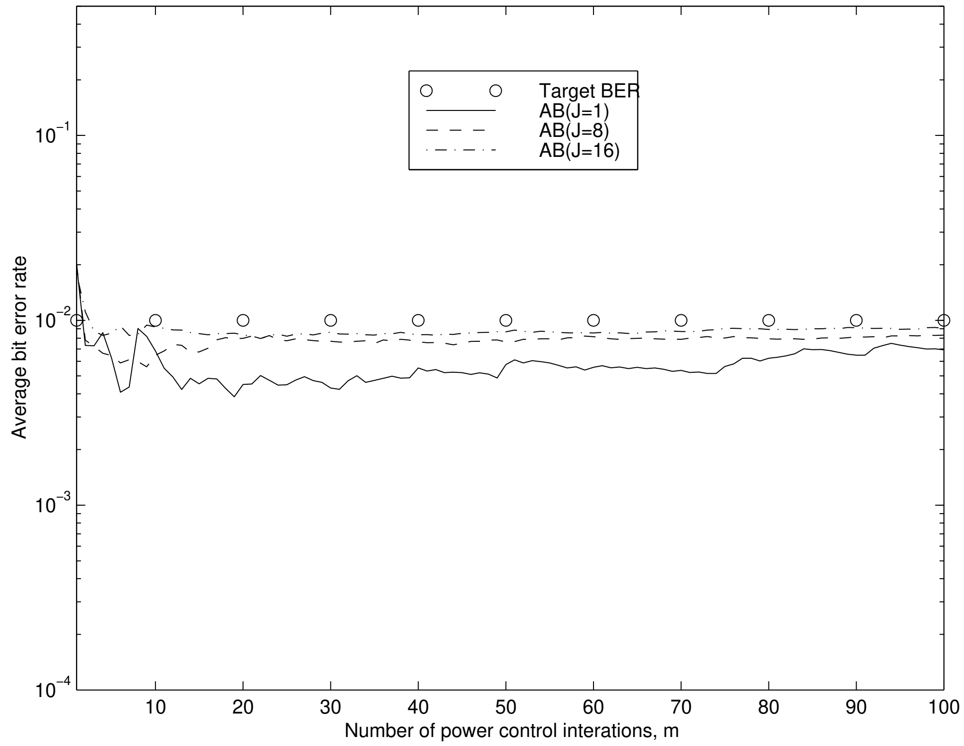

Figure 7.4: The average BER is shown as a function of the number of power control iterations for variable J. Here $a_m = 10^{13}/m$ and $P_j(0) = 0$.

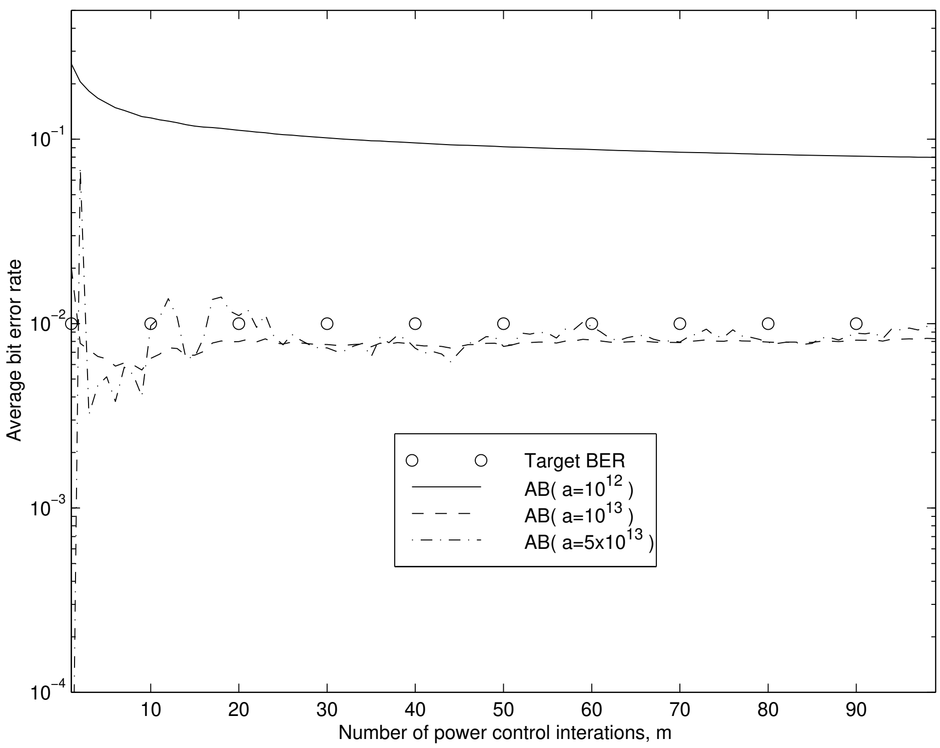

Figure 7.5: The average BER is plotted as a function of the number of power control iterations for variable a when $a_m = a/m$. Here $P_j(0) = 0$.

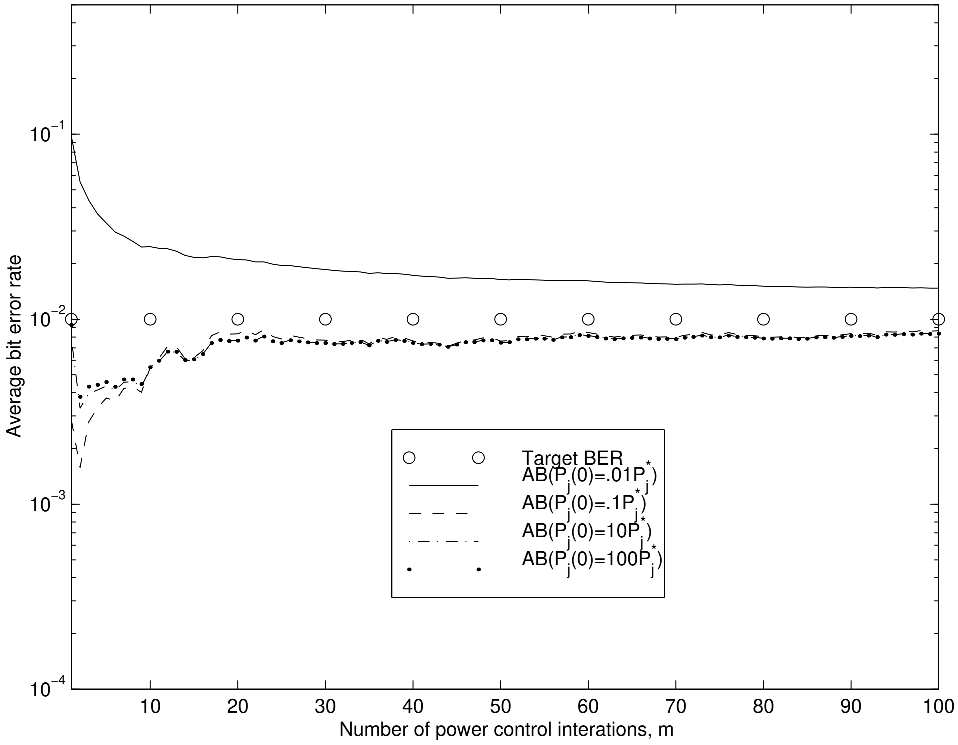

Figure 7.6: The average BER is shown as a function of the number of power control iterations for various $P_j(0)$, when equation (7.25) was used to select a. Here $J = 8$.

As expected, our empirical results showed that smaller values of a resulted in a slower convergence speed. On the other hand, larger values of a led to a wide variation in the initial transmitted power. These experimental results implied that neither a large a nor a small a was desirable for the mobile. This practical situation leads us to propose the following heuristic procedure to select the parameter a.

Let us assume that $P_j(0) > 0$. Using the target average power, Y_j^* and equation (7.8), we can estimate or approximate the target transmitted power, P_j^* as follows.

$$\hat{P}_j^* = \frac{\left(Y_j^* - \sigma^2\right) P_j(0)}{Y_j[P_j(0), \mathbf{N_j}(0)] - \sigma^2} \tag{7.22}$$

where $\hat{P}_j^*$ is the estimate of P_j^*. In order to be in the vicinity of P_j^* in the very first iteration, we will choose a so that

$$P_j(1) = \hat{P}_j^* \tag{7.23}$$

Equations (7.10) and (7.22) imply that equation (7.23) will be satisfied if

$$a = \frac{P_j(0)}{Y_j[P_j(0), \mathbf{N_j}(0)] - \sigma^2} \tag{7.24}$$

In equation (7.25), since $\mathbf{N_j}(0)$ is a random vector, a is a random variable and its magnitude depends on the initial transmitted power $P_j(0)$. For large J, equation (7.8) implies that $a \approx \left(J / \sum_{i=0}^{J-1} \zeta_j^{(i)}\right) \frac{1}{h_j}$ which is proportional to $\frac{1}{h_j}$. Thus equation (7.24) can be used to approximate h_j.

For small $P_j(0)$ and h_j, equation (7.24) may yield $a < 0$. However, the proof of Theorem 9 implies that in order to converge, the TP algorithm requires the parameter a to be positive. To handle this situation, we will modify equation (7.24) as follows.

$$a = \frac{P_j(0)}{|Y_j[P_j(0), \mathbf{N_j}(0)] - \sigma^2|} \tag{7.25}$$

In Figure 7.6, the effect of $P_j(0)$ on the TP algorithm is shown when equation (7.25) was used to select a. Here $J = 8$ and $P_j(0) = \kappa P_j^*$, where $\kappa = 10^{-2}, 10^{-1}, 10, 10^2$. Larger values of $P_j(0)$ yielded better estimates of P_j^* or smaller values of $|P_j(1) - P_j^*|$. As a result, the convergence speed of the power control was improved as $P_j(0)$ increased. For all values of $P_j(0)$, we observed that the mobile updated the transmitted power almost uniformly to achieve q_j^*.

7.5 Chapter Summary

For the varied QoS requirements of multimedia traffic in an asynchronous DS/CDMA system, this chapter has addressed a class of link quality objectives for a decentralized, truncated window multi-rate decorrelator. Both the average BER and worst case BER objectives can be achieved using the TP stochastic power control algorithm. The proposed algorithm is iterative, asynchronous and distributed and does not require the measurement of the uplink channel gain. It is proven that when each bit of a user has nonzero asymptotic efficiency, then the TP algorithm converges in the mean square sense to an optimal power. This theoretical result was verified by our empirical studies. In this chapter, a heuristic technique that assists the proposed stochastic power control algorithm in converging quickly has been also presented.

Chapter 8

Conclusions

8.1 Thesis Summary

This thesis has investigated the use of existing multi-user receivers such as decorrelating detectors and decision feedback decorrelators in multi-rate DS/CDMA systems. Objectives of this work were to develop multi-rate multi-user receivers of reasonable computational complexity and guarantee each user a target BER or QoS objective.

We have found that a dual-rate synchronous system with K_0 low rate users and K_1 high rate users can be modeled as an equivalent system of $K_0 + MK_1$ low rate users. However, the corresponding low rate decorrelator (LRD) for this system introduces an M bit processing delay for the high rate users and has a complexity that grows with M. This practical situation has led us to propose a decorrelator called the high rate decorrelator (HRD). The HRD generates bit decisions for each high rate user in every high rate bit interval. To decode a low rate user, a soft decoding rule applies maximal ratio combining on M separate decorrelated outputs of each low rate user. The HRD dramatically reduces the computational complexity of the LRD. However, the HRD is not as bandwidth efficient as the LRD. We have proven that the bit error rate of the LRD is less than or equal to the HRD. By evaluation, we found that when the signature sequences had good correlation properties, the HRD performed as well as the LRD and for highly correlated signature waveforms, performance degradation for the HRD versus the LRD was observed.

In addition, this thesis has proposed a signature assignment technique for a dual-rate DS/CDMA system. Under this signature sequence assignment technique, M low rate users share the signature of a single high rate user without wasting bandwidth. Based on the signature assignment technique, a decorrelator that generates bit decisions for each high rate user in every high rate bit interval has been proposed. In order to decode a low rate user, an orthogonal projection is applied to M separate decorrelated outputs of each low rate user. This proposed receiver was called the two stage decorrelator (2SD). The 2SD significantly reduces the computational complexity of the LRD. Due to the structural simplicity, the proposed receiver suffers in terms of bit error rate. However, we have found that in several cases the 2SD achieves the LRD performance.

This thesis has also proposed a decision feedback decorrelator called the high rate decision feedback decorrelator (HRDF) for a dual-rate synchronous DS/CDMA system. Our proposed decision feedback decorrelator is as bandwidth efficient as the LRD while retaining all the desirable properties of the HRD. The HRDF is implemented via modified correlators. It initiates the bit decision process at the end of the high rate bit interval and decodes a bit by utilizing the decisions of all previously decoded users. Each bit decoding process is executed by ordering users according to their nondecreasing orthogonal energies, or OEs, where OE of a user is the fraction of its received energy associated with the subspace orthogonal to the interfering users. The motivation behind this ordering technique is to reduce the likelihood of early decision feedback errors which have an impact on the decoding of lower ordered users. Using simulation, we showed that the technique that ordered users according to non decreasing OEs outperformed significantly the technique that ordered users according to non increasing OEs. It was also observed that the HRDF outperformed the HRD as well as the LRD and as the interferers grew stronger relative to the desired user, the performance of the HRDF for decoding the desired user approached the single user bound.

For an asynchronous multi-rate DS/CDMA system, we have developed a decentralized, truncated window decorrelator called the asynchronous multi-rate decorrelator (AMD). The AMD decodes a user by employing a set of modified correlators whose signals are simply time shifted versions of one another. Due to the decentralization of the AMD, each user is able to suppress the multiuser interference as long as that user has non-zero asymptotic efficiency over its observation window. The decentralized model of the AMD permits a simple proof that the performance of any truncated window decorrelator improves monotonically with the observation window length. However, a longer observation window results in greater computational complexity. Thus, in order to realize a truncated window decorrelator, a user should only extend the observation window over reasonable number of bits. For a given observation window, upper and lower bounds on the performance of the infinite window decorrelator are developed. These bounds follow naturally from the implementation of the AMD and are functions of the observation window length. The upper and lower bounds can be used to characterize practical window sizes. Our experimental results showed that as the observation window length increased that the upper and lower bounds converged rapidly to the performance of the infinite window decorrelator.

The varied QoS requirements of multimedia traffic necessitate the use of power control for CDMA wireless systems employing multiuser detection. Using a decorrelator in a multi-rate DS/CDMA system, it is necessary for different users to combat the noise enhancement and the propagation losses to varying degrees depending on the individual QoS requirement. In this context, this thesis has proposed a class of BER based link quality objectives for the AMD, such as 1) the fixed BER objective, 2) the average BER objective and 3) the worst case BER objective. If the uplink channel gain of the mobile is known then it is simple to provide each user its QoS objective. In practice, however, the measurement of the channel gain is non-trivial and neglects the stochastic behavior of the channel. This practical situation has led us to develop a stochastic approximation method that uses the AMD outputs to iteratively converge to a target QoS objective without the knowledge of the uplink channel gain. We have called this stochastic approximation method as the target power or TP algorithm. Our proposed power control algorithm is suitable for the average BER and worst case BER objectives. When asymptotic efficiencies of the desired user are nonzero, the TP algorithm converges in the mean square sense to an optimal power at which the user achieves its QoS requirement. We have presented a heuristic technique that assists the TP algorithm to converge quickly.

8.2 Suggestions for Further Study

8.2.1 Decorrelators in Multi-cell

Further study is needed in the area of implementation of a decorrelating receiver in a multi-cell multi-rate DS/CDMA system. Since the existence of a decorrelator depends on the number of users and it is difficult for a base station to know all the signatures that are used in other cells, it may not be possible to develop a multi-rate decorrelator in a multi-cell system with many users. One way to handle this problem is to orthogonalize the intra-cell interferers only. As a result, every user will still suffer from the inter-cell interference. Let us call a receiver that follows this working principle a *partial decorrelator*. Considering random signature sequences, Appendix D provides a comparative study between the partial decorrelator and the conventional receiver for an AWGN synchronous multi-cell CDMA system. Here it is assumed that the power spectral density of the white Gaussian noise is σ^2. Since, the bit error rate is hard to analyze for both the partial decorrelator and the conventional receiver, average signal-to-interference ratio (SIR) is considered as a system performance measure. In this study, σ_1^2 denotes the second moment of the intra-cell interference for the conventional receiver and σ_2^2 is the second moment of the inter-cell interference for the conventional receiver. When K' is the number of intra-cell users and L is the processing gain, we prove that a sufficient condition for the partial decorrelator to outperform the conventional receiver is $K'/L < 1/(1+F)$, where $F = \left(\sigma_2^2 + \sigma^2\right)/\sigma_1^2$; see Theorem 16. In a practical system, σ_2^2/σ_1^2 is approximately 0.55 [10, 69]. For $F \approx 0.6$, we get $K'/L < 0.6$ for the partial decorrelator to be better. However, for conventional systems, $K'/L \approx 0.2$. This suggests that within the operating region of the conventional receiver, the partial decorrelator outperforms the conventional receiver. As a result, the partial decorrelator will yield at least the same system capacity of the conventional receiver.

The above analysis has used the restrictive model of an AWGN synchronous channel. It would be desirable to extend this work by relaxing these assumptions through considering an AWGN asynchronous channel which is observed in mobile radio systems. Besides this analysis, an extensive full scale system simulation is necessary to understand fully the performance of the partial decorrelator in an AWGN asynchronous multi-cell environment.

8.2.2 Multi-modulation Scheme for Multi-rate Decorrelators

Under both the fixed chip rate and variable processing gain and multi-code access strategies, we can view a multi-rate DS/CDMA system of base rate R as a single rate system in which a rate R' user is equivalent to R'/R effective rate R users. As a result, compared to the multi-rate system, the equivalent single rate system has a higher number of users. On the other hand, in the multi-modulation access strategy, both the multi-rate and equivalent single rate systems have the same number of users. This happens because under this access strategy, a rate R' user is equivalent to a rate R user with a higher level modulation scheme (QAM). The above discussions imply that among the above three access strategies, the multi-modulation method generates the least number of effective users. Since both the complexity and the performance of a decorrelating receiver deteriorate as the number of users increases, the multi-modulation method may be more suitable access strategy for multi-rate DS/CDMA systems with decorrelators than any of the variable processing gain and multi-code access strategies. Furthermore, in Chapter 1, we have discussed that in a conventional multi-rate DS/CDMA system, the multi-modulation scheme may cause a severe near/far problem. However, this near/far problem of the multi-modulation scheme will be eradicated by a multi-rate decorrelator. We feel this area is particularly interesting from a decorrelator point of view and should be explored in some depth.

Appendix A

Proof of Theorem 3

Proof: Without loss of generality, we will concentrate on the 1st bit of user $(K_1, 1)$. Let us denote the set of signature sequences which are being used by the users as S_a, where $S_a = \{S_{k,1} : 1 \leq k \leq J + K_1\}$. Let us assume that Gram-Schmidt orthogonalization on the set S_a yields $(J + K_1)$ normalized basis functions,

$$\Psi = \{\Psi_j : j = 1, \ldots, J + K_1\}$$

Using Theorem 4, we can write the asymptotic efficiency of the 2SD for decoding the 1st transmitted bit of customer $(K_1, 1)$ as

$$\zeta_{K_1,1} = 1/\hat{\Gamma}^{-1}_{J+K_1,J+K_1} = \left(S^{\top}_{J+K_1,1}\Psi_{J+K_1}\right)^2 \tag{A.1}$$

Let us define a set of vectors as $\{\Omega_{m,i}\}$ where $m = 1, \ldots, J + K_1$ and $i = 1, \ldots, M$. The size of the vector $\Omega_{m,i}$ is $L_0 \times 1$ and its elements numbered from $(i-1)\,L_1 + 1$ to iL_1 are only non-zero and matched to Ψ_m. As an example, we can write

$$\Omega^{\top}_{3,1} = \left[\Psi^{\top}_3, 0, \ldots, 0\right]$$

For the LRD system model, the set $\{\Omega_{m,i}\}$ forms the basis for the sub-space corresponding to the signature sequences of the $K_0 + MK_1$ or $M(J + K_1)$ users. Here, the 1st bit of user $(K_1, 1)$ will observe $M(J+K_1)-1$ interfering signatures. The set of basis functions which spans this interfering sub-space is represented by $\hat{\Omega}$, where $\hat{\Omega}$ contains all the elements of $\{\Omega_{m,i}\}$ except $\Omega_{J+K_1,1}$.

Let us define a $L_0 \times 1$ vector $\bar{S}_{J+K_1,1}$ as

$$\bar{S}^{\top}_{J+K_1,1} = \left[S^{\top}_{J+K_1,1}, 0, \ldots, 0\right]$$

Theorem 4 implies that the square root of the asymptotic efficiency of the LRD for decoding the 1st transmitted bit of customer $(K_1, 1)$ is

$$\begin{array}{lll} \max_{\Phi} & \Phi^{\top}\bar{S}_{J+K_1,1} & \\ \text{subject to} & \Phi^{\top}\Omega_{m,i} = 0 & (m,i) \neq (J+K_1,1) \\ & \Phi^{\top}\Phi = 1 & \end{array} \tag{A.2}$$

The vector $\bar{S}_{J+K_1,1}$ can be expressed as $\bar{S}_{J+K_1,1} = \sum_{m=1}^{J+K_1}\sum_{i=1}^{M}\alpha_{m,i}\Omega_{m,i}$, where $\alpha_{m,i} = \bar{S}_{J+K_1,1}^{\top}\Omega_{m,i}$. Let us assume that Φ_o is a feasible solution to the optimization problem (A.2). Using the Schwarz inequality, we can write

$$\Phi_o^{\top}\bar{S}_{J+K_1,1} = \sum_{m=1}^{J+K_1}\sum_{i=1}^{M}\alpha_{m,i}\Phi_o^{\top}\Omega_{m,i} \tag{A.3}$$

$$\leq \alpha_{J+K_1,1} \tag{A.4}$$

In equation (A.4), $\alpha_{J+K_1,1}^2$ is the asymptotic efficiency [28] of the LRD for decoding the 1st transmitted bit of customer $(K_1, 1)$. It is easy to show that $\alpha_{J+K_1,1}^2 = \zeta_{K_1,1}$ $\square$

Appendix B

Additional Proofs for Chapter 7

Proof: Lemma 1 Using $Y_j^* = (E_j^*/J) \sum_{i=0}^{J-1} \zeta_j^{(i)} + \sigma^2$ in equation (7.13), we can write

$$\mu_1(\xi) = E[X_j(m)|P_j(m) = \xi] = \left\{ \frac{h_j}{J} \sum_{i=0}^{J-1} \zeta_j^{(i)} \right\} \left(\xi - P_j^*\right) = c_0 \left(\xi - P_j^*\right) \tag{B.1}$$

where $c_0 = \frac{h_j}{J} \sum_{i=0}^{J-1} \zeta_j^{(i)} > 0$ is a constant related to the system parameters. □

Proof: Lemma 2 From the definition of $\mu_2(\xi)$, we can write

$$\mu_2(\xi) = E\left[\left[\frac{1}{J}\sum_{i=0}^{J-1}\left(\zeta_j^{(i)} h_j \left(\xi - P_j^*\right) + 2\sqrt{\zeta_j^{(i)} h_j \xi}\, b^{(i)} N_j^{(i)} + \left\{\left(N_j^{(i)}\right)^2 - \sigma^2\right\}\right)\right]^2\right] \tag{B.2}$$

Now we observe that $\{x_i\}$ is a set of real numbers, then successive use of inequality $(x_0 + x_1)^2 \leq 2\left(x_0^2 + x_1^2\right)$ yields

$$\left(\sum_{i=0}^{J-1} x_i\right)^2 \leq 2x_0^2 + 2\left(\sum_{i=1}^{J-1} x_i\right)^2 \leq \ldots \leq \left(\sum_{i=0}^{J-1} \omega_i x_i^2\right) \tag{B.3}$$

where $\omega_i = 2^{i+1}$ for $0 \leq i < J-1$ and $\omega_{J-1} = \omega_{J-2}$. We will use (B.3) repeatedly with equation (B.2) in the following fashion.

$$\mu_2(\xi) \leq \frac{1}{J^2} E\left[\sum_{i=0}^{J-1} \omega_i \left(\zeta_j^{(i)} h_j \left(\xi - P_j^*\right) + 2\sqrt{\zeta_j^{(i)} h_j \xi}\, b^{(i)} N_j^{(i)} + \left\{\left(N_j^{(i)}\right)^2 - \sigma^2\right\}\right)^2\right] \tag{B.4}$$

$$\leq \frac{1}{J^2} \sum_{i=0}^{J-1} \omega_i E\left[2\left(\zeta_j^{(i)} h_j\right)^2 \left(\xi - P_j^*\right)^2 + 16\zeta_j^{(i)} h_j \xi \left(N_j^{(i)}\right)^2 + 4\left\{\left(N_j^{(i)}\right)^2 - \sigma^2\right\}^2\right] \tag{B.5}$$

Taking the expectation of equation (B.5) with respect to $N_j^{(i)}$, we can write

$$\mu_2(\xi) \quad \leq \quad \frac{2}{J^2} \sum_{i=0}^{J-1} \omega_i \left\{ \left(\zeta_j^{(i)} h_j\right)^2 \left(\xi - P_j^*\right)^2 + 8\zeta_j^{(i)} h_j \xi \sigma^2 + 4\sigma^4 \right\} \tag{B.6}$$

$$= \quad \frac{2}{J^2} \sum_{i=0}^{J-1} \omega_i \left\{ \left(\zeta_j^{(i)} h_j \left(\xi - P_j^*\right) + 4\sigma^2\right)^2 + 8\zeta_j^{(i)} h_j P_j^* \sigma^2 - 12\sigma^4 \right\} \tag{B.7}$$

Applying (B.3) to (B.7) yields the inequality

$$\mu_2(\xi) \leq \frac{2}{J^2}\sum_{i=0}^{J-1}\omega_i\left\{2\left(\zeta_j^{(i)}h_j\right)^2\left(\xi-P_j^*\right)^2+32\sigma^4+8\zeta_j^{(i)}h_jP_j^*\sigma^2-12\sigma^4\right\} \quad \text{(B.8)}$$

$$= \frac{4}{J^2}\sum_{i=0}^{J-1}\omega_i\left\{\left(\zeta_j^{(i)}h_j\right)^2\left(\xi-P_j^*\right)^2+4\zeta_j^{(i)}h_jP_j^*\sigma^2+10\sigma^4\right\} \quad \text{(B.9)}$$

The result of Lemma 2 follows from equation (B.9) by defining constants

$$c_1 = \frac{4h_j^2}{J^2}\sum_{i=0}^{J-1}\omega_i\left(\zeta_j^{(i)}\right)^2 \quad \text{(B.10)}$$

$$c_2 = \frac{16E_j^*\sigma^2}{J^2}\sum_{i=0}^{J-1}\omega_i\zeta_j^{(i)}+\frac{40\sigma^4}{J^2}\sum_{i=0}^{J-1}\omega_i \quad \text{(B.11)}$$

□

Proof: Theorem 7 Subtracting P_j^* from both sides of equation (7.10), squaring the result, and then using equation (7.13), we obtain

$$\left[P_j(m+1)-P_j^*\right]^2 = \left[P_j(m)-P_j^*\right]^2 - 2a_mX_j(m)\left[P_j(m)-P_j^*\right]+a_m^2X_j^2(m) \quad \text{(B.12)}$$

We denote the conditional second moment of the transmitter power error by

$$\Theta_{m+1}(\xi) = E\Big[\left[P_j(m+1)-P_j^*\right]^2|P_j(m)=\xi\Big] \quad \text{(B.13)}$$

Taking the conditional expectation of equation (B.12) given $P_j(m)=\xi$ yields

$$\Theta_{m+1}(\xi) = \left(\xi-P_j^*\right)^2-2a_m\mu_1(\xi)\left(\xi-P_j^*\right)+a_m^2\mu_2(\xi) \quad \text{(B.14)}$$

Lemmas 1 and 2 yield an upper bound on equation (B.14) as follows.

$$\Theta_{m+1}(\xi) \leq \left(1-2a_mc_0+a_m^2c_1\right)\left(\xi-P_j^*\right)^2+a_m^2c_2 \quad \text{(B.15)}$$

Taking the expectation with respect to $P_j(m)$ of equation (B.15) and using equation (7.11), we obtain the desired result of Theorem 7. □

Proof: Theorem 8 We can express Θ_m of inequality (7.16) in terms of Θ_0 as follows.

$$\Theta_m \leq \left(1-2ac_0+a^2c_1\right)^m\Theta_0+a^2c_2\sum_{i=0}^{m}\left(1-2ac_0+a^2c_1\right)^m \quad \text{(B.16)}$$

Since $|1-2ac_0+a^2c_1|<1$, as m approaches to infinity, inequality (B.16) yields

$$\begin{aligned}\lim_{m\to\infty}\Theta_m &\le \Theta_0\lim_{m\to\infty}\left(1-2ac_0+a^2c_1\right)^m \\ &\quad +a^2c_2\lim_{m\to\infty}\sum_{i=0}^{m}\left(1-2ac_0+a^2c_1\right)^m \qquad \text{(B.17)}\\ &= \frac{ac_2}{2c_0-ac_1} \qquad \text{(B.18)}\end{aligned}$$

□

Proof: Theorem 9 The sequence a_m of equation (7.19) is monotone decreasing in m. Therefore, there exists an m' such that

$$1-2a_mC_0+a_m^2C_1 \le 1-(2-\delta)\,a_mC_0$$

and

$$1-(2-\delta)\,a_mC_0>0 \qquad 0\le\delta\le 2$$

for all $m\ge m'$. Thus, for $m\ge m'$, inequality of equation (7.16) can be weakened as

$$\Theta_{m+1}\le\Theta_m\{1-(2-\delta)\,a_mC_0\}+a_m^2C_2 \tag{B.19}$$

Then starting at $m=m'$ and executing the recursion repeatedly we get

$$\Theta_m\le\Theta_{m'}\beta_{m'-1,m-1}+C_2\sum_{i=m'}^{m-1}a_i^2\beta_{i,m-1} \tag{B.20}$$

in which

$$\beta_{i,m-1}=\begin{cases}\Pi_{j=i+1}^{m}\{1-a_jC_0\,(2-\delta)\} & 0\le i\le m\\ 0 & i\ge m\end{cases} \tag{B.21}$$

Using the inequality $\ln(1-x)\le -x$, we can write

$$\beta_{n,m}\le\exp\left\{-(2-\delta)\,C_0\sum_{j=n+1}^{m}a_j\right\} \tag{B.22}$$

As the first condition of a_j defined in equation (7.19) is assumed to diverge and $(2-\delta)\,C_0>0$, therefore

$$\lim_{m\to\infty}\beta_{m'-1,m-1}=0 \tag{B.23}$$

Equation (B.23) implies that the first term of equation (B.20) approaches to zero as m goes to infinity. Now we will consider the second term of equation (B.20). Then

$$\begin{aligned}
\lim_{m\to\infty} C_2 \sum_{i=m'}^{m-1} a_i^2 \beta_{i,m-1} &= C_2 \lim_{m\to\infty} \sum_{i=m'}^{\infty} a_i^2 \beta_{i,m-1}\{1 - u(i-m)\} \\
&= C_2 \sum_{i=m'}^{\infty} a_i^2 \lim_{m\to\infty} \beta_{i,m-1}\{1 - u(i-m)\} \\
&= 0 \qquad \text{(B.24)}
\end{aligned}$$

where $u(x)$ is a unit step function. Note that the interchange of limit and sum is justified, since the sum is absolutely convergent. The last equality holds because the second condition of a_k defined in equation (7.19) is assumed to converge. Finally, using equations (B.23) and (B.24) with equation (B.20), we can conclude

$$\lim_{m\to\infty} \Theta_m = \lim_{m\to\infty} \mathrm{E}\Big\{ \big(P_j(m) - P_j^*\big)^2 \Big\} = 0 \qquad \text{(B.25)}$$

$\square$

Appendix C

Calculation of the Target Received Power

From equation (7.2), the target received power $E_j^* = h_j P_j^*$ can be calculated by using several numerical methods. Among all such methods, here we will present a simple iterative technique that offers significantly fast convergence to E_j^* from any initial point. The proposed iterative method is based on the definitions of Yates' *standard interference functions* [75]. Reference [75] shows that if it is possible to develop a set of iterative functions $\mathbf{I}(\mathbf{Y})$ that satisfy three properties of the standard interference functions which will be discussed shortly, then iterative algorithm $Y = \mathbf{I}(\mathbf{Y})$ will converge to a unique fixed point $\mathbf{Y}^*$ from any initial vector $\mathbf{Y}_0$. In this study, we will formulate an iterative function from equation (7.2) and then prove that this iterative function is a standard interference function. Hence, the iterative function will converge to E_j^* from any initial point E_0.

In the following section, we will summarize the necessary results of [75]. Note that these results were addressed in [75] in the context of the power control problem for the matched filters.

C.1 Standard Interference Functions

For an arbitrary vector function $\mathbf{I}(\mathbf{Y}) = [I_1(\mathbf{Y}), \ldots, I_n(\mathbf{Y})]$, reference [75] develops the following definition.

Definition: The interference function $\mathbf{I}(\mathbf{Y})$ is standard if for all $\mathbf{Y} \geq 0$ the following properties are satisfied.

- *Positivity* $\mathbf{I}(\mathbf{Y}) > 0$.

- *Monotonicity* If $\mathbf{Y} \geq \acute{\mathbf{Y}}$, then $\mathbf{I}(\mathbf{Y}) \geq \mathbf{I}(\acute{\mathbf{Y}})$.

- *Scalability* For all $\alpha > 1$, $\alpha\mathbf{I}(\mathbf{Y}) > \mathbf{I}(\alpha\mathbf{Y})$.

Reference [75] adopts the convention that the vector inequality $\mathbf{Y} > \acute{\mathbf{Y}}$ is a strict inequality in all components. In [75], convergence of the synchronous iteration

$$\mathbf{Y}(n) = \mathbf{I}(\mathbf{Y}(n)) \tag{C.1}$$

is addressed in the following family of theorems.

Theorem 10 *If the standard power control algorithm has a fixed point, then that fixed point is unique.*

Theorem 11 *If* $\mathbf{I}(\mathbf{Y})$ *is feasible and the initial vector* $\mathbf{Y}_0 \geq \mathbf{I}(\mathbf{Y}_0)$*, then* $\mathbf{I}^n(\mathbf{Y}_0)$ *is a monotone decreasing sequence of feasible power vectors that converges to a fixed point* $\mathbf{Y}^*$*.*

Theorem 12 *If* $\mathbf{I}(\mathbf{Y})$ *is feasible and the initial vector* $\mathbf{Y}_0 \leq \mathbf{I}(\mathbf{Y}_0)$*, then* $\mathbf{I}^n(\mathbf{Y}_0)$ *is a monotone increasing sequence of feasible power vectors that converges to a fixed point* $\mathbf{Y}^*$*.*

Applying Theorem 10 with Theorems 11 and 12, reference [75] proves that

Theorem 13 *If* $\mathbf{I}(\mathbf{Y})$ *is feasible then for any initial power vector* $\mathbf{Y}_0$*, the standard power control algorithm converges to a unique fixed point* $\mathbf{Y}^*$*.*

C.2 Iterative Function

We will now develop an iterative function $\mathbf{f}(E_j)$ that calculates E_j^* for the AB objective. Using equation (7.2), let us define a function $\mathbf{f}_1(E_j)$ as

$$\mathbf{f_1}(E_j) = \frac{\log\left(1/q_j^*\right)}{\log\left[M/\sum_{i=1}^{M} Q\left(\sqrt{c_i E_j}\right)\right]} E_j \tag{C.2}$$

where $c_i = \zeta_j^{(i)}/\sigma^2$. If $E_0 > 0$ is the minimum value of E_j that the iterative algorithm must use, then using $\mathbf{f_1}(E_j)$ and E_0, we will write the iterative function $\mathbf{f}(E_j)$ as follows.

$$\mathbf{f}(E_j) = \max\left\{\mathbf{f_1}(E_j), E_0\right\} \tag{C.3}$$

C.2.1 Convergence of the Iterative Function

Now our goal is to prove that $\mathbf{f}(E_j)$ satisfies all three properties of a standard interference function. In this respect, we will make use of the following results which can be easily verified.

Lemma 3 *The constant interference function* $\mathbf{I^q}(\mathbf{Y}) = q$ *is a standard interference function.*

Theorem 14 *If* $\mathbf{I_1}(\mathbf{Y})$ *is a scalable monotone interference function, then*

$$\mathbf{I}(\mathbf{Y}) = \max\left\{\mathbf{I_1}(\mathbf{Y}), q\right\}$$

is a standard interference function.

Theorem 14 implies that the iterative function, $\mathbf{f}(E_j)$ of equation (C.3) will be standard iff $\mathbf{f_1}(E_j)$ is a scalable monotone function.

We will sequentially prove the monotonicity and scalability of $\mathbf{f_1}(E_j)$. To show $\mathbf{f_1}(E_j)$ is a monotone interference function, the following theorem from [6] will be found useful.

Theorem 15 Log sum Inequality: *For non-negative numbers,* $\{a_i\}_{i=1}^n$, $\{b_i\}_{i=1}^n$,

$$\sum_{i=1}^{n} a_i \log \frac{a_i}{b_i} \geq \left(\sum_{i=1}^{n} a_i\right) \log \frac{\left(\sum_{i=1}^{n} a_i\right)}{\left(\sum_{i=1}^{n} b_i\right)} \tag{C.4}$$

with equality if and only if $\frac{a_i}{b_i}$ *=constant.*

Multiplying both sides of equation (C.4) by -1, we can write

$$\sum_{i=1}^{M} a_i \log \frac{b_i}{a_i} \leq \left(\sum_{i=1}^{M} a_i\right) \log \frac{\left(\sum_{i=1}^{M} b_i\right)}{\left(\sum_{i=1}^{M} a_i\right)} \tag{C.5}$$

Proof: Monotonicity of $\mathbf{f_1}(E_j)$ To prove the monotonicity of $\mathbf{f_1}(E_j)$, we need to show that $\frac{\mathrm{d}\mathbf{f_1}(E_j)}{\mathrm{d}E_j} \geq 0$. Some algebra will verify that $\frac{\mathrm{d}\mathbf{f_1}(E_j)}{\mathrm{d}E_j} \geq 0$ iff

$$\left[\sum_{i=1}^{M} Q\left(\sqrt{c_i E_j}\right)\right] \log \left[M/\sum_{i=1}^{M} Q\left(\sqrt{c_i E_j}\right)\right] - \frac{1}{2\sqrt{\pi}} \sum_{i=1}^{M} \sqrt{\frac{c_i E_j}{2}} \exp(-\frac{c_i E_j}{2}) \geq 0 \tag{C.6}$$

In this study, we will establish $\frac{\mathrm{d}\mathbf{f_1}(E_j)}{\mathrm{d}E_j} \geq 0$ by proving inequality (C.6).

Let us assume that $\{x_i\}$ is a set of non-negative real numbers. Using the result of reference [26, equation 11], we can write

$$Q\left(\sqrt{2}x_i\right)\log\left[1/Q\left(\sqrt{2}x_i\right)\right] - \frac{1}{2\sqrt{\pi}}x_i\exp(-x_i^2) \geq 0 \tag{C.7}$$

Since inequality (C.7) is true for all i, we get

$$\sum_{i=1}^{M} Q\left(\sqrt{2}x_i\right)\log\left[1/Q\left(\sqrt{2}x_i\right)\right] - \frac{1}{2\sqrt{\pi}}\sum_{i=1}^{M} x_i\exp(-x_i^2) \geq 0 \tag{C.8}$$

Denoting $\sqrt{c_iE_j} = \sqrt{2}x_i$, from equation (C.8) we obtain

$$\sum_{i=1}^{M} Q\left(\sqrt{c_iE_j}\right)\log\left[1/Q\left(\sqrt{c_iE_j}\right)\right] - \frac{1}{2\sqrt{\pi}}\sum_{i=1}^{M}\sqrt{\frac{c_iE_j}{2}}\exp(-\frac{c_iE_j}{2}) \geq 0 \tag{C.9}$$

As inequality (C.5) implies that

$$\sum_{i=1}^{M} Q\left(\sqrt{c_iE_j}\right)\log\left[1/Q\left(\sqrt{c_iE_j}\right)\right] \leq \left\{\sum_{i=1}^{M} Q\left(\sqrt{c_iE_j}\right)\right\}\log\left[M/\sum_{i=1}^{M} Q\left(\sqrt{c_iE_j}\right)\right] \tag{C.10}$$

we can weaken the inequality (C.9) as follows.

$$\left[\sum_{i=1}^{M} Q\left(\sqrt{c_iE_j}\right)\right]\log\left[M/\sum_{i=1}^{M} Q\left(\sqrt{c_iE_j}\right)\right] - \frac{1}{2\sqrt{\pi}}\sum_{i=1}^{M}\sqrt{\frac{c_iE_j}{2}}\exp(-\frac{c_iE_j}{2}) \geq 0 \tag{C.11}$$

□

Proof: Scalability of $\mathbf{f_1}(E_j)$ For $\alpha > 1$, we can write

$$\begin{aligned}\mathbf{f_1}(\alpha E_j) &= \frac{\log(1/q^*)}{\log\left\{M/\sum_{i=1}^{M} Q\left(\sqrt{c_i\alpha E_j}\right)\right\}}\alpha E_j \\ &< \frac{\log(1/q^*)}{\log\left\{M/\sum_{i=1}^{M} Q\left(\sqrt{c_iE_j}\right)\right\}}\alpha E_j = \alpha\mathbf{f_1}(E_j)\end{aligned} \tag{C.12}$$

□

Appendix D

A Comparison of the Partial Decorrelator and the Conventional Receiver in a Multi-cell DS/CDMA System

Considering random signature sequences, we will perform a comparative study between the partial decorrelator and the conventional receiver. Since, the bit error rate is difficult to analyze for both the partial decorrelator and the conventional receiver, average signal-to-interference ratio (SIR) will be used as a system performance measure. Average SIR is defined as the ratio of the average signal power and the average total interference power. We implement the partial decorrelator by modified correlators. When the desired user's signature is not a linear combination of the other intra-cell users' signatures, the desired modified correlator signal is normalized to have unit energy, otherwise, it is a zero signal. In Chapters 3 and 6, we have seen that in order to decode the desired user, the decorrelator eliminates the multiuser interference at the cost of reduced received energy. Since the partial decorrelator orthogonalizes the intra-cell interference, the desired user's received energy will be reduced at the receiver output. Note that, in this case, the energy loss factor is the asymptotic efficiency of the desired user given that the other cell interference is zero.

For the sake of simplicity, this study considers a single rate synchronous multi-cell DS/CDMA system. The given analysis has three parts. In the first part of the analysis, we develop a lower bound on the average energy loss factor of the desired user for the partial decorrelator. The second part of the analysis proves that the second moment of the inter-cell interference is higher for the conventional receiver than the partial decorrelator. Using these results, in the third part of our analysis, we develop an upper bound on the number of intra-cell users for which the partial decorrelator performs better than the conventional receiver in terms of average SIR. This upper bound is a function of the processing gain, the second moments of the intra-cell and inter-cell interferences for the conventional receiver and the power spectral density of the additive white Gaussian noise.

D.1 Analysis

In our single rate synchronous multi-cell DS/CDMA system, the chip, $p[t]$ duration is T_c and the bit duration is T. Thus, the processing gain of each user is $L = T/T_c$. The number of users in the system is K and the jth user has signature waveform

$$S_j(t) = \sum_{m=1}^{L} \{a_j(m) \frac{1}{\sqrt{L}} p[t-(m-1)T_c]\} \qquad t \in [0,T] \qquad 1 \leq j \leq K$$

where $a_j(m) \in \{-1, 1\}$ denotes the random signature sequence of user j. Note that $\int_0^T [S_j(t)]^2 dt = 1$. All users are transmitting over an AWGN channel, where the power spectral density of the AWGN is σ^2.

In the interval $[0, T]$, user j transmits bit b_j with received energy E_j using the signature $S_j(t)$. If the vector representation of the signature $S_j(t)$ is S_j, then the received signal vector of the jth user in the interval $[0, T]$ is

$$r_j = b_j \sqrt{E_j} S_j \qquad 1 \leq j \leq K \tag{D.1}$$

Note that the size of S_j is $L \times 1$.

Let us choose a cell arbitrarily from the multi-cell CDMA system and denote the number of intra-cell users by K'. We number these K' intra-cell users from 1 to K'. There are $K - K'$ other cell users which are numbered as $K'+1, \ldots, K$. In our analysis, we will consider the K'th intra-cell user as the user of our interest.

Using the above notations, we will now develop a lower bound on the average energy loss factor of the desired user for the partial decorrelator.

Lemma 4 *For random signature sequences, the average energy loss factor of the desired user for the partial decorrelator is lower bounded as follows.*

$$\bar{\zeta}_{K'} = E[\zeta_{K'}] \geq 1 - \left(K' - 1\right)/L \tag{D.2}$$

Proof:

Let us assume that for a given set of signatures $\{S_j\}$, the first $K'-1$ intra-cell interfering signatures generate $\{f_j\}_{j=1}^{K''}$ orthonormal basis vectors, where each f_j is a vector of size $L \times 1$ and $K'' \leq K'-1$. Note that K'' is a random variable and its mean $\mathrm{E}[K''] \leq K'-1$.

For given $\{S_j\}$, using equations (6.12) and (6.21), we can write the energy loss factor of the K'th user for the partial decorrelator as follows.

$$\zeta_{K'} = 1 - \sum_{j=1}^{K''} \left(f_j^\top S_{K'}\right)^2 = 1 - \sum_{j=1}^{K''} f_j^\top S_{K'} S_{K'}^\top f_j \tag{D.3}$$

Since

$$\mathrm{E}\left[S_{K'} S_{K'}^\top\right] = (1/L) \times \text{identity matrix of size } L \times L \qquad \text{and} \qquad f_j^\top f_j = 1 \tag{D.4}$$

taking expectation with respect to $S_{K'}$ on both sides of equation (D.3), we obtain

$$\mathrm{E}_{S_{K'}}[\zeta_{K'}] = 1 - K''/L \tag{D.5}$$

We will now take expectation with respect to K'' on both sides of equation (D.5). Since $\mathrm{E}[K''] \leq K'-1$, we will then get

$$\bar{\zeta}_{K'} = 1 - \mathrm{E}\big[K''\big]/L \geq 1 - \big(K'-1\big)/L \tag{D.6}$$

□

The near-far resistance of the decorrelator is the same as its asymptotic efficiency. Again, the near-far resistance of the decorrelator equals the near-far resistance of the LMMSE receiver; see [31]. Using complex matrix algebra, for random signatures, reference [30] has calculated a lower bound on the average near-far resistance of the LMMSE receiver which is the same as equation (D.3). However, the proof of Lemma 4 presents a simple technique to calculate the lower bound on the near-far resistance of the decorrelator or the LMMSE [30].

We will now present the second part of our analysis.

Lemma 5 *For random signature sequences, the second moment of the inter-cell interference is higher for the conventional receiver than the partial decorrelator.*

Proof:

To simplify the proof, we will use the term $\Phi_{K'}(t)$ or $\Phi_{K'}$ to denote the desired correlator signal or the desired receiver filter. The desired receiver filter $\Phi_{K'}$ can be either the signature waveform, $S_{K'}$ or the partial decorrelator filter. Note that if $\Phi_{K'} = S_{K'}$, then $||\Phi_{K'}||^2 = 1$. However, for the partial decorrelator, $||\Phi_{K'}||^2 = 1$ holds only when the desired user's signature is not a linear combination of the intra-cell interfering signatures, otherwise, $\Phi_{K'}$ is a zero vector or $||\Phi_{K'}||^2 = 0$. Since $S_{K'}$ has the possibility to be a linear combination of the intra-cell interfering signatures, the proof of this lemma has the following steps. First, we will determine the second moment of the inter-cell interference for both the receivers given that $S_{K'}$ is not a linear combination of the intra-cell interfering signatures. We will then calculate the second moment of the inter-cell interference for both the receivers given that $S_{K'}$ is a linear combination of the intra-cell interfering signatures. At the end, using these conditional second moments of the inter-cell interference, we will prove the above lemma.

Let us now consider the case, when the desired signature $S_{K'}$ is not a linear combination of the intra-cell interfering signatures. In this case, $||\Phi_{K'}||^2 = 1$ for both the receivers. If the sum of received signal vectors of the other cell terminals is r_o, then equation (D.1) yields

$$r_o = \sum_{j=K'+1}^{K} r_j = \sum_{j=K'+1}^{K} b_j \sqrt{E_j} S_j \tag{D.7}$$

We denote the other cell interference at the desired receiver filter output by $\bar{r}_o$, where

$$\bar{r}_o = \Phi_{K'}^{\top} r_o = \sum_{j=K'+1}^{K} b_j \sqrt{E_j} \Phi_{K'}^{\top} S_j \tag{D.8}$$

Squaring both sides of equation (D.8), we get

$$\bar{r}_o^2 = \Phi_{K'}^{\top} r_o r_o^{\top} \Phi_{K'} = \sum_{j=K'+1}^{K} \sum_{k=K'+1}^{K} b_j b_k \sqrt{E_j} \sqrt{E_k} \Phi_{K'}^{\top} S_j S_k^{\top} \Phi_{K'} \tag{D.9}$$

Our goal is to calculate the second moment of $\bar{r}_o$ given that $S_{K'}$ is not a linear combination of the intra-cell interfering signatures. In equation (D.9), we assume that the transmitted bits are independent. Taking the expectation with respect to transmitted bits b on both sides of equation (D.9), we can write

$$\mathrm{E}_b(\bar{r}_o^2) = \sum_{j=K'+1}^{K} \sum_{k=K'+1}^{K} \mathrm{E}_b(b_j b_k)\sqrt{E_j}\sqrt{E_k}\Phi_{K'}^\top S_j S_k^\top \Phi_{K'} = \sum_{j=K'+1}^{K} E_j \Phi_{K'}^\top S_j S_j^\top \Phi_{K'} \tag{D.10}$$

We will now take the expectation with respect to normalized signatures S_j on equation (D.10). Using equation (D.4) and $||\Phi_{K'}||^2 = 1$, we will write the conditional second moment of the inter-cell interference as

$$\mathrm{E}_{S_j}\left[\mathrm{E}_b(\bar{r}_o^2)\right] = \sum_{j=K'+1}^{K} E_j/L \tag{D.11}$$

Equation (D.11) implies that if the signature sequences are random and $||\Phi_{K'}||^2 = 1$, the second moment of the inter-cell interference does not depend on the correlator signal $\Phi_{K'}$. As a result, for random signatures, the second moment of the inter-cell interference is the same for both the conventional receiver and the partial decorrelator given that $S_{K'}$ is not a linear combination of the other intra-cell signatures.

We will now consider the case when the desired signature $S_{K'}$ is a linear combination of the intra-cell interfering signatures, i.e. $||\Phi_{K'}||^2 = 0$ for the partial decorrelator. In this situation, the second moment of the inter-cell interference for the partial decorrelator is zero. However, the second moment of the inter-cell interference for the conventional receiver is the same as equation (D.11). Thus, if the second moment of the inter-cell interference for the partial decorrelator is $\hat{\sigma}_2^2$ and the second moment of the inter-cell interference for the conventional receiver is σ_2^2, then using equation (D.11), we can write

$$\hat{\sigma}_2^2 \leq \sum_{j=K'+1}^{K} E_j/L = \sigma_2^2 \tag{D.12}$$

□

Let us assume that $\hat{\sigma}^2$ denotes the background noise variance for the partial decorrelator. Applying the similar technique used in the proof of Lemma 5, we can show that the background noise variance for the partial decorrelator is less than or equal to the background noise variance, σ^2 for the conventional receiver, i.e.

$$\hat{\sigma}^2 \leq \sigma^2 \tag{D.13}$$

Using some algebra similar to equations (D.10) and (D.11), the second moment of the intra-cell interference, σ_1^2 for the conventional receiver can be written as

$$\sigma_1^2 = \sum_{j=1}^{K'-1} E_j/L \tag{D.14}$$

Denoting $F = \left(\sigma_2^2 + \sigma^2\right)/\sigma_1^2$, we will now prove the following theorem.

Theorem 16 *If $K' < \frac{L}{1+F} + 1$, then the partial decorrelator provides higher average SIR than the conventional receiver.*

Proof: Since the average SIR is the ratio of the average signal power and the average total interference power, using equations (D.12) and (D.14), we can write the average SIR of the desired user under the conventional receiver as

$$\mathrm{SIR}_{\mathrm{con}} = \frac{E_{K'}}{\sigma_1^2 + \sigma_2^2 + \sigma^2} \tag{D.15}$$

Lemmas 4- 5 and equation (D.13) yield a lower bound on the average SIR of the desired user under the partial decorrelator as follows.

$$\mathrm{SIR}_{\mathrm{par}} = \frac{\bar{\zeta}_{K'}}{\hat{\sigma}_2^2 + \hat{\sigma}^2} E_{K'} \geq \frac{1-(K'-1)/L}{\hat{\sigma}_2^2 + \hat{\sigma}^2} E_{K'} \geq \frac{1-(K'-1)/L}{\sigma_2^2 + \sigma^2} E_{K'} \tag{D.16}$$

It is straightforward to show that if $\frac{1-(K'-1)/L}{\sigma_2^2+\sigma^2} E_{K'} > \mathrm{SIR}_{\mathrm{con}}$ then

$$K' < \frac{L}{1+F} + 1 \tag{D.17}$$

Equation (D.16) implies that inequality (D.17) satisfies $\mathrm{SIR}_{\mathrm{par}} > \mathrm{SIR}_{\mathrm{con}}$ $\square$

References

[1] A. Baier, U-C. Fiebig, W. Granzow, W. Koch, P. Teder, and J. Thielecke. Design Study for a CDMA-based Third-generation Mobile Radio System. *IEEE Journal on Selected Areas in Communications*, 12(4):733–743, May 1994.

[2] Y. Bar-Ness and N. Sezgin. Maximum Signal-to-noise Ratio Data Combining for One-Shot Asynchronous Multiuser CDMA Detector. In *Proceedings of the sixth IEEE International Symposium on Personal, Indoor and Mobile Radio Communications*, volume 1, pages 188–192, September, 27-29 1995.

[3] D. G. Brennan. Linear Diversity Combining Techniques. In *Proceedings of IRE*, volume 47, pages 1075–1102, June 1959.

[4] D. S. Chen and S. Roy. An Adaptive Multiuser Receiver for CDMA Systems. *IEEE Journal on Selected Areas in Communications*, 12(5):808–816, June 1994.

[5] J. Chen and U. Mitra. Further Results for Multi-rate Decorrelators for Synchronous DS/CDMA Systems. In *Proceedings of 34th Annual Allerton Conference on Communication, Control and Computing*, Monticello, IL, October, 26 1996.

[6] T. M. Cover and J. A. Thomas. *Elements of Information Theory.* John Wiley & Sons, USA, 1991.

[7] R. C. Dixon. *Spread Spectrum Systems.* John Wiley and Sons, USA, 1994.

[8] A. Duel-Hallen. Decision-Feedback Multiuser Detector Synchronous for Code-Division Multiple Access Channel. *IEEE Transactions on Communications*, 41:285–290, February 1993.

[9] A. Duel-Hallen. A Family of Multiuser Decision-Feedback Detectors for Asynchronous for Code-Division Multiple Access Channels. *IEEE Transactions on Communications*, 43(2/3/4):421–434, February/March 1995.

[10] A. Duel-Hallen, J. Holtzman, and Z. Zvonar. Multiuser Detection for CDMA Systems. *IEEE Personal Communications*, pages 46–58, April 1995.

[11] G. J. Foschini and Z. Miljanic. A Simple Distributed Autonomous Power Control Algorithm and its Convergence. *IEEE Transactions on Vehicular Technology*, 42(4):641–646, November 1993.

[12] H. Ge and Y. Bar-Ness. Multi-shot Multiuser Detector for Asynchronous CDMA Channel. In *Proceedings of the Conference on Information Science and Systems*, volume 1, pages 590–595, March, 20-22 1996.

[13] K.S. Gilhousen, I.M. Jacobs, R. Padovani, A.J. Viterbi, L. A. Weaver Jr., and C.E. Wheatley III. On the Capacity of a Cellular CDMA System. *IEEE Transactions on Vehicular Technology*, 40:303–311, May 1991.

[14] G. H. Golub and C. F. Van Loan. *Matrix Computations.* The John Hopkins University Press, Baltimore, MD, 1989.

[15] N. Guo and S. D. Morgera. The Grade of Service for Integrated Voice/Data Wireless DS-CDMA Networks. In *Proceedings of Supercomm/IEEE International Conference on Communications*, pages 1104–1110, 1994.

[16] S. V. Hanly. An Algorithm for Combined Cell-Site Selection and Power Control to Maximize Cellular Spread Spectrum Capacity. *IEEE Journal on Selected Areas in Communications*, 13(7):1332–1340, September 1995.

[17] M. Honig, U. Madhow, and S. Verdú. Blind Adaptive Multiuser Detection. *IEEE Transactions on Information Theory*, 41(4):944–960, July 1995.

[18] M. L. Honig and S. Roy. Multi-user Communication with Multiple Symbol Rates. In *Proceedings of the IEEE Symposium on Information Theory, Whistler, BC, Canada*, page 381, September 1995.

[19] A. Hottinen, H. Holma, and A. Toskala. Multiuser Detection for Multi-rate CDMA Communications. In *Proceedings of IEEE International Conference on Communications*, 1996.

[20] C.-L. I and R. D. Gitlin. Multi-code CDMA Wireless Personal Communications Networks. In *Proceedings of IEEE International Conference on Communications*, volume 2, pages 1060–1064, Seattle, WA, June 18-22 1995.

[21] A. Johansson and A. Svensson. Successive Interference Cancellation Schemes in Multi-rate DS/CDMA Systems. In *Proceedings of 45th IEEE Vehicular Technology Conference*, volume 2, pages 704–708, Chicago, USA, July, 25-28 1995.

[22] M. J. Juntti and B. Aazhang. Linear Finite Memory-length Multiuser Detectors. In *Proceedings of 3rd IEEE Communication Theory Mini-Conference, Global Telecommunications Conference*, pages 126–130, Singapore, November 13 - 17 1995.

[23] M. J. Juntti and J. O. Lilleberg. Linear FIR Multiuser Detection for Multiple Data Rate CDMA Systems. In *Proceedings of 47th IEEE Vehicular Technology Conference*, volume 2, pages 455–459, Phoenix, USA, May 4-7 1997.

[24] T. Kailath. *Linear Systems.* Prentice-Hall, Inc., Englewood Cliffs, N.J. 07632, 1980.

[25] P. S. Kumar and J. Holtzman. Power Control for a Spread Spectrum System with Multiuser Receivers. In *Proceedings of IEEE International Symposium on Personal, Indoor and Mobile Radio Communications*, volume 3, pages 955–959, September 1995.

[26] P. S. Kumar, R. D. Yates, and J. Holtzman. Power Control Cased on Bit Error Rate (BER) Measurements. In *Military Communications Conference (MILCOM)*, volume 2, pages 617–620. IEEE, October 1995.

[27] W. C. Y. Lee. *Mobile Communications Engineering.* McGraw-Hill, Inc., USA, 1993.

[28] R. Lupas and S. Verdú. Linear Multiuser Detectors for Synchronous Code-Division Multiple-Access Channels. *IEEE Transactions On Information Theory*, 35(1):123–136, January 1989.

[29] R. Lupas and S. Verdú. Near-Far Resistance of Multiuser Detectors in Asynchronous Channels. *IEEE Transactions On Communications*, 38(4):496–508, April 1990.

[30] U. Madhow and M. L. Honig. MMSE Detection of Direct-Sequence CDMA Signals: Performance Analysis for Random Signature Sequences. (submitted).

[31] U. Madhow and M. L. Honig. MMSE Interference Suppression for Direct-Sequence Spread-Spectrum CDMA. *IEEE Transactions on Communications*, 42(12):3178–3188, December 1994.

[32] N. Mandayam, J. M. Holtzman, and S. Barberis. Erlang Capacity of an Integrated Voice/Data CDMA Systems. In *Proceedings of IEEE International Symposium on Personal, Indoor and Mobile Radio Communications*, volume 3, pages 1078–1082, September 1995.

[33] N. Mandayam and S. Verdú. Analysis of an Approximate Decorrelating Detector. In *Proceedings of Thirty-third Annual Allerton Conference on Communication, Control and Computing*, Monticello, IL, October, 4-6 1995.

[34] N. B. Mandayam and B. Aazhang. An Adaptive Multiuser Interference Rejection Algorithms for Direct-Sequence Code Division Multiple Access. In *Proceedings of IEEE International Symposium of Information Theory*, page 135, Trondheim, Norway, June 27 - July 1 1994. (published in IEEE Transactions on Communications).

[35] S. Miller. An Adaptive Direct-sequence Code-division Multiple-access Receiver for Multi-user Interference Rejection. *IEEE Transactions On Communications*, 43(2/3/4):1746–1755, February/March/April 1995.

[36] U. Mitra. Observations on Jointly Optimal Detection for Multi-rate DS/CDMA Systems. In *Proceedings of 4th IEEE Communication Theory Mini-Conference, Global Telecommunications Conference*, UK, November 18 - 22 1996.

[37] T. Ottosson and A. Svensson. Multi-rate Schemes in DS/CDMA Systems. In *Proceedings of 45th IEEE Vehicular Technology Conference*, volume 2, pages 1006–1010, Chicago, USA, July 1995. (accepted for publication in Wireless Personal Communications).

[38] B.-P. Paris. Finite Precision Decorrelating Receivers for Multiuser CDMA Communication Systems. *IEEE Transactions on Communications*, 44(4):496–507, April 1996.

[39] P. Patel and J. Holtzman. Analysis of a Simple Successive Interference Cancellation Scheme in a DS/CDMA. *IEEE Journal on Selected Areas in Communications*, 12(5):796–807, June 1994.

[40] H. V. Poor. *An Introduction to Signal Detection and Estimation*. Spinger-Verlag, New York, 1988.

[41] J.G. Proakis. *Digital Communication.* McGraw-Hill, Inc., USA, 1989.

[42] P. B. Rapajic and B. S. Vucetic. Adaptive Receiver Structures for Asynchronous CDMA Systems. *IEEE Journal on Selected Areas in Communications*, 12(4):685–697, May 1994.

[43] J. Rapeli. UMTS: Targets, System Concept, and Standardization in a Global Framework. *IEEE Personal Communications*, pages 20–28, February 1995.

[44] D. J. Sakrison. Stochastic Approximation: A Recursive Method for Solving Regression Problems. *Advances in Communication Systems*, 2:51–106, 1966.

[45] A. Sampath, P. S. Kumar, and J. M. Holtzman. Power Control and Resource Management for a Multimedia CDMA Wireless. In *Proceedings of IEEE International Symposium on Personal, Indoor and Mobile Radio Communications*, volume 1, pages 21–25, September 1995.

[46] M. Saquib and R. Yates. A Two Stage Decorrelator for a Dual Rate Synchronous DS/CDMA System. In *Proceedings of Supercomm/IEEE International Conference on Communications*, Montreal, Canada, 1997.

[47] M. Saquib, R. Yates, and A. Ganti. Quality of Service for an Asynchronous Multi-rate Decorrelator, Part I : Detection. *IEEE Transactions on Communications.* (submitted).

[48] M. Saquib, R. Yates, and A. Ganti. Quality of Service for an Asynchronous Multi-rate Decorrelator, Part II : Power Control. *IEEE Transactions on Communications.* (submitted).

[49] M. Saquib, R. Yates, and A. Ganti. An Asynchronous Decentralized Multi-rate Decorrelator. In *Proceedings of the Conference on Information Science and Systems*, volume 1, pages 462–467, Johns Hopkins University, USA, March, 19-21 1997.

[50] M. Saquib, R. Yates, and A. Ganti. Stochastic Power Control with Bit Error Rate for a Multi-rate Decorrelating Detector. In *Proceedings of 35th Annual Allerton Conference on Communication, Control and Computing*, Monticello, IL, October, 26 1997.

[51] M. Saquib, R. Yates, and N. Mandayam. A Decision Feedback Decorrelator for a Dual Rate Synchronous DS/CDMA System. *Wireless Networks, special issue on "Multi-user Detection in Wireless Communications".* (accepted).

[52] M. Saquib, R. Yates, and N. Mandayam. Decorrelating Detectors for a Dual Rate Synchronous DS/CDMA System. *Wireless Personal Communications.* (accepted).

[53] M. Saquib, R. Yates, and N. Mandayam. A Decision Feedback Decorrelator for a Dual Rate Synchronous DS/CDMA System. In *Proceedings of IEEE Global Telecommunications Conference*, volume 3, pages 1804–1808, UK, November 18 - 22 1996.

[54] M. Saquib, R. Yates, and N. Mandayam. Decorrelating Detectors for a Dual Rate Synchronous DS/CDMA System. In *Proceedings of 46th IEEE Vehicular Technology Conference*, volume 1, pages 377–381, Atlanta, USA, April 28 - May 1 1996.

[55] Z. Siveski, Y. Bar-Ness, and D. W. Chen. Error Performance of Synchronous Multiuser Code Division Multiple Access Detector with Multidimensional Adaptive Canceler. *European Transactions on Telecommunications and Related Technologies*, 5(6):719–724, November-December 1994.

[56] M. K. Tsatsanis and G. B. Giannakis. Optimal Decorrelating Receivers for DS-CDMA Systems: A Signal Processing Framework. *IEEE Transactions on Signal Processing*, 44(12):3044–3055, December 1996.

[57] S. Ulukus and R. Yates. Adaptive Power Control with MMSE Multiuser Detectors. In *Proceedings of Supercomm/IEEE International Conference on Communications*, Montreal, Canada, 1997.

[58] S. Ulukus and R. D. Yates. Stochastic Power Control for Cellular Radio Systems. In *Proceedings of 34th Annual Allerton Conference on Communication, Control and Computing*, Monticello, IL, September, 29 - October, 1 1996.

[59] H. L. Vantrees. *Detection, Estimation and Modulation Theory, Part I.* Wiley, New York, 1968.

[60] M. Varanasi. Power Control for Multiuser Detection. In *Proceedings of the 30th Annual Conference on Information Sciences and Systems*, Princeton University, March 1996.

[61] M. K. Varanasi and B. Aazhang. Multistage Detection in Asynchronous Code-Division Multiple-Access Communications. *IEEE Transactions On Communications*, 38(4):509–519, April 1990.

[62] M. K. Varanasi and B. Aazhang. Near-Optimum Detection in Synchronous Code-Division Multiple-Access Systems. *IEEE Transactions On Communications*, pages 725–736, May 1991.

[63] S. Vembu and A. J. Viterbi. Two Different Philosophies in CDMA - A Comparison. In *Proceedings of 46th IEEE Vehicular Technology Conference*, volume 2, pages 869–873, Atlanta, USA, April 28 - May 1 1996.

[64] S. Verdú. Computational complexity of optimum multiuser detection.

[65] S. Verdú. Multiuser Detection. EE-539 Class notes, Princeton University.

[66] S. Verdú. *Optimum Multi-user Signal Detection.* PhD thesis, University of Illinois at Urbana-Champaign, 1984.

[67] S. Verdú. Minimum Probability of Error for Asynchronous Gaussian Multiple-access Channels. *IEEE Transactions on Information Theory*, IT-32:85–96, January 1986.

[68] S. Verdú. Multiuser Detection, Advances in Statistical Signal Processing. *JAI Press Inc.*, 2:369–409, 1993.

[69] A.J. Viterbi. The Orthogonal-Random Waveform Dichotomy for Digital Mobile Personal Communications . *IEEE Personal Communications*, (First Quarters):18–24, 1994.

[70] X. Wang and H. V. Poor. Blind Adaptive Interference Suppression for CDMA Communications Based on Eigenspace Tracking. In *Proceedings of the Conference on Information Science and Systems*, Johns Hopkins University, USA, March, 19-21 1997.

[71] S. S. H. Wijayasuriya, G. H. Norton, and J. P. McGeehan. A Sliding Window Decorrelating Receiver for Multiuser DS-CDMA Mobile Radio Networks. *IEEE Transactions on Vehicular Technology*, 45(3):503–521, August 1996.

[72] T.-H. Wu and E. Geraniotis. CDMA with Multiple Chip Rates for Multi-Media Communications. In *Proceedings of the 28th Annual Conference on Information Sciences and Systems, Princeton University*, pages 992–997, March 1994.

[73] R. Wyrwas, M. J. Miller, R. Anjaria, and W. Zhang. Multiple Access Options for Multi-media Wireless Systems. In *Proceedings of the 3rd Workshop on Third Generation Wireless Information Networks, WINLAB, Rutgers University*, pages 289–294, April 1992.

[74] Z. Xie, R. T. Short, and Rushforth. A Family of Sub-optimum Detectors for Coherent Multiuser Communications. *IEEE Journal on Selected Areas in Communications*, 8(4):683–690, March 1990.

[75] R. D. Yates. A Framework for Uplink Power Control in Cellular Radio Systems. *IEEE Journal on Selected Areas in Communications*, 13(7):1341–1347, September 1995.

[76] J. Zander. Performance of Optimum Transmitter Power Control in Cellular Radio Systems. *IEEE Transactions on Vehicular Technology*, 41(1):57–62, February 1992.

[77] F.-C. Zheng and S. K. Barton. Near-Far Resistant Detection of CDMA Signals via Isolation Bit Insertion. *IEEE Transactions on Communications*, 43(2/3/4):1313–1317, February/March/April 1995.

[78] R. E. Ziemer and R. L. Peterson. *Digital Communications and Spread Spectrum Systems*. MacMillan, New York, 1985.

Vita

Mohammad Saquib

1991 B.Sc. in Electrical and Electronics Engineering, Bangladesh University of Engineering & Technology, Bangladesh.

1991-92 System Engineer, Energy Research Corporation, Danbury, CT.

1993-94 Teaching Assistant, Department of Electrical and Computer Engineering, Rutgers University, Piscataway, NJ.

1994-95 Graduate Research Assistant, Department of Electrical and Computer Engineering, Rutgers University, Piscataway, NJ.

1995-97 Graduate Research Assistant, WINLAB, Department of Electrical and Computer Engineering, Rutgers University, Piscataway, NJ.

1995 M.S. in Electrical and Computer Engineering, Rutgers, NJ.

1995 M. Saquib and R. Yates "Optimal Call Admission to a Mobile Cellular Network", *Proceedings of 45th IEEE Vehicular Technology Conference*, Chicago, IL.

1996 M. Saquib, R. Yates and N. Mandayam "Decorrelating Detectors for a Dual Rate Synchronous DS/CDMA System", *Proceedings of 46th IEEE Vehicular Technology Conference*, Atlanta, GA.

1996 M. Saquib, R. Yates and N. Mandayam "A Decision Feedback Decorrelator for a Dual Rate Synchronous DS/CDMA System", *Proceedings of IEEE Global Telecommunications Conference*, London, UK.

1997 M. Saquib, R. Yates and A. Ganti "An Asynchronous Decentralized Multirate Decorrelator", *Proceedings of the Conference on Information Science and Systems, Johns Hopkins University*, Baltimore, MD.

1997 M. Saquib and R. Yates "A Two Stage Decorrelator for a Dual Rate Synchronous DS/CDMA System", *Proceedings of Supercomm/IEEE International Conference on Communications*, Montreal, Canada.

1997 M. Saquib, R. Yates and A. Ganti "Power Control for an Asynchronous Multi-rate Decorrelator", invited to *Thirty-fifth Annual Allerton Conference on Communication, Control and Computing*, Monticello, IL.

1998 M. Saquib, R. Yates and N. Mandayam "Decorrelating Detectors for a Dual Rate Synchronous DS/CDMA System", accepted for publication in *Wireless Personal Communications.*

1998 M. Saquib, R. Yates and N. Mandayam "A Decision Feedback Decorrelator for a Dual Rate Synchronous DS/CDMA System", accepted for publication in *ACM Journal of Wireless Networks.*

1998 Ph.D. in Electrical and Computer Engineering, Rutgers, NJ.